JOURNAL OF CAVE AND KARST STUDIES

September 2018
Volume 80, Number 3
ISSN 1090-6924
A Publication of the National Speleological Society

DEDICATED TO THE ADVANCEMENT OF SCIENCE, EDUCATION, EXPLORATION, AND CONSERVATION

Published By
The National Speleological Society

http://caves.org/pub/journal

Office
6001 Pulaski Pike NW
Huntsville, AL 35810 USA
Tel:256-852-1300
nss@caves.org

The *Journal of Cave and Karst Studies* , ISSN 1090-6924, CPM Number #40065056, is a multi-disciplinary, refereed journal published four times a year by the National Speleological Society. The *Journal* is available by open access on its website, or check the website for current print subscription rates. Back issues are available from the NSS office.

POSTMASTER: send address changes to the National Speleological Society Office listed above.

The Journal of Cave and Karst Studies is covered by the following ISI Thomson Services Science Citation Index Expanded, ISI Alerting Services, and Current Contents/Physical, Chemical, and Earth Sciences.

Front cover: A lobster stalagmite located in Victoria Arch at Wombeyan Caves, New South Wales, Australia. Photograph by Scott Engel.

L. Land and A. Rinehart. Geophysical surveys of a potentially extensive cave system, Guadalupe Mountains, New Mexico, USA. *Journal of Cave and Karst Studies*, v. 80, no. 3, p. 109-120. DOI:10.4311/2017ES0108

GEOPHYSICAL SURVEYS OF A POTENTIALLY EXTENSIVE CAVE SYSTEM, GUADALUPE MOUNTAINS, NEW MEXICO, USA

Lewis Land[1] and Alex Rinehart[2]

Abstract

Between 2012 and 2015 National Cave and Karst Research Institute (NCKRI) personnel conducted electrical resistivity and microgravity surveys over Manhole Cave, located on public land administered by the US Bureau of Land Management (BLM) in the Guadalupe Mountains of southeastern New Mexico. Manhole Cave is a relatively shallow pit cave, but it is thought by many cavers to be a second entrance to Lechuguilla Cave, the second deepest cave in the continental United States. Digging in Manhole Cave has been occurring sporadically for many years, following airflow through cemented breakdown. Results of resistivity surveys conducted over the cave show a high-resistivity anomaly southwest of the cave entrance, consistent with microgravity survey results that show a negative gravity anomaly in the same area. Combined geophysical results indicate that a substantial void is present in the subsurface a few tens of meters below ground level and extending to the south of the dig.

Background

The study area is located in the Delaware Basin region of southeastern New Mexico and west Texas. The Delaware Basin is one of the deepest sedimentary basins in North America, containing more than 7300 m of sedimentary rock that provide reservoirs for water, oil, and natural gas resources. A thinner sedimentary section overlaps the northern edge of the basin, extending for over 100 km beyond the basin margin across the Northwest Shelf (Fig. 1).

The Delaware Basin is rimmed by the Capitan Reef, a fossil reef of middle Permian (Guadalupian) age, that is exposed along the southeast escarpment of the Guadalupe Mountains. Here, it is the host rock for Carlsbad Cavern, the centerpiece of Carlsbad Caverns National Park (Fig. 2). Northeast of the Park, the reef plunges into the subsurface and passes beneath the city of Carlsbad, where it is a karstic aquifer that is the principal source of fresh water for that community (Hiss, 1975a). During middle Permian time, fine-grained sediments were deposited in shallow waters of the backreef area, behind the reef in a broad lagoon that extended across the Northwest Shelf. These sediments make up the carbonate and evaporite rocks of the backreef Artesia Group (Fig. 1; King, 1948; Hayes, 1964; Kelley, 1971; Land, 2003).

Caves, and other karst features in the Delaware Basin region, form in a semi-arid environment in a variety of geologic settings, in both carbonate and gypsum bedrock. Most caves in the Guadalupe Mountains are formed in limestones of the Capitan Reef Formation, or in dolomites of the backreef Artesia Group. For many years the prevailing theory of cave formation in the Guadalupe Mountains was that they were of epigenic origin, forming by carbonic acid dissolution near the water table (Bretz, 1949). However, since the 1980s, it is now widely accepted that caves in the Guadalupe Mountains are, for the most part, of hypogene origin, excavated by ascending artesian groundwater charged with sulfuric acid (Hill, 1987; Klimchouk, 2007).

Manhole Cave (known to many in the caving community as Big Manhole) is an approximately 20 m deep pit cave in the Guadalupe Mountains of southeastern New Mexico (Fig. 2), formed in backreef dolomites of the middle Permian Seven Rivers Formation (Fig. 1). The cave's entrance opens vertically beneath a dolomite ledge, and is protected by a steel gate to prevent unauthorized entry (Fig. 3). Its single chamber is approximately circular, and bells out from an entrance diameter of about one by three meters to a diameter averaging 27 m at the floor of the main chamber. The floor of the cave slopes upward from south to north, and the northern wall is within a meter of the ceiling (Lange, 1992). Most of the floor is covered with flowstone-cemented breakdown, which has been explored and excavated to a depth of about 30 m below the surface (Fig. 4).

Manhole Cave is located on federal land administered by the US Bureau of Land Management (BLM); its location places it less than 300 m north of the boundary with Carlsbad Caverns National Park. The cave is also located approximately 300 m (map distance) from the easternmost passages of Lechuguilla Cave, which lies within the boundaries of Carlsbad Caverns National Park (Figs. 2 and 5). Lechuguilla Cave is currently the second deepest cave in the continental United States (489 m; Gulden, 2016a) and, at 223 km, the seventh longest cave in the world (Gulden, 2016b). Lechuguilla Cave is generally assumed to have formed by hypogenic processes involving ascending, sulfuric acid-enriched

[1]National Cave and Karst Research Institute, New Mexico Institute of Mining and Technology, 400-1 Cascades Ave., Carlsbad, New Mexico 88220, USA. Lewis.land@nmt.edu.
[2]New Mexico Bureau of Geology and Mineral Resources, New Mexico Institute of Mining and Technology, 801 Leroy Pl., Socorro, New Mexico 87801, USA. Alex.rinehart@nmt.edu.

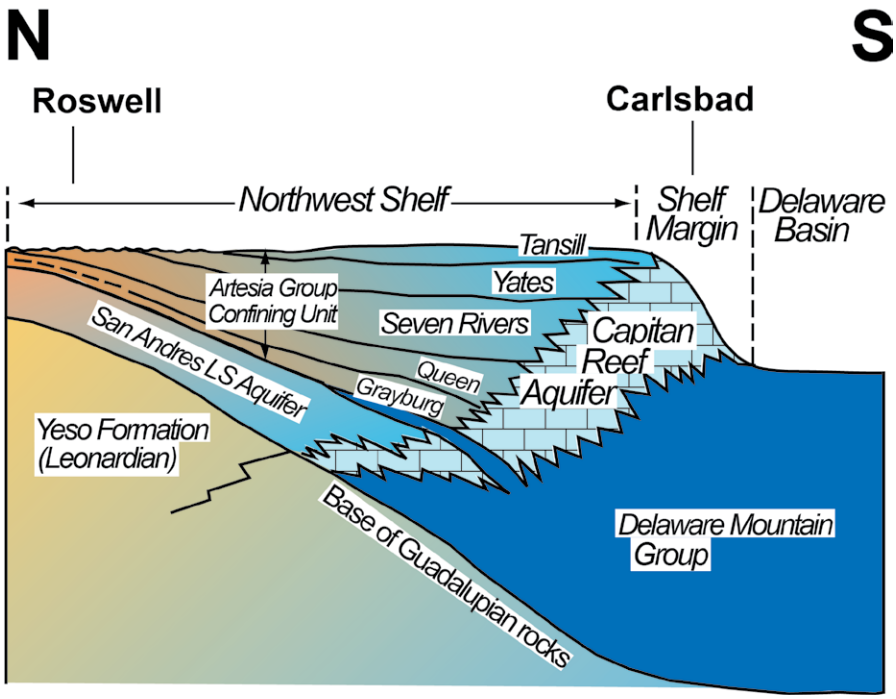

Figure 1. Regional stratigraphy of Guadalupian (middle Permian) rocks in southeastern New Mexico. Modified from Hiss (1975b).

groundwater, derived from oil and gas accumulations in the Delaware Basin of southeastern New Mexico and west Texas (Hill, 1987; Palmer and Palmer, 2000). The cave contains a remarkable assemblage of rare speleothems and communities of chemolithoautotrophic bacteria, which are thought to have contributed to enlargement of the cave (Northup, et al., 2000). Access to Lechuguilla Cave is limited to scientific research and survey of its extent as approved by the National Park Service (NPS).

Strong airflow emerging from cracks in the flowstone-covered floor of Manhole Cave indicates that the cave probably extends beyond its mapped limits. This phenomenon, and Manhole's proximity to Lechuguilla Cave, has generated speculation that Manhole Cave may represent an entrance to one of the most distant points in Lechuguilla. Beginning in 1986, this airflow has motivated exploratory digging by caver volunteers beneath the south wall of the cave (Fig. 4).

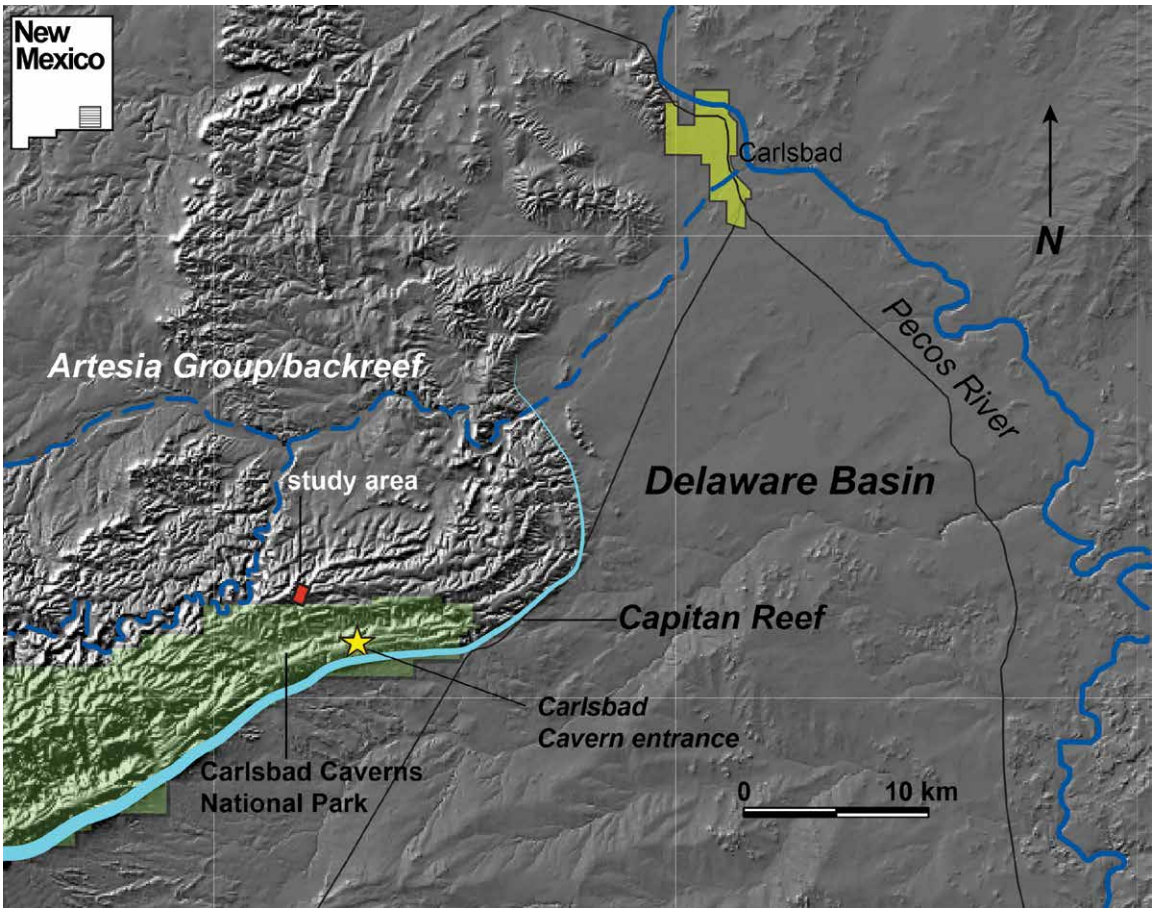

Figure 2. Map showing location of study area. Carlsbad Caverns National Park is shown by green shading. Capitan Reef outcrop is shown by blue shading along the Guadalupe Mountain front.

Figure 3. Manhole Cave entrance, formed in backreef carbonates of the Artesia Group/Seven Rivers Formation.

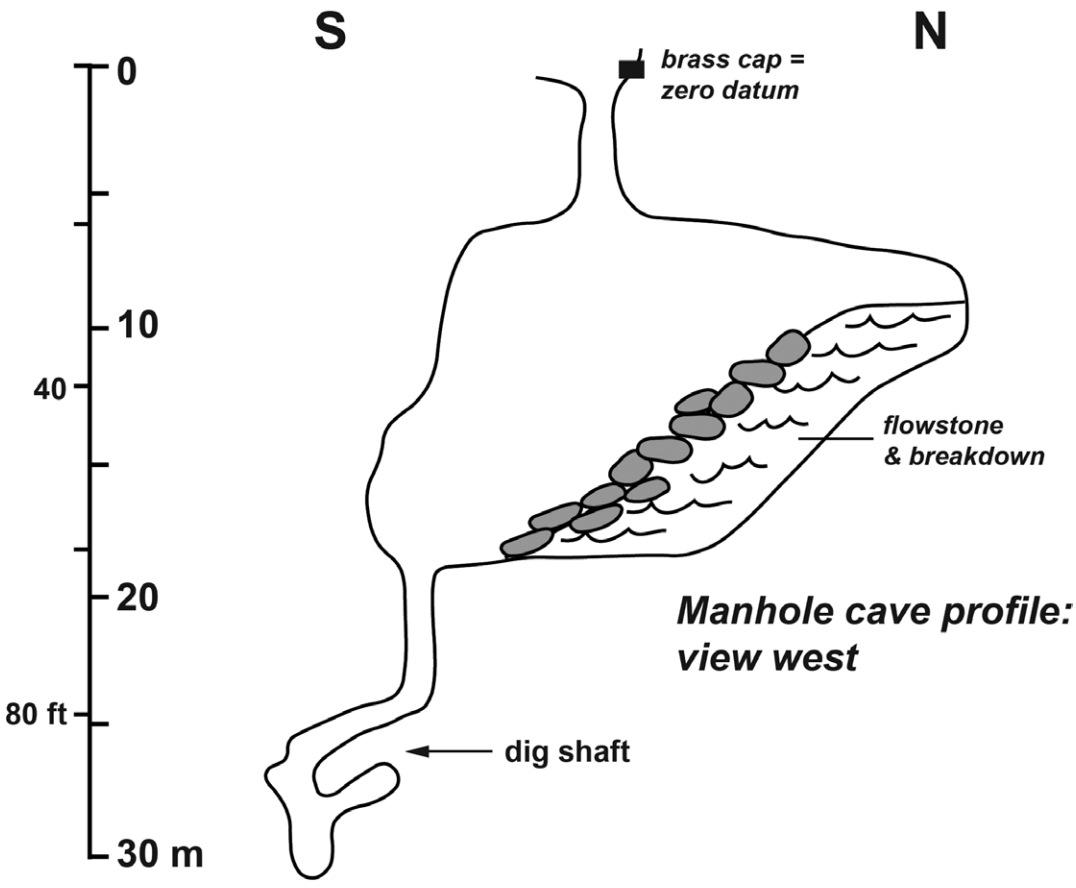

Figure 4. Manhole Cave profile.

Previous Work

In 1992, the Geophysics Group conducted a natural potential (NP) survey over Manhole Cave (Lange, 1992). The survey consisted of a grid of eight lines oriented north-south, with the medial lines passing directly over the mapped cave. Results of the survey show a large positive NP anomaly, south-southeast of the cave entrance. Lange (1992) interpreted this anomaly as indicating the presence of conduits or cave galleries that extended beyond the limits of the survey grid.

In 2004 and 2005, John McLean (2005) conducted 2D electrical resistivity surveys over Manhole Cave, using dipole-dipole arrays with 15 and 30 m electrode spacing. These surveys identified a large, high-resistivity anomaly, presumably caused by an air-filled cavity located about 30 to 60 m south of the Manhole Cave entrance at a depth of about 40 m. One branch of the anomaly passes within 20 m of the cave. Several shallow, high-resistivity zones were also identified in the northeast and southwest parts of the survey area, which McLean suggested might represent small, independent caves or parts of a larger hypogenic cave system. The deep resistivity anomaly generally agrees with the NP anomalies identified by Lange (1992).

Methods

During the winter of 2012-2013, the National Cave and Karst Research Institute (NCKRI), assisted by BLM personnel and volunteers, conducted six 2D resistivity surveys over and adjacent to the entrance to Manhole Cave

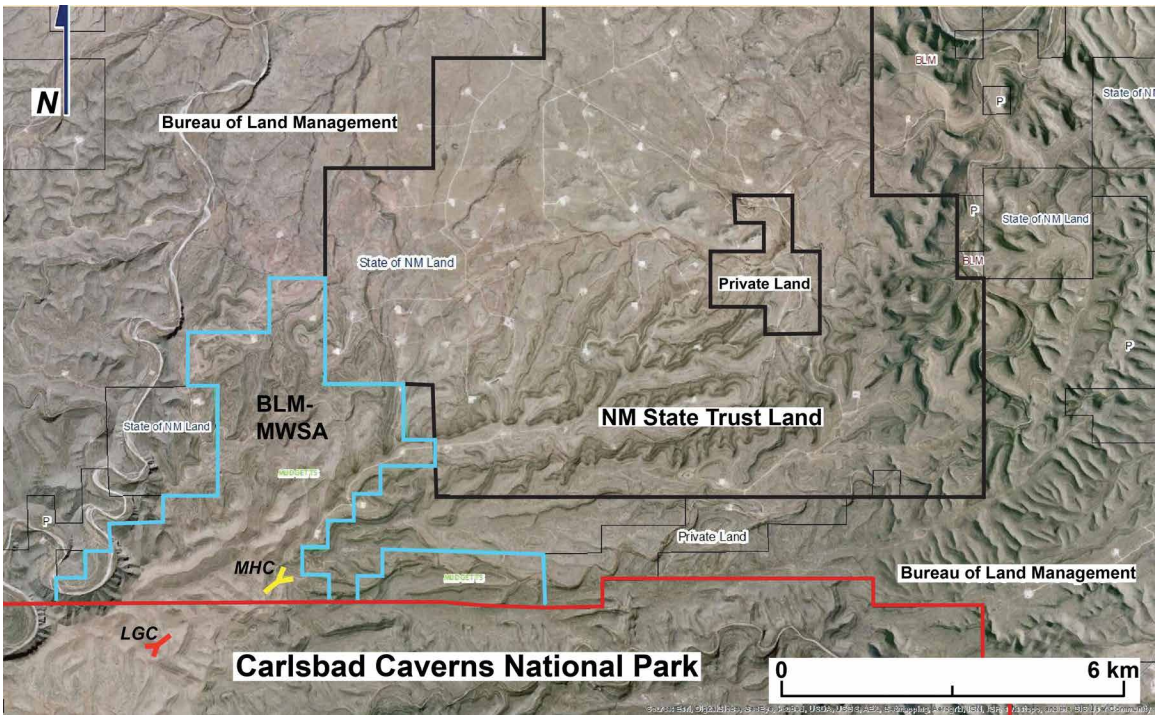

Figure 5. Detail of study area showing surrounding area land status. MWSA = Mudgetts Wilderness Study Area. MHC = Manhole Cave. LGC shows approximate location of Lechuguilla Cave entrance.

(Fig. 6), using 56 electrode dipole-dipole arrays at 6-m electrode spacing for higher resolution than previous resistivity studies. The survey lines were spaced 6 m apart, and data from these surveys were subsequently merged to develop a 2.5D resistivity model using EarthImager 3D™ software.

Electrical resistivity (ER) surveys are a common and effective geophysical method for detection of subsurface voids. The basic operating principle for an ER survey involves generating a direct current between two metal electrodes implanted in the ground, while measuring the ground voltage between two other implanted electrodes. Given the current flow and voltage drop between the electrodes, differences in subsurface electrical resistivity can be determined and mapped. Modern resistivity surveys employ an array of multiple electrodes connected with electrical cable. Over the course of a survey, pairs of electrodes are activated by means of a switchbox and resistivity meter. The depth of investigation for a typical ER survey is approximately one-fifth the length of the array of cable.

Resistivity profiles illustrate vertical and lateral variations in subsurface resistivity. The presence of water, water-saturated soil, or bedrock will strongly affect the results of a resistivity survey. Air-filled caves or air-filled pore space in the vadose zone are easy to detect using the ER method, since air has near-infinite resistivity, in contrast with 10 to 15 orders of magnitude more conductive surrounding bedrock. Previous work (Land and Veni, 2012; Land, 2013) has shown that resistivity surveys are one of the most effective methods for identifying water-filled and air-filled voids due to their electrical contrast with surrounding bedrock.

During the spring of 2015, NCKRI personnel completed a microgravity survey in the vicinity of Manhole Cave, using a Scintrex CG-5 gravity meter with 5-microgal resolution. Because of the highly irregular topography (steep cliffs and deep canyons), detailed terrain corrections had to be applied to the gravity data, instead of the simpler Bouguer slab correction. Gaps in the survey grid (Fig. 7) reflect areas of near-vertical topographic relief, where it was not possible to deploy the gravity meter. High wind conditions introduced additional challenges in data acquisition, since wind-induced vibration required longer measurement times at each station to reduce standard deviations to acceptable levels. Deployment of portable wind barriers met with limited success.

Microgravity surveys are frequently conducted in conjunction with ER surveys. Gravity surveys estimate spatial variations in gravitational acceleration. These changes vary as a function of the density of the shallow subsurface according to Newton's Law (Blakely, 1995). Conceptually, these measurements are made by precisely measuring the force required to balance a mass on a spring. To understand changes in the shallow subsurface, variations in gravitational acceleration from six-to-eight significant figures are required. With advances in materials, mechanical design, and electronic controls, it is now routine to perform these measurements (Hinze et al., 2013).

The Scintrex CG-5 uses a weighted quartz spring, balanced by a capacitor with an internal feedback control system, for raw measurements. The CG-5 reports measurements with internal drift and tidal corrections. During a survey, a reference station is reoccupied periodically to account for additional instrument drift and tares ("jumps" in the gravity

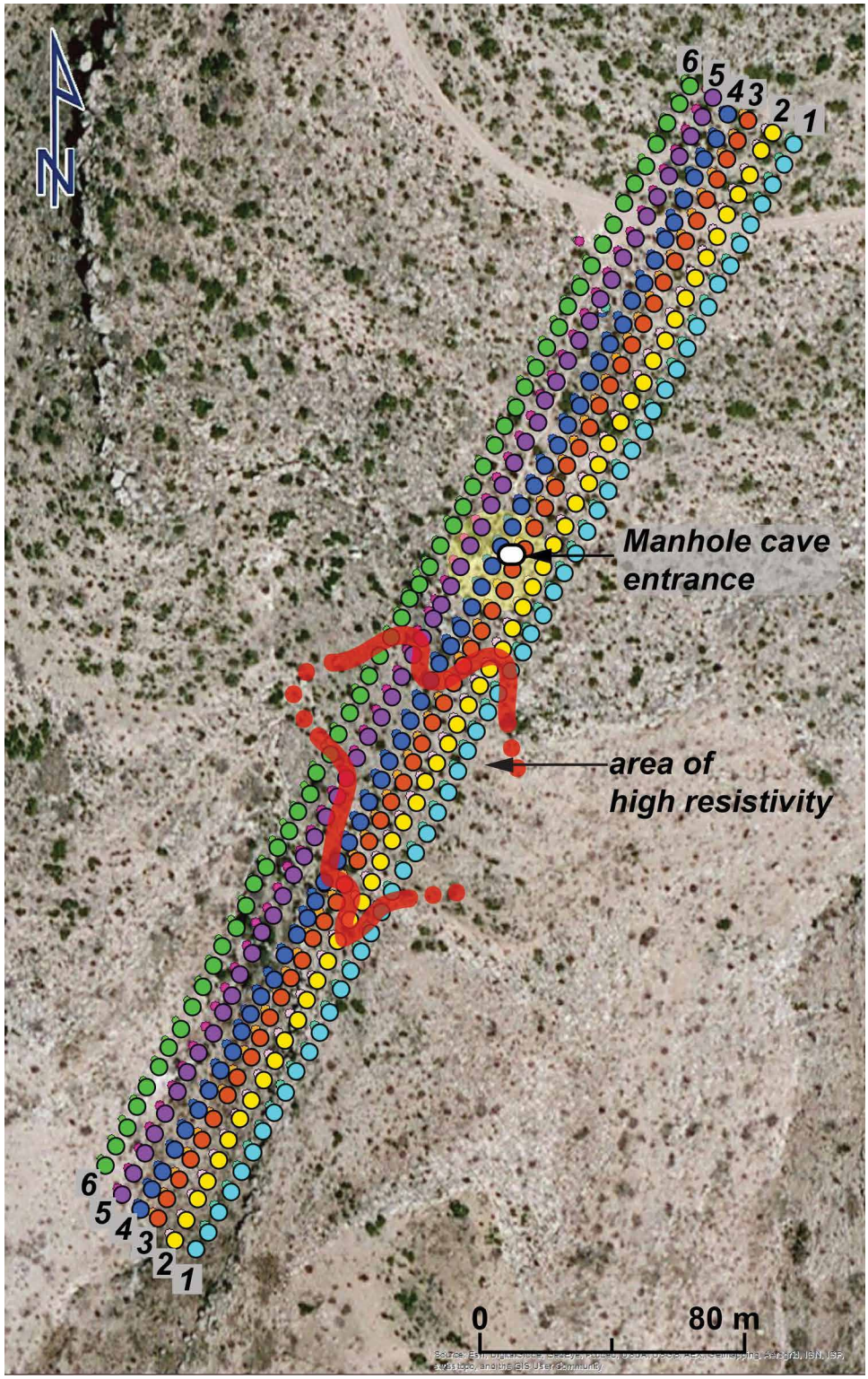

Figure 6. Electrical resistivity survey lines. Individual electrodes are shown by filled circles. White oval shows location of cave entrance. Line numbers reference ER profiles shown in Figure 7. Data sources, BLM, NCKRI, ESRI base maps. Cartography by Andrea K. Goodbar.

readings when the instrument is moved). With the electromechanical system, the internal corrections and the drift corrections with base station reoccupations, the maximum accuracy of the CG-5 is 5 microgal (approximately 10^{-8} m s^{-2}).

To interpret the shallow subsurface structure, a number of corrections must be made to remove other, undesired effects. In many cases, the complete terrain-corrected Bouguer anomaly can be used to understand subsurface structures (Hinze et al., 2013). This anomaly remains after correcting for:

- the attraction of the reference geoid;
- the centrifugal acceleration as a function of latitude, reflecting changes in the shape of the geoid;

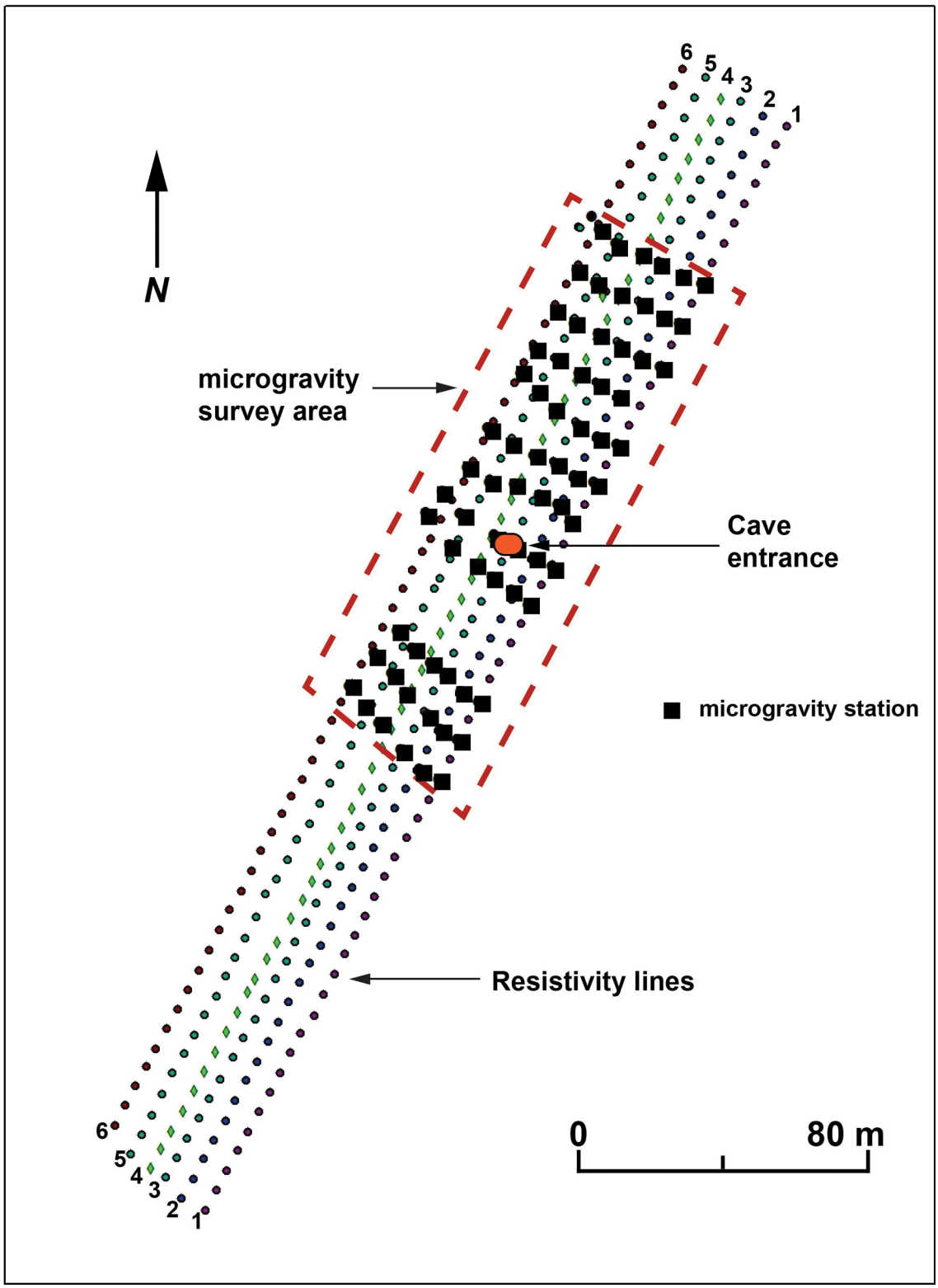

Figure 7. Comparison of resistivity survey lines and microgravity survey area. Orange oval shows location of cave entrance. Line numbers reference ER profiles shown in Figure 8. Black squares show locations of microgravity survey stations. NW-SE gravity survey lines are spaced approximately 12 m apart. Spacing of individual stations within each survey line is approximately 6 m.

- the elevation of the measurement location above the geoid, or free air anomaly;
- earth tides;
- an estimate of the "normal" rock density above the geoid, or slab Bouguer anomaly; and
- effects from variations in terrain around the measurement point (Longman, 1959; Blakely, 1995).

With the CG-5, tidal corrections are made internally using the correction of Longman (1959). We made all of the other corrections, except for the terrain correction, based on site locations, using the simple formula in Blakely (1995). The terrain correction was computed numerically. We assumed a mean density of 2.6 g cm^{-3} for bedrock, and broke the

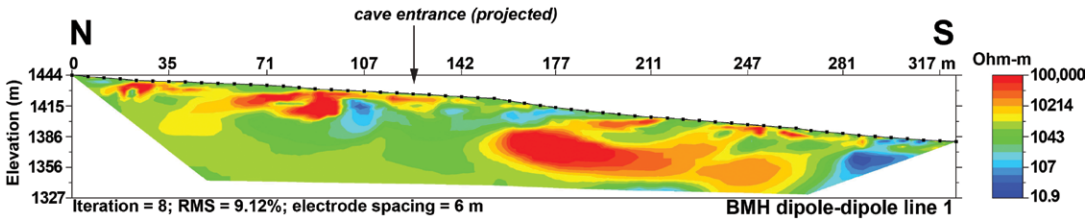

Figure 8a. Manhole Cave ER line 1. Cave entrance is about 13 m east of the survey line, and is projected onto the resistivity profile. Locations of this and subsequent profiles are shown in Fig. 5.

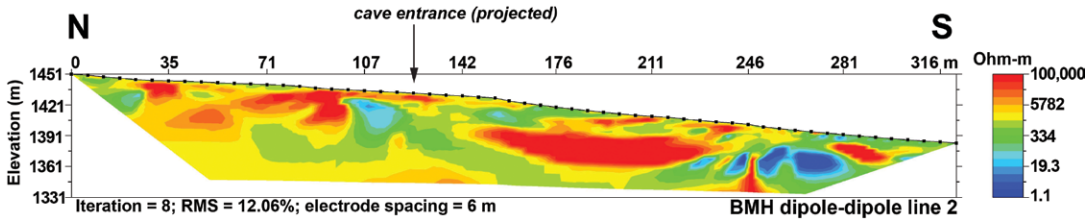

Figure 8b. Manhole Cave ER line 2. Cave entrance is about 7 m east of the survey line, and is projected onto the resistivity profile.

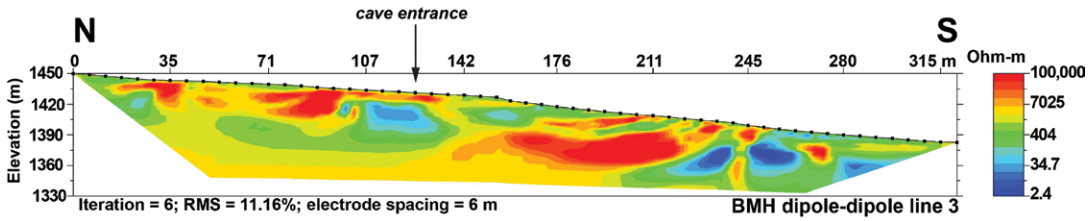

Figure 8c. Manhole Cave ER line 3. This survey line passes less than one m east of the cave entrance. Note the presence of a zone of slightly lower resistivity that connects the Manhole Cave anomaly with the larger resistivity anomaly to the south.

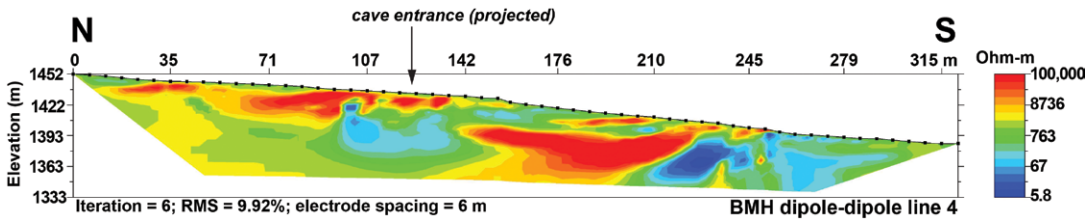

Figure 8d. Manhole Cave ER line 4. Cave entrance is about 5 m west of the survey line, and is projected onto the resistivity profile.

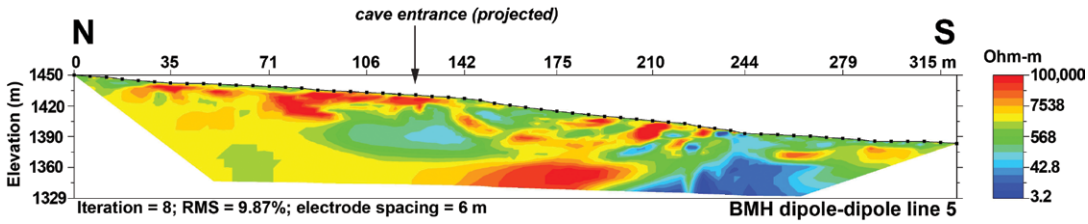

Figure 8e. Manhole Cave ER line 5. Cave entrance is about 11 m west of the survey line, and is projected onto the resistivity profile.

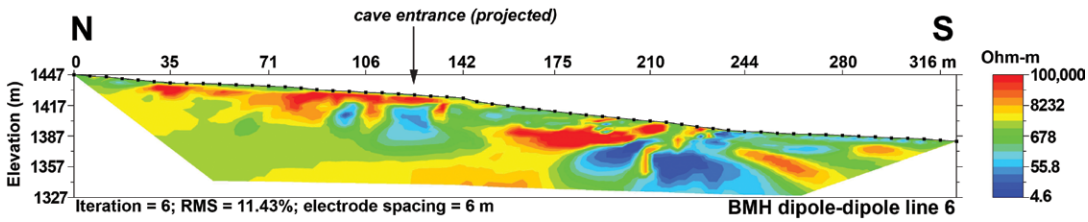

Figure 8f. Manhole Cave ER line 6. Cave entrance is about 17 m west of the survey line, and is projected onto the resistivity profile.

terrain into prisms using a 10 m digital elevation model (DEM). The vertical component of gravitational attraction from each prism is computed for every measurement point out to a radius of 150 km from the measurement point (Blakely, 1995), and then is removed from the measured gravity.

Results and Discussion

Resistivity Surveys

Terrain-corrected electrical resistivity surveys, conducted in the vicinity of Manhole Cave, achieved an investigation depth of approximately 60 to 90 m below ground level (bgl) (Figs. 8a-8f). The ER data are exceptionally noisy, probably the result of high contact resistance in the survey area, which is comprised largely of exposed dolomite bedrock with very thin and patchy soil cover. In many cases, a hammer drill was necessary to drill holes in the bedrock pavement for installation of electrodes. We achieved lower contact resistance in those cases by filling the holes with saltwater before

insertion of the electrodes. We also used a data misfit histogram provided by EarthImager™ software to remove data outliers and reduce the root mean square error during data processing.

ER line 3 passes less than one m east of the cave entrance (Fig. 8c). The entrance to the cave is projected onto the remaining five survey lines. Manhole Cave is shown by a shallow zone of high resistivity, at approximately 125 m on all six profiles. It is worth noting that Manhole Cave's relatively shallow, 20 m, depth results in it not appearing prominently displayed because of the vertical scale of the ER profiles (e.g., line 3, Fig. 8c). Additional high-resistivity anomalies are visible at the northern end of all six lines, at depths ranging from approximately five to 40 m. These anomalies may represent shallow caves or conduits independent of Manhole Cave. McLean (2005) identified similar shallow, resistivity anomalies north of the Manhole Cave entrance.

A distinctive feature of Lines 1 through 4 is a broad zone of high resistivity 35 to 120 m south of the cave entrance. This anomaly is visible on Line 1 at depths ranging from approximately 20 to 65 m bgl (Fig. 8a). Resistivity values range from 10,000 to 100,000 ohm-m, consistent with air-filled, void space in the subsurface. A similar high-resistivity anomaly is present on Line 2 (Fig. 8b) 15 to 55 m bgl, on Line 3 (Fig. 8c) at about 10 to 60 m bgl, and on Line 4 (Fig. 8d) at 10 to 60 m bgl.

The southern end of the large ER anomaly, visible on Lines 1 to 4, appears to curve upward toward the surface, although we encountered no evidence of cave entrances in that area during the ER surveys. Line 3 (Fig. 8c) also shows

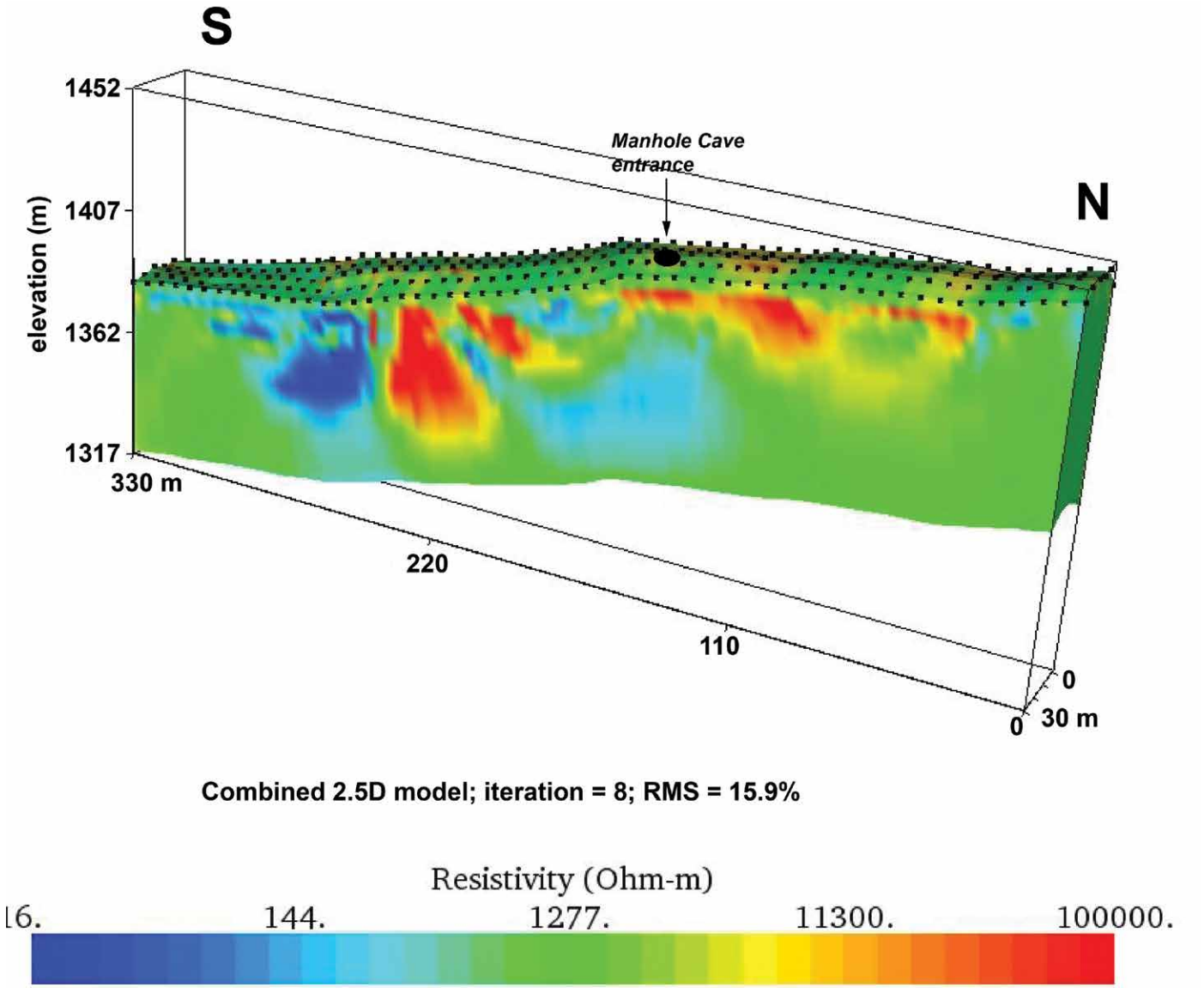

Figure 9. 2.5D model, view to west.

a narrow zone of slightly lower resistivity (about 5000 to 7000 ohm-m) that connects the Manhole Cave resistivity anomaly with the larger anomaly to the south at an angle of approximately 30°. If the resistivity anomaly to the south represents a larger cave, this feature may indicate the presence of a breakdown-choked passage linking the two caves. Smaller high-resistivity anomalies are visible at the south end of Lines 2 and 3, which may represent isolated cavities not connected to the larger void; or they may be the result of data-processing artifacts that are more common at the ends of resistivity profiles, where fewer data points are available for interpretation.

A high-resistivity feature is still present south of Manhole Cave on Line 5 (Fig. 8e) about 55 to 75 m bgl, overlain by several smaller and shallower anomalies. A southern anomaly is also present on Line 6 (Fig. 8f) at a significantly shallower depth, 10 to 30 m bgl, that may correlate with the shallow anomalies observed on Line 5. These features may represent shallower corridors and/or galleries above the main void space south of Manhole Cave. If this interpretation is correct, it suggests that the southern cave system may turn to the southeast, beyond the limits of the ER surveys (Fig. 6).

EarthImager 3D™ software was used to merge the six 2D resistivity lines to create a 2.5D model of the survey area (Fig. 9). The software was then used to generate slices at depth increments of five meters through the 2.5D model (Figs. 10a-10g). The slices terminate at varying distances from the northern end of the model because of steep topography in the survey area, causing the horizontal slices to extend into what would be open air above a broad arroyo.

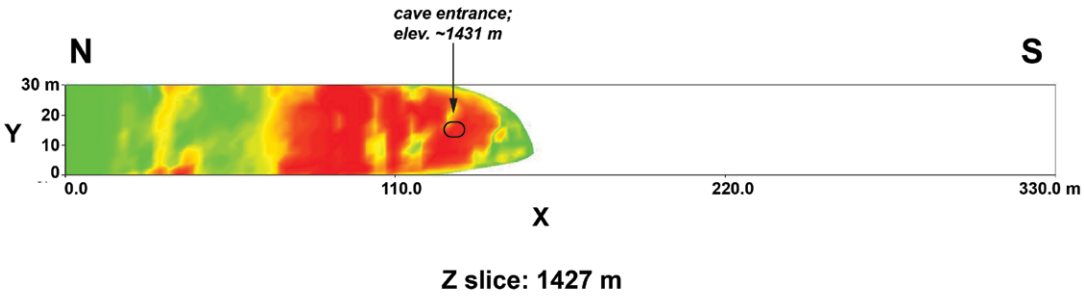

Figure 10a. 1427 m layer, approximately four m bgl at the cave entrance. Steep terrain in the survey area causes this layer (and subsequent ones) to terminate to the south, where the horizontal slice projects into open air above an arroyo. High resistivity in this slice indicates the presence of air-filled void space in Manhole Cave, and additional shallow zones of high resistivity north of the cave entrance.

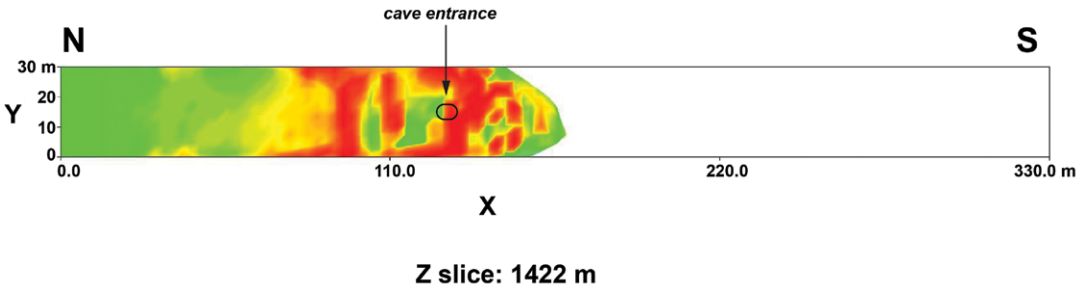

Figure 10b. 1422 m layer. High resistivity results from air-filled void space near the center of Manhole Cave.

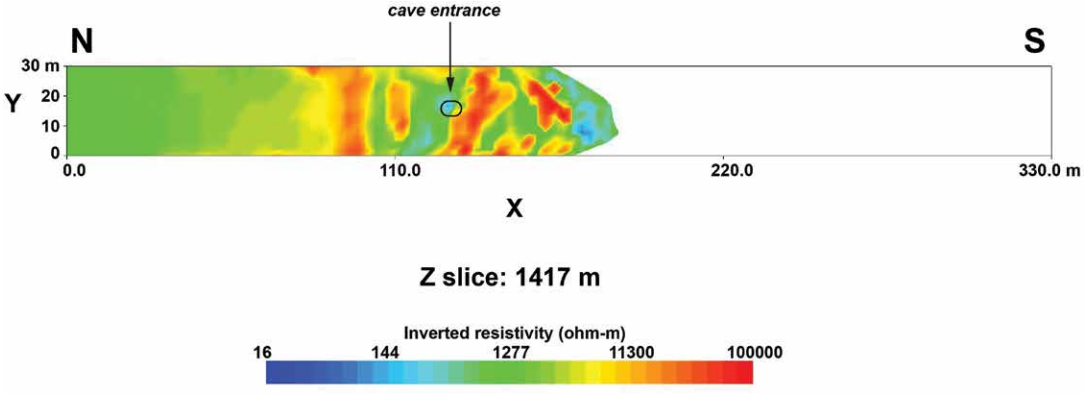

Figure 10c. 1417 m layer, just above the cave floor.

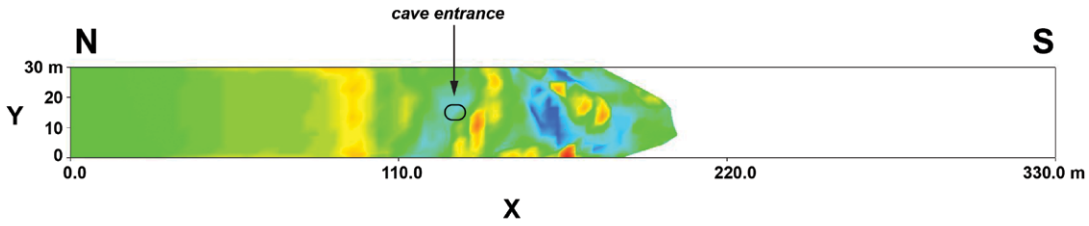

Figure 10d.1412 m layer. The absence of any zones of high resistivity reflect the fact that this slice is below the level of Manhole Cave.

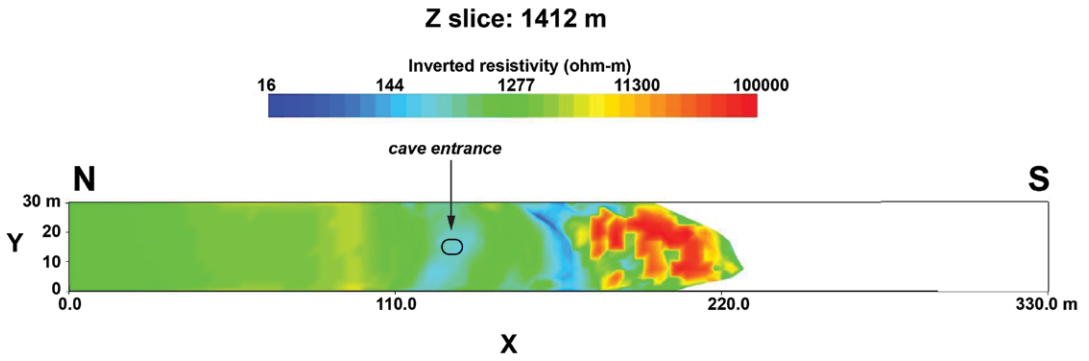

Figure 10e. 1407 m layer. Zones of high resistivity on this and the two subsequent slices show the presence of a large, high-resistivity anomaly observed on 2D Lines 1 through 5.

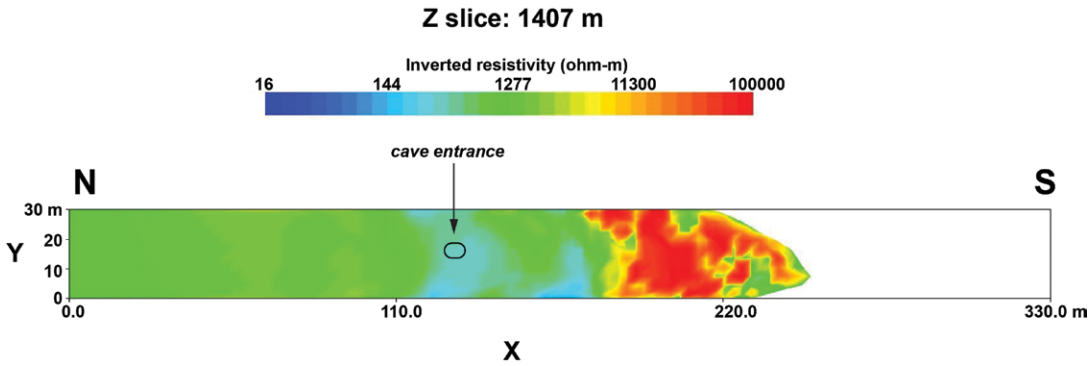

Figure 10f. 1402 m layer.

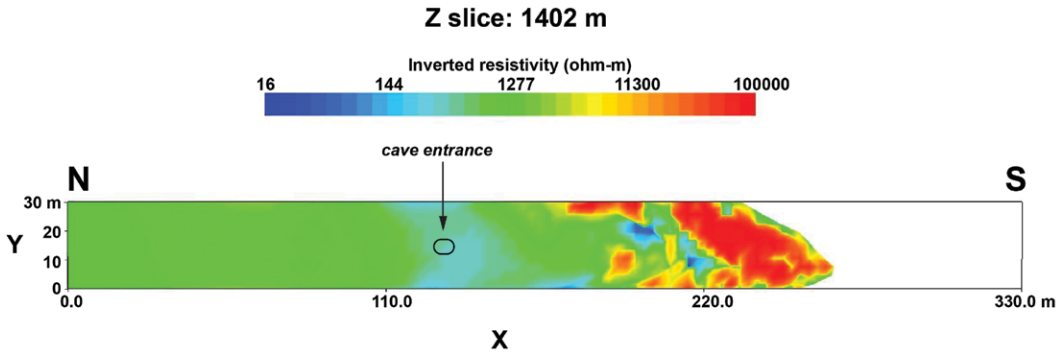

Figure 10g. 1397 m layer.

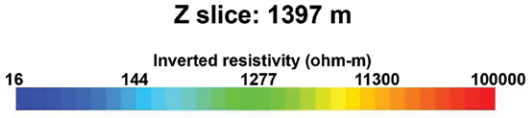

Fig. 10a shows a slice at 1427 m elevation, or about 4 m below the cave entrance. High-resistivity values at the south end of this slice reflect the air-filled void space represented by Manhole Cave. A high resistivity anomaly is also present on the 1422 m layer (Fig. 10b), resulting from the presence of air-filled void space near the center of the cave. These high-resistivity values begin to break up in the 1417 m layer, just above the cave floor (Fig. 10c), and are absent in the 1412 m slice (Fig. 10d), reflecting the absence of any cavities below the cave floor. However, the high-resistivity

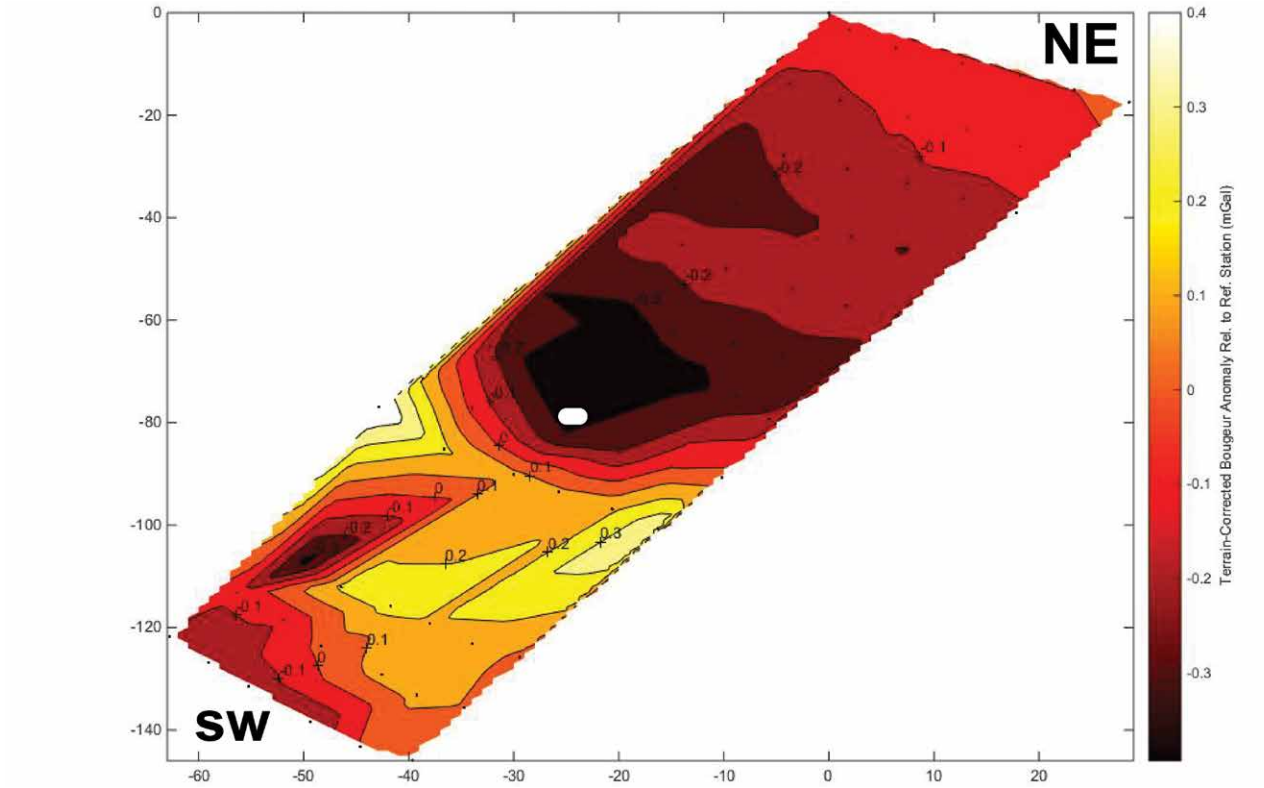

Figure 11. Terrain-corrected Bouguer gravity anomaly map. White oval shows location of cave entrance. Contour interval = 0.1 mg.

anomaly to the south of Manhole Cave is clearly indicated on the three slices at 1397, 1402, and 1407 m depth (Figs. 10e, 10f, and 10g).

Microgravity surveys

Microgravity data were collected at 72 stations in the vicinity of Manhole Cave using a Scintrex CG-5 gravity meter (Fig. 7). A complete Bouguer gravity correction was applied to the data to account for the extreme topography of the survey area. Microgravity survey results clearly indicate a negative gravity anomaly in the vicinity of Manhole Cave. Another gravity low is visible south-southwest of the cave entrance (Fig. 11). The gravity data are consistent with resistivity surveys, suggesting the presence of a large cave system south of Manhole Cave. However, the more southerly gravity low is only defined by two stations. The somewhat ambiguous character of the microgravity data, in contrast with the resistivity results, may indicate the presence of a large, breakdown-filled passage, as opposed to open void space, which would produce a high electrical resistivity signal, but a less clearly-defined microgravity anomaly.

An alternative explanation for the smaller anomaly to the south is that the southern cave is deeper than Manhole Cave, and is not entirely surrounded by the gravity survey. Gravity anomalies integrate subsurface density distribution weighted by $1/r^2$, thus density variations at greater depths will have a smaller surface manifestation. In general, deeper subsurface anomalies have a smaller and smoother signature than shallower anomalies. Complicating the interpretation, the gravity survey does not surround the entire negative anomaly, further smoothing the image.

The absence of a gravity anomaly in the southeast corner of the gravity survey, where ER data indicate subsurface void space (Fig. 8A), may be due to inadequacies in the 10 m DEM-based terrain correction, which may simply not have resolved the ruggedness of the terrain. Less than ideal field conditions (steep cliffs, deep canyons, and strong winds) may have also contributed to the ambiguous gravity results.

Conclusions

Resistivity surveys conducted over Manhole Cave show a laterally-extensive, high-resistivity anomaly approximately 35-120 m south-southwest of the cave entrance. Given the geologic setting, the high-resistivity signal identified on the ER lines probably indicates the presence of a large, air-filled cavity 25 to 30 m below ground level. Microgravity survey results are less conclusive, but consistent with analysis of the resistivity data. The results of these geophysical surveys suggest that additional digging should eventually result in intersection with deeper cave passages southwest of Manhole Cave.

The entrance to Manhole Cave is located less than 300 m north of the Carlsbad Caverns National Park boundary. Lechuguilla Cave is located within the Park, but at its closest point Lechuguilla is only 300 m (map distance) from BLM administered land. If a connection is ultimately established between Manhole and Lechuguilla caves, it will create a unique situation, wherein a world-class scientific resource is subject to dual management by two federal agencies with different agendas and management styles. BLM and NPS personnel have already discussed joint management of this resource, but as one BLM resource manager has observed, the devil is in the details.

References

Blakely, R.J., 1995, Potential theory in gravity and magnetic applications: New York (NY): Cambridge University Press, 441 p. https://doi.org/10.1017/CBO9780511549816.

Bretz, J.H., 1949, Carlsbad Caverns and other caves of the Guadalupe Block, New Mexico: Journal of Geology 57, no. 5, p. 447−463. https://doi.org/10.1086/625660.

Gulden, B., 2016a, USA deepest caves: National Speleological Society Geo 2. http://www.caverbob.com/usadeep.htm. [accessed February 7, 2017]

Gulden, B., 2016b, World's longest caves: National Speleological Society Geo 2. http://www.caverbob.com/wlong.htm. [accessed February 7, 2017]

Hayes, P.T., 1964, Geology of the Guadalupe Mountains, New Mexico: U.S. Geological Survey Professional Paper, p. 446.

Hill, C.A., 1987, Geology of Carlsbad Cavern and other caves in the Guadalupe Mountains, New Mexico and Texas: New Mexico Bureau of Mines and Mineral Resources Bulletin, p. 117.

Hinze, W.J., von Frese, R.R.B., and Saad, A.H., 2013, Gravity and magnetic exploration: Principles, practices, and applications: New York, NY, Cambridge University Press. https://doi.org/10.1017/CBO9780511843129.

Hiss, W.L., 1975a, Stratigraphy and ground-water hydrology of the Capitan Aquifer, southeastern New Mexico and western Texas: [Ph.D. dissertation]. Boulder, Colo.: University of Colorado, 396 p.

Hiss, W.L., 1975b, Chloride ion concentration in ground water in Permian Guadalupian rocks, southeast New Mexico and west Texas: New Mexico Bureau of Mines and Mineral Resources, Resource Map 4.

Kelley, V.C., 1971, Geology of the Pecos country, southeastern New Mexico: New Mexico Bureau of Mines and Mineral Resources, Memoir 24.

King, P.B., 1948, Geology of the southern Guadalupe Mountains, Texas. U.S.: Geological Survey Professional Paper 215.

Klimchouk, A., 2007, Hypogene speleogenesis: Hydrogeological and morphogenetic perspective: National Cave and Karst Research Institute Special Paper no. 1.

Land, L., 2003, Regional geology of the Pecos Country, *in* Johnson, P.S., Land, L., Price, L.G., Titus, F., eds., Water Resources of the Lower Pecos Region, New Mexico: Science, Policy, and a Look to the Future: New Mexico Bureau of Geology and Mineral Resources, 2003 New Mexico Decision Makers Guidebook, p. 9−13.

Land,.L, Veni, G., 2012, Electrical resistivity surveys of anthropogenic karst phenomena, southeastern New Mexico: New Mexico Geology 34, no. 4, p. 117−125.

Land, L., 2013, Evaporite karst in the Permian Basin region of west Texas and southeastern New Mexico: The human impact, *in* Land, L., Doctor, D.H., Stephenson, J.B., eds., Proceedings of the Thirteenth Multidisciplinary Conference on Sinkholes and the Engineering and Environmental Impact of Karst, Carlsbad, New Mexico: National Cave and Karst Research Institute Symposium 2. Carlsbad, NM, National Cave and Karst Research Institute, p. 113−121. https://doi.org/10.5038/9780979542275.1119.

Lange, A.L., 1992, Natural-potential survey over Big Manhole Cave, Eddy County, New Mexico: Unpublished report submitted to U.S. Bureau of Land Management, Carlsbad, New Mexico, 13 April, 1992.

Longman, I.M., 1959, Formulas for computing the tidal accelerations due to the moon and the sun: Journal of Geophysical Research 64, p. 2351−2355. https://doi.org/10.1029/JZ064i012p02351.

McLean, J.S., 2005, Earth resistivity measurements at Big Manhole Cave: Southwest Region, National Speleological Society, Winter Technical Meeting, Carlsbad, New Mexico, December 3rd, 2005. Abstract.

Northup, D.E., Dahm, C.N., Melim, L.A., Spilde, M.N., Crossey, L.J., Lavoie, K.H., Mallory, L.M., Boston, P.J., Cunningham, K.I., and Barns, S.M., 2000, Evidence for geomicrobiological interactions in Guadalupe caves: Journal of Cave and Karst Studies, v. 62, no. 2, p. 80−90.

Palmer, A.N. and Palmer, M.V., 2000, Hydrochemical interpretation of cave patterns in the Guadalupe Mountains, New Mexico. Journal of Cave and Karst Studies, v. 62, no. 2, p. 91−108.

D. Vardeh, J. Woodhouse, B. Neilan. Microbial diversity of speleothems in two southeast Australian limestone cave arches. *Journal of Cave and Karst Studies*, v. 80, no. 3, p. 121-132. DOI:10.4311/2017MB0119

MICROBIAL DIVERSITY OF SPELEOTHEMS IN TWO SOUTHEAST AUSTRALIAN LIMESTONE CAVE ARCHES

David P. Vardeh[1], Jason N. Woodhouse[1,2], Brett A. Neilan[1,3 C]

Abstract

Peculiar cave structures, nicknamed lobsters, and shaped by drip water, wind, aeolian particles and microbial biofilms, are described from cave entrance arches at Jenolan and Wombeyan caves in southeast Australia. Subaerial biofilms on rock surfaces support complex microbial assemblages adapted to temperature, desiccation, and low irradiance stress. The community composition of active and inactive speleothems was elucidated by next generation sequencing. Active biofilms showed high abundances of cyanobacterial taxa, morphologically and phylogenetically belonging to the genera *Chroococcidiopsis* and *Gloeocapsa,* representing an endolithic lifestyle in desiccated and low light conditions. Significant differences were found between caves and between actively accreting and inactive and weathered structures. Functional taxa putatively occupying the same niches were found on active structures in both locations. A temporal succession is proposed, with dominance shifting from *Chroococcales* to *Actinomycetales* and highly desiccation-resistant and oligotrophic *Rubrobacterales* with decreasing water availability.

Introduction

Subaerial biofilms occupy the realm between air and rock surface, which is an ancient and hostile niche. Under favorable conditions, complex and less tolerant eukaryotic taxa, such as algae and fungi, dominate subaerial biofilms. However, under adverse conditions, prokaryotic taxa remain the only microorganisms capable of enduring the extreme environmental conditions characterized by inhospitable habitats like deserts and caves (Gorbushina, 2007). Colonization of a rock substrate is initiated by photosynthetic organisms that enrich the surface and provide a base for heterotrophic taxa (Crispim and Gaylarde, 2005). In subaerial habitats, a constant, close interplay between lithosphere, atmosphere, and colonizing microbes has a direct impact on the biogeochemistry within the biofilm and the underlying minerals (Warscheid and Braams, 2000; Buedel et al., 2004).

The organisms that inhabit subaerial biofilms present on cave structures, are influenced by a series of factors including light availability, the abundance and nature of mineral-enriched drip water, and the physical structure of the rock (Gorbushina, 2007). Substrate micro-topography influences niche availability (Golubic et al., 1981) and colonization speed, with smooth surfaces harder to colonize and favoring small coccoid organisms, such as cyanobacteria of the genus *Gloeocapsa*. Rougher surfaces with declivities, protecting organisms from wind, solar irradiation, or predation, are colonized faster and provide additional microniches (Miller et al., 2006) resulting in a greater abundance and diversity of organismal shape and metabolism (Gorbushina, 2007).

Cave entrances, as opposed to hypogeal environments, are strongly influenced by surface, physical parameters, including fluctuations in temperature, desiccation and light restriction. The extracellular polymeric substances (EPS) that envelop cell assemblages in microbial mats provide protection from these fluctuations (Kemmling et al., 2004) and govern mineral precipitation (Tourney and Ngwenya, 2009).

Lobster-type speleothems are unique, elongated, narrow structures present within cave entrances, which extend toward the main direction of wind in the cave arch systems (James et al., 1982; Cox et al., 1989b; Lundberg and McFarlane, 2011). Two cave arches in the Blue Mountains area of New South Wales, Australia, are the sites of the first description of this morphology, namely Nettle Cave in Jenolan Karst Conservation Reserve and Victoria Arch in Wombeyan Karst Conservation Reserve (Cox, 1984; James et al., 1982). Their nickname, lobsters or craybacks, originates from the crenulations and elevated ridges across the narrow axis that give the speleothems the appearance of a segmented, crustacean carapace (Cox et al., 1989a). Due to influx of allochthonous matter into the open caves, a plausible explanation for the formation of the lobster ridges is the introduction of particulate irregularities on the surface. Once a particle becomes attached to the surface, it creates a shaded area that phototrophic organisms will avoid, thus causing increased calcification and, ultimately, a ridge in the lighter part (Cox et al., 1989b). The width of the structures is at least partly determined by the height of the cave roof, whereby higher travel distance of the drops from above result in larger splash diameters and wider structures.

Cox and co-workers proposed that the growth of the lobsters is partially biogenic. They also confirmed the presence of *Gloeocapsa* spp. (Cox et al., 1989b), and *Chroococcales* have been shown to contribute to calcification in accreted

[1]School of Biotechnology and Biomolecular Sciences and the Australian Centre for Astrobiology, University of New South Wales (UNSW), Sydney, Australia
[2] Leibnitz-Institute of Freshwater Ecology and Inland Fisheries
[3] School of Environmental and Life Sciences, University of Newcastle, Australia
[C] Corresponding author: brett.neilan@newcastle.edu.au

structures, formed by the action of microbes, i.e. microbialites (Saghaï et al., 2015). Extremely little is known about the microbial communities of cave speleothems and there are only a handful of reports worldwide on the peculiar morphology of crayback or lobster stalagmites (Mulec et al., 2007; Lundberg and McFarlane, 2011). Purely physical, carbonate precipitation, driven by evaporation of the water film on the speleothem surface, usually leads to randomly structured precipitate (Hill et al., 1997). In contrast, cyanobacterial photosynthesis induces smooth, laminar precipitation. Seasonality contributes to layering within the structure, with solid or coralline layers deposited in wet seasons and allochthonous layers of dust, grains, and animal matter deposited in dry seasons (Cox et al., 1989b). Decreased, wind-driven evaporation of the scarce water conveys an advantage to organisms settling there (Lundberg and McFarlane, 2011).

Here, we characterize, for the first time, the microbial assemblage, in regard to composition and putative ecological roles, of lobster speleothems in cave arches. We address the extent of any heterogeneity that might occur between sites within a cave system, as well as between cave systems. Also, a sampling regime was enacted to shed light on the succession of microbial communities as speleothems transition from active to the inactive and weathered form over time.

Materials and Methods

Site description and sampling

Samples were collected from Nettle Cave (Jenolan Caves, Blue Mountains, NSW, 33.8206° S, 150.0214° E) in March 2013 and from Victoria Arch (Wombeyan Caves, NSW, 34.3167° S, 149.9833° E) in April 2013. Nettle Cave is the upper part of an 80 m high and 40 m wide tunnel called Devils Coachhouse that runs in a southwest-northeast direction. Almost all speleothems are located on this upper level, which receives light mainly from the smaller, narrow Nettle Cave exit, a roof hole, and to some extent, the large Devils Coachhouse opening (Cox et al., 1989a). Site 1 (sample J1) is an old, weathered and dry lobster (Fig. 1B) with white and flaking surface, and it is about 4 m away from the walkway to the right. This site, and all other sites, is located about 20 m from the Nettle cave exit. Site 2 (J2 and J3) is a small blue-green, extremely faint, ridged lobster at the edge of a crevice on the left side of the walkway. It is located directly beneath an old steel cable. Site 3 (Fig. 1A) is a well-ridged speleothem with blue-green surface (J4 and J5), as well as coarse, dry, green sides (J6 and J7). It is located 2 m behind Site 2. Site 4 (J8 and J9) is an elongate, only faintly blue-green speleothem underneath the walkway in the vicinity of sites 2 and 3. It was partially removed to allow construction of the walkway. Rock (J10) and soil (J11) samples were collected from between sites.

Victoria Arch at Wombeyan has roughly the same dimensions as Nettle Cave and runs in a north-south direction (Osborne, 1993). As opposed to Nettle Cave, it is at ground level. Site 1 (W1 and W2) is a conspicuous, large (1 m high) lobster with blue-green coloration 10 m from the entrance on the left side. Site 2 (W3−W5) is an elongate lobster 12 m further into the cave and directly to the right of the path. It is ridged and deep blue-green with light-green growth on the sides. Site 3 (W6 and W7) is a soft, deep grey-green flowstone, 1 m high and 3 m wide and about 10 m from the opposite cave opening. Site 4 (W8) is a weathered, chipped and white lobster close to site 2. Rock (W9) and soil (W10) samples are adjacent to site 4. Specimens were drilled to a depth of about 5 mm using a hand-held, battery-powered drill, equipped with a 20 mm diamond-coated, circular drill bit which was ethanol-sterilized between samples. Samples were kept at 4 °C for 1−2 days in sterile containers prior to DNA extraction. As of 2015, sampling core holes were still clearly visible.

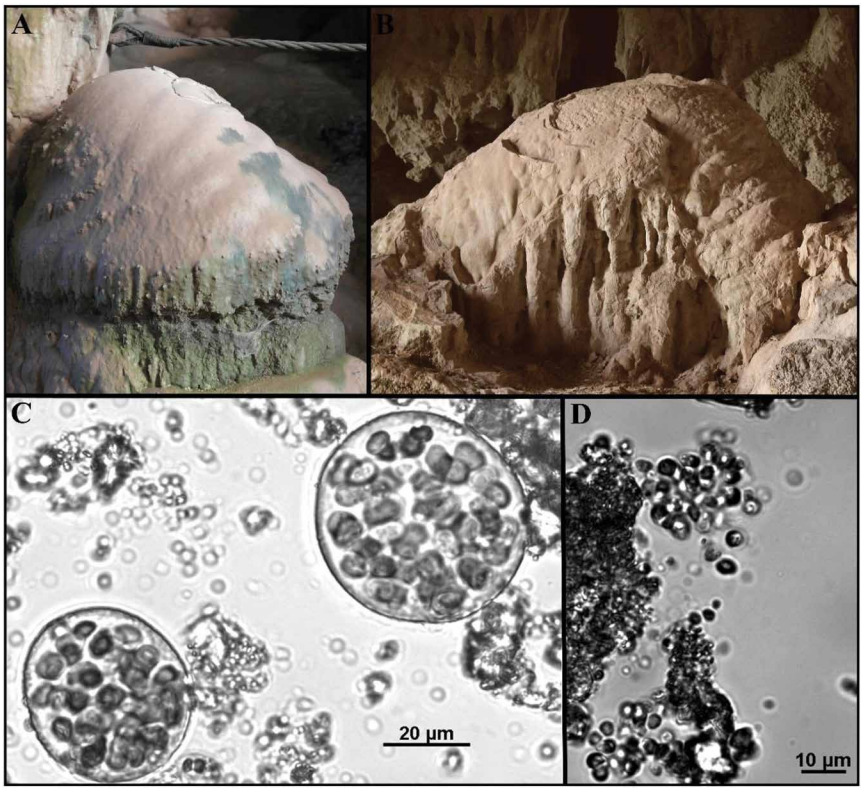

Figure 1. Representative active blue-green (A) and inactive weathered (B) Lobster speleothems from Jenolan Caves and light microscopy pictures of *Chroococcidiopsis-Gloeocapsa* morphologies with (C) and without (D) gelatinous envelopes.

Illuminance at the Jenolan lobster site was previously measured at low values of

50−100 lux on a summer midday, depending on exact location and positioning of the structure (Cox et al. 1989a). No measurements from the Wombeyan site are available, but due to the similarity in cave shape and speleothem positioning, a similar light intensity is presumed. Conditions at Jenolan Caves (792 m above sea level, station number 63036) were unusually wet in the weeks preceding, with February rainfall being registered at about three times the mean for that month (Bureau of Meteorology, 2013a). In contrast, conditions had been unusually dry at Wombeyan Caves (580 m above sea level, station no 63093) before sampling. Only 29.6 mm of rain fell in the month leading up to the sampling date and March and April were much drier than average (Bureau of Meteorology, 2013b). Both caves are open to the public and receive high numbers of visitors year-round, but most speleothem structures are not directly accessible. As this is an exploratory study covering large sampling areas, small-scale differences in environmental factors are likely, but these will need to be investigated using a narrower approach that includes more physical measurements. Wind, exposure to outside contamination and annual temperature fluctuations are comparable across all samples for the scope of this study. Average monthly temperatures are between 0.5 °C and 26 °C in both locations.

DNA extraction, amplification and sequencing

For each core, 400−500 mg of sample was ground coarsely and sample replicates from the same specimen and the same appearance were pooled. A FastDNA Spin Kit for Soil was used according to manufacturer's instructions (MP Bio). The final buffer was left on the column at 55 °C to enhance elution and re-centrifuged over the column once to increase yield. DNA was kept at −20 °C. DNA concentration and quality were measured using a NanoDropTM 1000 Spectrophotometer (Thermo Fisher Scientific). DNA concentrations ranged from 10-40 ng μL^{-1} at 260/280-absorbance ratios between 1.59 and 2.02.

PCR for the V1−V3 region of the 16S rRNA gene was performed using oligonucleotides 27F and 519R, each featuring a unique sample specific 8 nt multiplex identifier (MID) tag (Caporaso et al., 2012). A 19.5 µL master mix containing 1× Tris-HCl buffer (Bioline), 1 mM $MgCl_2$, 1 mM BSA, 1.5 mM dNTPs and 0.3 U BioTaq DNA Polymerase (Bioline), and 0.1 U *Pfu* proofreading DNA Polymerase (Promega) was pipetted into a sterile PCR tube along with 50 pmol forward primer, 50 pmol reverse primer, and 5−20 ng of sample DNA. PCR cycling was performed as follows: Initial denaturing for 5 min at 95 °C, 30 cycles of denaturation for 15 s at 95 °C, annealing for 30 s at 55 °C, elongation for 60 s at 68 °C, and a final elongation step for 7 min at 72 °C. Single-stranded DNA was digested at 37 °C for 15 min by the addition of 0.05 U Exonuclease I and 0.25 U Shrimp Alkaline Phosphatase (New England Biolabs). The enzymes were inactivated at 80 °C for 20 min. PCR products (~530 bp) were confirmed by gel electrophoresis on a 1 % agarose gel and then normalised and pooled using a SequalPrep Normalisation Plate (Thermo Fisher Scientific).

Concentration and quality of the pooled library were checked with Qubit and the library size confirmed using the Agilent 2200 TapeStation. The Agencourt AMPure XP bead clean-up kit (Beckman Coulter) was used on the pool to reduce primer dimers. The libraries were sequenced at the Ramaciotti Centre for Genomics, UNSW, Australia, on an Illumina MiSeq instrument using a MiSeq Reagent Kit v3 with a 2 × 300 bp run format and default run parameters including adaptor trimming.

Bioinformatic analysis

Only the 27F-derived sequences were used for taxonomic assignment, as it ensures comparable taxonomic assignment, while reducing an overestimation of operational taxonomic unit (OTU) richness due to progressively deteriorating sequencing quality (Caporaso et al., 2012). The following analysis was performed using the Mothur v. 1.36.0 package (Schloss et al., 2009). Sequence files were trimmed using a scanning window average (window size = 50, minimum quality score = 30). Sequences that were shorter than 270 bp in length, contained ambiguous bases, or homopolymers of length greater than 8 bp were removed. Unique sequences were aligned with the SILVA database (version 102). Sequences were pre-clustered allowing for a 1 bp mismatch per 100 bp and Uchime, as implemented in Mothur, was used to identify and remove chimeric sequences (Edgar et al., 2011).

Taxonomic annotation was first done with the RDP trainset9_032012 (Cole et al., 2013) reference and lineages, classified as mitochondria, Archaea, Eukarya, or unknown were removed. Sequences classified as chloroplast were retained to ensure that all cyanobacterial sequences were retained. The second taxonomic annotation was done using the GreenGenes 13_8_99 reference file with cut-off 0.8. Subsampling was performed at a level of 9351, consistent with the lowest, observed sampling depth, resulting in 196,371 sequences in total. Of these, 9,508 unique sequences were clustered into OTUs using average neighbor clustering and a distance threshold of 0.03. Taxonomy of each OTU was assigned using a consensus method and a cut-off of 0.8. A total of 1089 OTUs representing 17,136 sequences could not be classified beyond the level of kingdom.

Phylogenetic analysis

A phylogenetic tree was constructed by obtaining representatives for each OTU containing at least 10 sequences that annotated to the orders *Nostocales* or *Chroococcales*, in addition to any unclassified cyanobacterial sequences. For each OTU representative, the corresponding 519R sequence was recovered and the sequences assembled to form

~450 bp sequences. Reference sequences from NCBI GenBank nucleotide database (accessed June 2015) and OTU sequences were aligned in the BioEdit version 7.2.5. (Hall, 1999) with implementation of the Clustal W (Thompson et al., 1994) multiple alignment algorithm. Phylogenetic inference of the resulting alignment was made with PhyML (Guindon et al., 2010) using a gamma time-reversible model and 1,000 bootstrap replicates. The resulting tree was visualized with Dendroscope version 3.2.10 (Huson and Scornavacca, 2012).

Statistical analysis

Richness, diversity (inverse Simpson index) and evenness (log-based Shannon index) of the microbial community were calculated from the OTU matrix using Primer 6 (version 6.1.11, Primer-E Ltd., UK). Cluster analysis was performed on a Bray-Curtis similarity resemblance matrix derived from the square root transformed OTU matrix. PERMANOVA was performed using the Primer 6 PERMANOVA+ version 1.0.1 (http://www.primer-e.com/permanova.htm) add-on using location (Jenolan and Wombeyan caves) and group (Table 1) as fixed factors.

Indicator species analysis was performed to identify OTUs representative of each group using the Indicator Species package in R (de Cáceres et al., 2010). For inclusion in this analysis, OTUs were required to contribute at least 1 % to the total sequence number in a given sample. A correlation table was constructed featuring each OTU, the site (or sites) that it was an indicator of, the indicator value, and the observed p-value (see Supplementary Table 1). Visualisation of the relationships between indicator OTUs and the morphotypes as an indicator value, edge-weighted, spring-embedded network was performed using Cytoscape version 3.2.1 (http://www.cytoscape.org/index.html).

Results

Microbial composition of cave entrance subaerial biofilms

The most abundant taxa found on the active speleothems in Jenolan (groups 2 and 3) were *Cyanobacteria* (28.6 ± 21.3 %), *Actinobacteria* (25.5 ± 10.2 %), unclassified *Bacteria* (20.7 ± 9.7 %), *Alphaproteobacteria* (11.8 ± 9.8 %), and *Acidobacteria* (6.1 ± 2.3 %). The inactive speleothem in Jenolan (group 1) was dominated by *Actinobacteria* (69.3 ± 11.2 %), followed by unclassified *Bacteria* (10.2 ± 9.8 %) and *Alphaproteobacteria* (6.4 ± 2.8 %). The most abundant taxa in active Wombeyan biofilms (groups 6−8) were *Acidobacteria* (20.2 ± 11.4 %), *Actinobacteria* (21.3 ± 8.9 %), *Cyanobacteria* (19.1 ± 15.8 %), *Alphaproteobacteria* (7.3 ± 4 %), and unclassified *Bacteria* (5.5 ± 2 %). Weathered speleothems and rock controls (group 4) were dominated by *Actinobacteria* (79.9 ± 2.8 %), followed by *Cyanobacteria* (3.1 ± 4.4 %), most of which were identified as chloroplasts and *Alphaproteobacteria* (1.7 ± 0.9 %). Soil communities (group 5) contained *Actinobacteria* (44.3 ± 6.5 %), *Proteobacteria* (27.4 ± 1.2 %), unclassified *Bacteria* (3 ± 1.6 %), and *Cyanobacteria* (2 ± 2.1 %). Of the 14.1 ± 17.2 % of sequences annotated as belonging to the phylum *Cyanobacteria*, the major groups were *Chroococcales* (6 ± 9.4 %), unclassified *Cyanobacteria* (5 ± 9.5 %), and chloroplast sequences (2.1 ± 2.9 %).

Bray-Curtis similarities of square root transformed OTU abundances revealed several distinct groups of samples that are less than 30 % similar to one another (Fig. 2). These groups, consistent with the morphological appearance of the subaerial biofilms, are subsequently annotated as: blue-green mat (two per cave), green mat (Jenolan), grey-green flowstone (Wombeyan), soil controls, and a group containing old inactive speleothems and bare rock controls (shared by both caves, Table 1). Except for one instance, these groups coincided with the respective speleothem specimen from which they were sampled. The exception is sample J3 from the subsurface layer (ca 2−5 mm) of one active speleothem in Jenolan sharing about 40 % OTU similarity with the cores from site 4, a pale lobster with only faint hues of blue-green coloration.

Table 1. Groups from Jenolan and Wombeyan samples identified from cluster analysis and morphological description of sampling sites.

Samples	Group	Description
J3, J8, J9	1	Subsurface sample from blue-green speleothem (J3) and samples from inactive faint blue-green speleothem
J2, J4, J5	2	Blue-green speleothem
J6, J7	3	Dry green coarse mat on vertical side of group 2 speleothem
J1, J10, W8, W9	4	Old weathered speleothems without any visible mat (J1, W8) and bare non-speleothem rock (J10, W9)
J11, W10	5	Soil
W1, W2	6	Blue-green speleothem at cave entrance
W3, W4, W5	7	Blue-green speleothem with some dry green growth
W6, W7	8	Green-grey wet soft flowstone

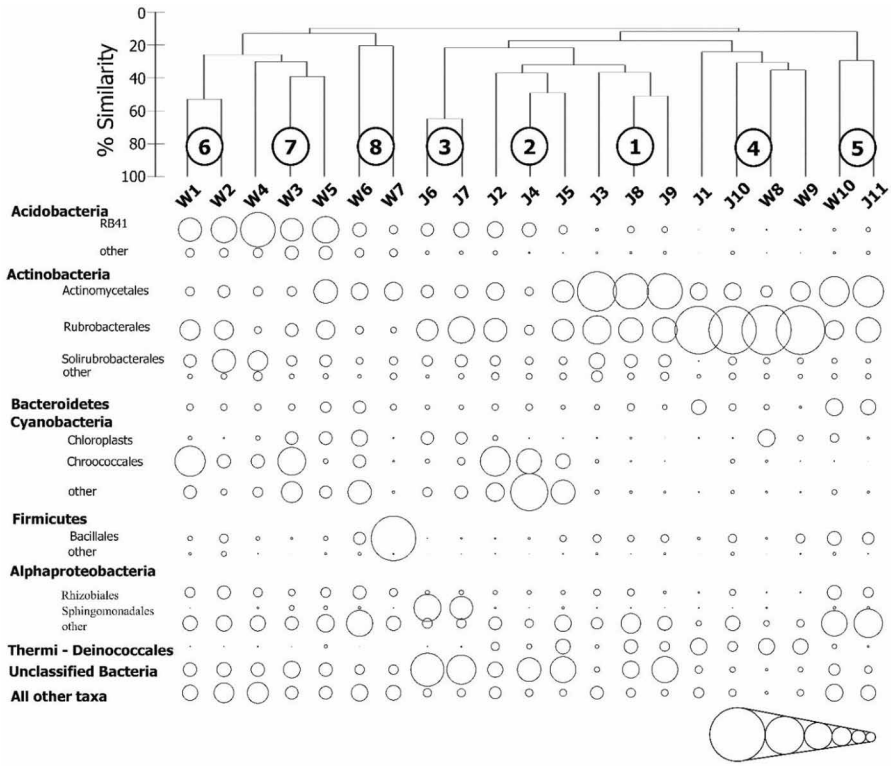

Figure 2. Abundances of the major taxa (contributing >2 % of total sequences) and clustering of Jenolan and Wombeyan samples into 8 distinct groups. Scale represents 60-40-20-10-5-2.5 % of total abundance. For samples and groups see Table 1.

Microbial heterogeneity between geographically isolated speleothems

Soil and rock controls from Wombeyan or Jenolan caves were not found to be substantially different, based on the Bray-Curtis similarities, although the lack of replicate samples did not permit this to be demonstrated statistically. PERMANOVA supported a distinction between Jenolan and Wombeyan active speleothem OTU communities (p = 0.001, Pseudo-F = 4.1555) and a distinction amongst groups (p = 0.0001, Pseudo-F = 3.1621). Differences between the groups were investigated by post-hoc, pairwise t-test. Significant differences were identified between rock controls and Site 1 (t = 0.038) and Site 2 (t = 0.039) from Jenolan Cave and Site 7 (t = 0.023) from Wombeyan Cave entrances.

There was a significant difference (t = 0.0334) in richness of subaerial biofilm communities between Jenolan and Wombeyan caves, but not of evenness (t = 0.0638) or diversity (t = 0.0950). A significant effect of Bray-Curtis similarity-defined groupings (p < 0.0001, F = 18.23) and, to a lesser extent, morphotype (p = 0.0281, F = 3.604) on the richness was observed. A significant effect on evenness was observed for Bray-Curtis groupings (p = 0.0008, F = 7.867), but not morphotype (p = 0.0559 F = 2.896). Pair-wise, the richness of microbial communities associated with subaerial biofilms in the Jenolan Cave entrance was not significantly different from bare rock and inactive speleothems in both caves. The richness of subaerial biofilms in the Wombeyan Cave arch was significantly different from that of the soil control for two of the three structures, namely the two blue-green speleothems, but not the green flowstone. No clear pattern was observed from the differences in evenness within or between caves.

The blue-green and green microbial mats of both Jenolan and Wombeyan caves were distinct from the rock and soil control samples by the presence of abundant cyanobacterial sequences (Fig. 2), consistent with microscopic analysis that confirmed an abundance of *Gloeocapsa* and *Chroococcidiopsis* morphotypes. Phylogenetic analysis (Fig. 3) of dominant cyanobacterial 16S rRNA gene sequences indicated the presence of a number of diverse OTUs associated with cultured *Chroococcidiopsis* and *Nostoc* species. In addition, a subset of dominant cyanobacterial OTUs were identified that lacked phylogenetically-related, cultured representatives. Cyanobacterial OTUs were shown to vary in their relative contribution to the total sequence count, both within a cave and, more notably, between caves (Fig. 3).

Indicator species analysis of OTUs that contribute at least 1% to any given samples identified a number of species indicative of the distinct sites, and groups of sites, within each cave system (Fig. 4). A total of 95 indicator OTUs were identified (Supplementary Table 1). Active speleothems were characterized by a range of cyanobacterial OTUs, phylogenetically similar to *Chroococcidiopsis* and *Gloeocapsa*, as well as a few chloroplast, *Sphingomonas*, *Rhizobiales*, *Gemmatimonadetes,* and unclassified bacterial OTUs. Acidobacterial OTUs were only indicative of the Wombeyan active structures. One OTU of *Cyanobacteria* and *Solirubrobacterales* were indicative of all active structures in both caves. The cyanobacterial genus *Acaryochloris* was indicative of the coarse, green mat sampled on the side of a Jenolan microbialite. No cyanobacterial indicator was found to be exclusive to rock or soil control sites. Indicator OTUs for the soil samples were *Actinomycetales* and *Gammaproteobacteria*.

Discussion

This study represents the first description of the microbial community composition of subaerial biofilms associated with a unique speleothem structure in cave arches (James et al., 1982; Cox et al., 1989b). Speleothems provide a unique opportunity to study how microbial, meteorological and geographical processes interact to introduce heterogeneity into

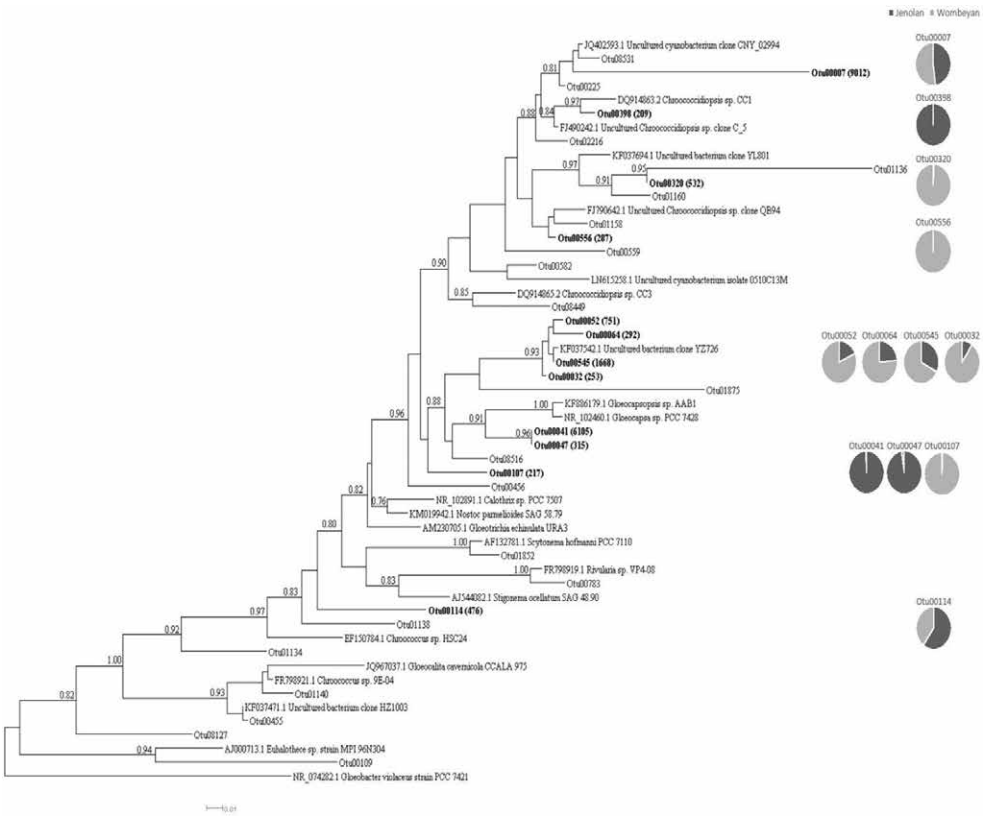

Figure 3. *Chroococcales*, *Nostocales* and unclassified cyanobacterial sequences from Jenolan and Wombeyan caves. Only OTUs with more than 10 sequences are included and relative shares of the most abundant OTUs (>200 sequences) are shown as pie charts and absolute sequence numbers are given in parentheses. Scale bar represents 0.01 substitutions per site.

landscapes. We sought to gain an understanding of the nature of microorganisms persisting in these biofilms, given the restricted availability of nutrients via drip water and dust. A focus has been placed on cyanobacteria as the main producers of organic matter within these systems, particularly with regards to the specific restrictions placed on this taxon by desiccation and low light.

Differences between and within caves

Despite significant differences between Jenolan and Wombeyan OTU community composition, no apparent differences in abundance of the major taxa were observed, except for the much higher abundance of *Acidobacteria* at Wombeyan sites (Fig. 2), suggesting that higher taxa and their respective metabolic and functional niches are represented by similar organisms. In both locations, cyanobacteria of the morphotypes *Chroococcidiopsis/Gloeocapsa* were the dominant primary producers and either share OTUs between caves or feature one representative of a putative, functional taxon (Fig. 3). This reflects an extent of functional redundancy to ecological roles and niche-specific adaptations (Yin et al., 2000). Given that the mechanisms of speleothem formation are likely the same in both caves, the key species in initial colonization influences subsequent biofilm growth. No clear pattern of richness, evenness and diversity was found between the caves, indicating that they experience similar environmental conditions and the differences in rainfall before sampling did not result in significant proliferation or decline of certain microbial clades, with the possible exception of an effect on *Acidobacteria*, discussed below.

Within caves, active blue-green mats were found to host a distinct microbial community compared to the weathered speleothems, bare rock or soil. Indicator OTU analysis showed that *Cyanobacteria* are indicators of active speleothems only, while *Actinobacteria* are mainly indicators of inactive structures and bare rock and soil (Fig. 4, Supplementary Table 1). Exceptionally abundant actinobacterial OTUs were distributed throughout the samples and are indicators for several sites, while multiple, less-abundant actinobacterial OTUs are associated with the aforementioned structures and controls. Therefore, a clear distinction in the importance of this taxon exists between active and inactive locations. Cyanobacterial indicators were closely related to the *Chroococcales* and uncultured species from extreme environments (Pointing et al., 2009; Wong et al., 2010). Jenolan active-site indicators were all cyanobacterial, whereas Wombeyan indicators are phylogenetically more diverse and include *Acidobacteria* and *Sphingomonas* OTUs. These taxa are also important constituents of soil and are able to degrade complex organic compounds (Juhasz and Naidu, 2000; Ward et al., 2009). A *Gemmatimonadete* OTU, indicative of all Wombeyan active mats, while poorly known, is well-adapted to desiccation (DeBruyn et al., 2011).

Low-light, desiccation tolerant Cyanobacteria represent a critical component of speleothem subaerial biofilms

Cyanobacteria (including chloroplasts) accounted for, on average, 18.6 % of the microbial community of active, speleothem-associated biofilms (Fig. 2). Consistent with their vibrant coloration, this value is likely to underestimate the cyanobacterial contribution to the total biomass in these systems, due to their large cell size. The microscopically- and phylogenetically-identified order *Chroococcales*, which includes the low-light adapted *Chroococcidiopsis* spp. and

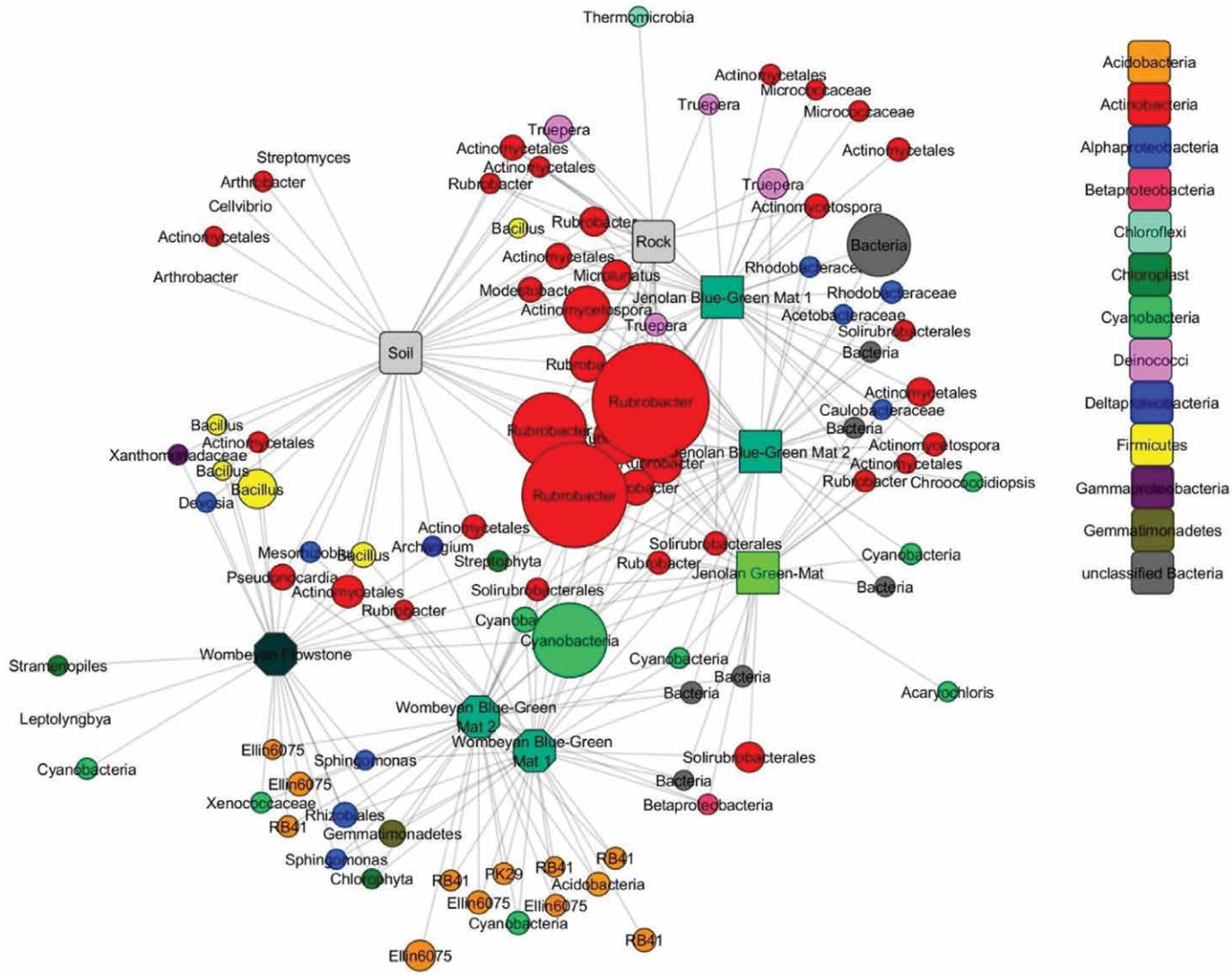

Figure 4. Indicator spring-embedded OTU network of sampled cave sites. Jenolan active and combined control sites in squares, Wombeyan active sites in octagons, OTUs in circles. Circle diameter corresponds to sequence abundance (not the same scale as Fig 2). Soil and rock denote bare cave soil and bare non-speleothem cave rock, respectively.

Gloeocapsa spp., contributed 8.3% of the total microbial community and were indicators (Fig. 4, Supplementary Table 1) of active biofilms. These findings are consistent with previous reports of biofilms on stone surfaces (Macedo et al., 2009) and caves (Asencio and Aboal, 2000; Lamprinou et al., 2009; Martinez and Asencio, 2010; Popović et al., 2015; Cox, 1984) and the premise that a biofilm established under low-light conditions would be dominated by cyanobacteria (Mulec et al., 2008). The morphotypes found in the cave arches possess thick sheaths (Baqué et al., 2013) and are prolific producers of EPS, which provide labile organic carbon for heterotrophs and offer protection from desiccation (Caiola et al., 1996) and freezing (Knowles and Castenholz, 2008). Production of EPS has also been proposed to support growth of low-light adapted photoautotrophs by facilitating the penetration of photons into deeper layers and minimizing shading of mineral grains and allochthonous particles in caves (Decho et al., 2003).

Low-light tolerance of the *Chroococcales* enables an endolithic lifestyle that mitigates desiccation stress (Potts, 1999), which is supported by very efficient DNA repair mechanisms conveyed by radiation resistance (Billi et al., 2000). Carbonate, which constitutes the cave speleothems, has high moisture retention and is more translucent than other common rock types and allows for colonization of *Chroococcidiopsis* (Smith et al., 2014). Retreat of endolithic cyanobacteria into the porous substrate ensures that the organisms receive sufficient water and light, while avoiding desiccation, temperature extremes, competition for space, and predation (Gorbushina, 2007).

It has been proposed that these cyanobacterial species contribute to the formation of cave structures (Cox et al., 1989a), leading to embedding of the biofilm. Several endolithic cyanobacteria have been found to precipitate intracellu-

lar, carbonate granules, thereby slowing down biomineralization (Benzerara et al., 2014). Decreased burial rate benefits both the primary producers and heterotrophic constituents of the subaerial biofilm. Büedel et al. (2002) proposed a three-story *Cyanobacteria*l biofilm based on endolithic *Chroococcidiopsis* and *Gloeocapsa* colonizing crevices and a medial layer of epiliths. The necessity to retain water efficiently makes a similar scaffold in cave biofilms likely, with the majority of the taxa building the understory.

An abundant cyanobacterial OTU related to cultured representatives of the genera *Acaryochloris* and *Loriellopsis* was observed in a shaded, vertical section of the Jenolan specimens. *Acaryochloris* inhabits deep-green, shaded limestone surfaces at Jenolan Caves and the genus is known to possess a red-shifted chlorophyll to facilitate growth at low-light (Behrendt et al., 2015). The branching filamentous *Loriellopsis cavernicola* has also been described from cave walls (Lamprinou et al., 2011).

Speleothem subaerial biofilms support the growth of oligotrophic microorganisms

Despite a high abundance of cyanobacteria within the speleothem biofilms, many of the heterotrophic groups resembled oligotrophic, rather than copiotrophic, taxa. Actinobacterial OTUs, similar to those identified from environments such as Roman catacombs (Saarela et al., 2004), lava caves (Hathaway et al., 2014), and granite walls (Laiz et al., 2009) represented the largest proportion of sequences present on both active and inactive speleothems, in accordance with previous reports on stone surfaces (Urzì et al., 2001). The next most common taxa were *Acidobacteria* and *Alphaproteobacteria*, both known to be abundant in caves (Schabereiter-Gurtner et al., 2004).

Filamentous *Actinobacteria* encompassed the family *Pseudonocardiaceae*, members that have been found to form net-like mycelia on weathered limestone (Cao et al., 2017), providing an advantage for the establishment of biofilms (Scheerer et al., 2009), and the family *Geodermatophilaceae,* described from a variety of stone surfaces (Urzì et al., 2001). *Pseudonocardia* is recognized for its capacity to degrade a variety of complex substrates (Reichert et al., 1998). The dominance of *Actinomycetes* on inactive structures is supported by their growth on recalcitrant organic matter and detrital particles. *Geodermatophilaceae* have been described from stone surfaces in various climates and are major colonizers of calcareous stone in the Mediterranean (Urzì, 2004). Heavy colonization by *Geodermatophilaceae* was associated with deterioration of stone surfaces (Urzì et al., 2001) and is potentially the cause for biodegradation at the weathered cave sites.

The presence of dominant OTUs, closely related to the gamma-radiation tolerant *Rubrobacter radiotolerans* (Yoshinaka et al., 1973), is consistent with the notion that radiation resistance in actinomycetes also conveys a level of desiccation tolerance via an efficient DNA repair mechanism. Tolerance to desiccation results in this group dominating and being indicators of the oldest, and therefore driest, cave structures (Fig. 2, Fig. 4 and Supplementary Table 1). Several OTUs also exhibited relatedness to *Rubrobacter bracarensis* that was isolated from biodeteriorated granite walls (47).

Most acidobacterial sequences recovered from the cave communities were associated with the taxon *RB41* (Fig. 2). Similar sequences have been recovered from lava caves (unpublished), rock surfaces (Yunnan stone forest, China, unpublished), and Antarctic soils (Yergeau et al., 2012). Abundance of this subgroup in soil is negatively correlated to pH (Jones et al., 2009), but the neutral pH of drip water in Wombeyan caves (McDonald et al., 2007) does not seem to support this finding and nutrient limitation might be the critical factor. *Acidobacteria* feature inconsistent nutrient utilization and preference patterns even within a subgroup (Naether et al., 2012). Nutrient-limited conditions were found to select for them, signifying their ability to degrade complex carbon sources in an oligotrophic environment (Rasche et al., 2011). Despite *Acidobacteria* often representing up to 20% of soil bacterial communities (Janssen, 2006), the origin of this taxon in the Wombeyan Cave structures does not seem to be aeolian. Sequence numbers are very low in the soil and rock controls, which indicates an enrichment on the Wombeyan speleothems rather than passive transport.

Various acidobacterial OTUs were indicators for the blue-green mats and flowstone sites in Wombeyan, but not in Jenolan (Fig. 4, Supplementary Table 1) caves. *Acidobacteria* have previously been reported in a comparative study of the walls of two caves, where visitor load might explain the differences in abundance (Schabereiter-Gurtner et al., 2004). In the caves, a difference in drip water chemistry is more likely to deter them from one site, but little is known about the physiology and ecology of *Acidobacteria* to explain this pattern, and without environmental data, it is difficult to understand it.

Most *Rhizobiales* sequences found were very similar (99-100%) to sequences of desiccation-tolerant *Dichotomicrobium thermohalophilum* isolated from a hypersaline lake (Hirsch and Hoffmann, 1989), and the families *Bradyrhizobium*, *Mesorhizobium,* and *Devosia*, from root nodules of various plants (Laranjo et al., 2014). *Bradyrhizobium* is a major nitrogen fixer and, in symbiosis with algae, provides a valuable service to microbial communities on oligotrophic substrates. Even though *Bradyrhizobium* was found in all but one cave sample, the relatively high biomass of the microbialite surfaces makes a contaminant origin unlikely.

For most chloroplast and a third of unclassified bacterial sequences, the closest homologue (>91%) is *Prasiolopsis* (*Trebouxiophyceae*), a widely distributed group and a common colonizer of stone surfaces in temperate regions (Rindi

et al., 2007; Hallmann et al., 2013). Almost all *Prasiolopsis*-like sequences were accounted for by the dry, green mat (group 3). This taxon forms lichens with fungi, which can stabilize a forming biofilm. It has also been found in dry valleys of Antarctica (de Wever et al., 2009) and on coastal rocks fertilized by bird guano (Heesch et al., 2012). This ability to grow in dry, oligotrophic conditions, where nutrient input is mainly via aerial transport and bird or bat droppings, might explain why this taxon might be prevalent, even though the low similarity to cultured organisms prevents detailed predictions.

Putative successional stages

The distinct groups observed in the caves are in line with the finding that, as opposed to algae and fungi, no significant spatial structure at the centimeter scale for bacteria can be found (Cutler et al., 2014). Cave locations were sampled at a centimeter to decimeter scale. While active sites have low numbers and roughly equal proportions of *Actinomycetales* and *Rubrobacterales*, this proportion shifts drastically in the inactive and weathered speleothems (groups 1 and 4), with almost no cyanobacterial sequences found. The proportion of *Actinomycetales* to *Rubrobacterales* shifts from about 2:1 in group 1 to about 1:4 in group 4.

A long-term temporal succession, most likely governed by water availability, may explain this pattern. On active, blue-green structures, where an intact, three-dimensional biofilm is maintained, water can be retained, and extremely desiccation-tolerant species are at much less of an advantage. The roofs of cave arches change over time, when crevices on the surface become clogged and new ones are created. Water availability for speleothems below fluctuates, leading to a shift from *Cyanobacteria*-driven primary production to a drought-induced collapse of cyanobacterial populations and retreat of coccoid genera such as *Chroococcidiopsis* and *Gloeocapsa* into endolithic niches. Oligotrophic *Actinobacteria* persevere on recalcitrant and complex organic molecules, dead cells, and aeolian particles. When desiccation stress becomes more intense, such as in the weathered speleothems and bare rock samples, only the highly desiccation-resistant *Rubrobacterales* prevail.

Conclusions

Significant differences between the microbial communities of speleothem biofilms of two cave arches were found. While rock and soil controls were especially similar between caves and dominated by *Actinobacteria*, active blue-green biofilms on speleothems were indicated by endolithic *Chroococcidiopsis* and *Gloeocapsa*-like cyanobacteria. Biofilms from both caves harbored similar cyanobacterial representatives, potentially fulfilling the same functions. As a consequence of desiccation-driven progression from active mats to inactive ones and to weathered speleothems, it is proposed that endolithic phototrophs retreat below the surface while oligotrophic *Actinomycetes* and, later, highly desiccation-resistant *Rubrobacterales*, dominate the speleothem surface. Inclusion of environmental long-term data would shed light on the dynamics through time, and reasons for distinct community compositions between sites, such as differences in the abundance of *Acidobacteria*.

Acknowledgements

This study was supported by the William Macleay Microbiology Research Fund, issued by the Linnean Society of New South Wales. DP Vardeh was supported by a University International Postgraduate Award by UNSW. Acting Managers Dan Cove from Jenolan Caves and David Smith from Wombeyan Caves are gratefully acknowledged for their help with sampling, as is Toby Mills for providing tools. Sampling was conducted under Office of Environment and Heritage (OEH) permit licence SL101114. This project was also supported by the Australian Research Council.

References

Asencio, A.D., and Aboal, M., 2000, A contribution to knowledge of chasmoendolithic algae in cave-like environments: Algological Studies, v. 98, p. 133–151.

Baqué, M., Viaggiu, E., Scalzi, G., and Billi, D., 2013, Endurance of the endolithic desert cyanobacterium *Chroococcidiopsis* under UVC radiation: Extremophiles, v. 17, p. 161–169. https://doi.org/10.1007/s00792-012-0505-5.

Behrendt, L., Brejnrod, A., Schliep, M., Sørensen, S.J., Larkum, A.W.D., and Kühl, M., 2015, Chlorophyll f-driven photosynthesis in a cavernous cyanobacterium: The ISME Journal, v. 9, p. 2108–2111. https://doi.org/10.1038/ismej.2015.14.

Benzerara, K., Skouri-Panet, F., Li, J., Férard, C., Gugger, M., Laurent, T., Couradeau, E., Ragon, M., Cosmidis, J., and Menguy, N., 2014, Intracellular Ca-carbonate biomineralization is widespread in cyanobacteria: Proceedings of the National Academy of Sciences, v. 111, p. 10933–10938. https://doi.org/10.1073/pnas.1403510111.

Billi, D., Friedmann, E.I., Hofer, K.G., Caiola, M.G., and Ocampo-Friedmann, R., 2000, Ionizing-radiation resistance in the desiccation-tolerant cyanobacterium *Chroococcidiopsis*: Applied and Environmental Microbiology, v. 66, p. 1489–1492. https://doi.org/10.1128/AEM.66.4.1489-1492.2000.

Buedel, B., Weber, B., Kuhl, M., Pfanz, H., Sultemeyer, D., and Wessels, D., 2004, Reshaping of sandstone surfaces by cryptoendolithic cyanobacteria: bioalkalization causes chemical weathering in arid landscapes: Geobiology, v. 2, p. 261–268. https://doi.org/10.1128/AEM.66.4.1489-1492.2000.

Buedel, B., Weber, H.-M., Porembski, S., and Barthlott, W., 2002, Cyanobacteria of inselbergs in the Atlantic rainforest zone of eastern Brazil: Phycologia, v. 41, p. 498–506. https://doi.org/10.2216/i0031-8884-41-5-498.1.

Bureau of Meteorology, 2013a, http://www.bom.gov.au/jsp/ncc/cdio/weatherData/av?p_nccObsCode=136&p_display_type=dailyDataFile&p_startYear=2013&p_c=-794902150&p_stn_num=63036.

Bureau of Meteorology, 2013b, http://www.bom.gov.au/jsp/ncc/cdio/weatherData/av?p_nccObsCode=136&p_display_type=dailyDataFile&p_startYear=2013&p_c=-796340020&p_stn_num=63093.

de Cáceres, M., Legendre, P., and Moretti, M., 2010, Improving indicator species analysis by combining groups of sites: Oikos, v. 119, p. 1674–1684. https://doi.org/10.1111/j.1600-0706.2010.18334.x.

Caiola, M.G., Billi, D., and Friedmann, E.I., 1996, Effect of desiccation on envelopes of the cyanobacterium *Chroococcidiopsis* sp.(Chroococcales): European Journal of Phycology, v. 31, p. 97–105. https://doi.org/10.1080/09670269600651251a.

Cao, C., Yuan, B., Qin, S., Jiang, J., Tao, F., and Lian, B., 2017, *Lentzea pudingi* sp. nov., isolated from a weathered limestone sample in a karst area: International Journal of Systematic and Evolutionary Microbiology, v. 67, p. 4873–4878. https://doi.org/10.1099/ijsem.0.002400.

Caporaso, J.G., Lauber, C.L., Walters, W.A., Berg-Lyons, D., Huntley, J., Fierer, N., Owens, S.M., Betley, J., Fraser, L., Bauer, M., Gormley, N., Gilbert, J.A., Smith, G., and Knight, R., 2012, Ultra-high-throughput microbial community analysis on the Illumina HiSeq and MiSeq platforms: ISME Journal, v. 6, p. 1621–1624. https://doi.org/10.1038/ismej.2012.8.

Cole, J.R., Wang, Q., Fish, J.A., Chai, B., McGarrell, D.M., Sun, Y., Brown, C.T., Porras-Alfaro, A., Kuske, C.R., and Tiedje, J.M., 2013, Ribosomal Database Project: Data and tools for high throughput rRNA analysis: Nucleic Acids Research, v. 42, p. D633–D642. https://doi.org/10.1093/nar/gkt1244.

Cox, G., 1984, Phototrophic stalagmites at Jenolan Caves, NSW: Helictite, v. 22, p. 55–56.

Cox, G., James, J.M., Armstrong, R.A.L., and Leggett, K.E.A., 1989a, Stromatolitic crayfish-like stalagmites: Proceedings of the University of Bristol Spelæological Society, v. 18, p. 339–358.

Cox, G., James, J.M., Leggett, K.E.A., and Osborne, A.L., 1989b, Cyanobacterially deposited speleothems : Subaerial stromatolites: Geomicrobiology Journal, v. 7, p. 245–252. https://doi.org/10.1080/01490458909377870.

Crispim, C.A., and Gaylarde, C.C., 2005, Cyanobacteria and biodeterioration of cultural heritage: A review: Microbial Ecology, v. 49, p. 1–9. https://doi.org/10.1007/s00248-003-1052-5.

Cutler, N.A., Chaput, D.L., Oliver, A.E., and Viles, H.A., 2014, The spatial organization and microbial community structure of an epilithic biofilm: FEMS Microbiology Ecology, v. 91, p. fiu027. https://doi.org/10.1093/femsec/fiu027.

DeBruyn, J.M., Nixon, L.T., Fawaz, M.N., Johnson, A.M., and Radosevich, M., 2011, Global biogeography and quantitative seasonal dynamics of Gemmatimonadetes in soil: Applied and Environmental Microbiology, v. 77, p. 6295–6300. https://doi.org/10.1128/AEM.05005-11.

Decho, A.W., Kawaguchi, T., Allison, M. a., Louchard, E.M., Reid, R.P., Stephens, F.C., Voss, K.J., Wheatcroft, R. a., and Taylor, B.B., 2003, Sediment properties influencing upwelling spectral reflectance signatures: The biofilm gel effect: Limnology and Oceanography, v. 48, p. 431–443. https://doi.org/10.4319/lo.2003.48.1_part_2.0431.

Edgar, R.C., Haas, B.J., Clemente, J.C., Quince, C., and Knight, R., 2011, UCHIME improves sensitivity and speed of chimera detection: Bioinformatics, v. 27, p. 2194–2200. https://doi.org/10.1093/bioinformatics/btr381.

Golubic, S., Friedmann, I., and Schneider, J., 1981, The lithobiontic ecological niche, with special reference to microorganisms: Journal of Sedimentary Research, v. 51, p. 475–478.

Gorbushina, A.A., 2007, Life on the rocks: Environmental Microbiology, v. 9, p. 1613–1631. https://doi.org/10.1111/j.1462-2920.2007.01301.x.

Guindon, S., Dufayard, J.-F., Lefort, V., and Anisimova, M., 2010, New alogrithms and methods to estimate maximum- likelihoods phylogenies: Assessing the performance of PhyML 3.0: Systematic Biology, v. 59, p. 307–321. https://doi.org/10.1093/sysbio/syq010.

Hall, T.A., 1999, BioEdit: A user-friendly biological sequence alignment editor and analysis program for Windows 95/98/NT: Nucleic Acids Symposium Series, v. 41, p. 95–98.

Hallmann, C., Stannek, L., Fritzlar, D., Hause-Reitner, D., Friedl, T., and Hoppert, M., 2013, Molecular diversity of phototrophic biofilms on building stone: FEMS Microbiology Ecology, v. 84, p. 355–372. https://doi.org/10.1111/1574-6941.12065.

Hathaway, J.J.M., Garcia, M.G., Balasch, M.M., Spilde, M.N., Stone, F.D., Dapkevicius, M.D.L.N.E., Amorim, I.R., Gabriel, R., Borges, P.A. V, and Northup, D.E., 2014, Comparison of bacterial diversity in Azorean and Hawai'ian lava cave microbial mats: Geomicrobiology Journal, v. 31, p. 205–220. https://doi.org/10.1080/01490451.2013.777491.

Heesch, S., Sutherland, J.E., and Nelson, W.A., 2012, Marine prasiolales (Trebouxiophyceae, Chlorophyta) from New Zealand and the Balleny Islands, with descriptions of *Prasiola novaezelandiae* sp. nov. and *Rosenvingiella australis* sp. nov: Phycologia, v. 51, p. 217–227. https://doi.org/10.2216/10-95.1.

Hill, C.A., Forti, P., and Shaw, T.R., 1997, Cave minerals of the world: National Speleological Society, Huntsville, AL, p. 238.

Hirsch, P., and Hoffmann, B., 1989, *Dichotomicrobium thermohalophilum*, gen. nov., spec, nov., budding prosthecate bacteria from the Solar Lake (Sinai) and some related strains: Systematic and Applied Microbiology, v. 11, p. 291–301. https://doi.org/10.1016/S0723-2020(89)80027-X.

Huson, D.H., and Scornavacca, C., 2012, Dendroscope 3: An interactive tool for rooted phylogenetic trees and networks: Systematic Biology, v. 61, p. 1061–1067. https://doi.org/10.1093/sysbio/sys062.

James, J.M., Jennings, J.N., and Dyson, H.G., 1982, Mineral decoration and weathering of the caves: Wombeyan Caves: Sydney Speleological Society, v. 8, p. 121–136.

Janssen, P.H., 2006, Identifying the dominant soil bacterial taxa in libraries of 16S rRNA and 16S rRNA genes: Applied and Environmental Microbiology, v. 72, p. 1719–1728. http://doi: 10.1128/AEM.72.3.1719.

Jones, R.T., Robeson, M.S., Lauber, C.L., Hamady, M., Knight, R., and Fierer, N., 2009, A comprehensive survey of soil acidobacterial diversity using pyrosequencing and clone library analyses: The ISME Journal, v. 3, p. 442–453. https://doi.org/10.1038/ismej.2008.127.

Juhasz, A.L., and Naidu, R., 2000, Bioremediation of high molecular weight polycyclic aromatic hydrocarbons: a review of the microbial degradation of benzo [a] pyrene: International Biodeterioration and Biodegradation, v. 45, p. 57–88. https://doi.org/10.1016/S0964-8305(00)00052-4.

Kemmling, A., Kämper, M., Flies, C., Schieweck, O., and Hoppert, M., 2004, Biofilms and extracellular matrices on geomaterials: Environmental Geology, v. 46, p. 429–435. https://doi.org/10.1007/s00254-004-1044-x.

Knowles, E.J., and Castenholz, R.W., 2008, Effect of exogenous extracellular polysaccharides on the desiccation and freezing tolerance of rock-inhabiting phototrophic microorganisms: FEMS Microbiology Ecology, v. 66, p. 261–270. https://doi.org/10.1111/j.1574-6941.2008.00568.x.

Laiz, L., Miller, A.Z., Jurado, V., Akatova, E., Sanchez-Moral, S., Gonzalez, J.M., Dionísio, A., MacEdo, M.F., and Saiz-Jimenez, C., 2009, Isolation of five *Rubrobacter* strains from biodeteriorated monuments: Naturwissenschaften, v. 96, p. 71–79. https://doi.org/10.1007/s00114-008-0452-2.

Lamprinou, V., Hernández-Mariné, M., Canals, T., Kormas, K., Economou-Amilli, A., and Pantazidou, A., 2011, Morphology and molecular evaluation of *Iphinoe spelaeobios* gen. nov., sp. nov. and *Loriellopsis cavernicola* gen. nov., sp. nov., two stigonematalean cyanobacteria from Greek and Spanish caves: International Journal of Systematic and Evolutionary Microbiology, v. 61, p. 2907–2915. https://doi.org/10.1099/ijs.0.029223-0.

Lamprinou, V., Pantazidou, A., Papadogiannaki, G., Radea, C., and Economou-Amilli, A., 2009, Cyanobacteria and associated invertebrates in Leontari Cave, Attica Greece: Fottea, v. 9, p. 155–164. https://doi.org/10.5507/fot.2009.014.

Laranjo, M., Alexandre, A., and Oliveira, S., 2014, Legume growth-promoting rhizobia: An overview on the *Mesorhizobium* genus: Microbiological Research, v. 169, p. 2–17. https://doi.org/10.1016/j.micres.2013.09.012.

Lundberg, J., and McFarlane, D.A., 2011, A note on the occurrence of a crayback stalagmite at Niah Caves, Borneo: International Journal of Speleology, v. 40, p. 39–43. https://doi.org/10.5038/1827-806X.40.1.5.

Macedo, M.F., Miller, A.Z., Dionísio, A., and Saiz-Jimenez, C., 2009, Biodiversity of cyanobacteria and green algae on monuments in the Mediterranean Basin: An overview: Microbiology, v. 155, p. 3476–3490. https://doi.org/10.1099/mic.0.032508-0.

Martinez, A., and Asencio, A.D., 2010, Distribution of cyanobacteria at the Gelada Cave (Spain) by physical parameters: Journal of Cave and Karst Studies, v. 72, p. 11–20. https://doi.org/10.4311/jcks2009lsc0082.

McDonald, J., Drysdale, R., Hill, D., Chisari, R., and Wong, H., 2007, The hydrochemical response of cave drip waters to sub-annual and inter-annual climate variability, Wombeyan Caves, SE Australia: Chemical Geology, v. 244, p. 605–623. https://doi.org/10.1016/j.chemgeo.2007.07.007.

Miller, A., Dionísio, A., and Macedo, M.F., 2006, Primary bioreceptivity: A comparative study of different Portuguese lithotypes: International Biodeterioration and Biodegradation, v. 57, p. 136–142. https://doi.org/10.1016/j.ibiod.2006.01.003.

Mulec, J., Kosi, G., and Vrhovsek, D., 2007, Algae promote growth of stalagmites and stalactites in karst caves (Skocjanske Jame, Slovenia): Carbonates and Evaporites, v. 22, p. 6–9. https://doi.org/10.1007/BF03175841.

Mulec, J., Kosi, G., and Vrhovšek, D., 2008, Characterization of cave aerophytic algal communities and effects of irradiance levels on production of pigments: Journal of Cave and Karst Studies, v. 70, p. 3–12.

Naether, A., Foesel, B.U., Naegele, V., Wuest, P.K., Weinert, J., Bonkowski, M., Alt, F., Oelmann, Y., Polle, A., Lohaus, G., Gockel, S., Hemp, A., Kalko, E.K. V, Linsenmair, K.E., et al., 2012, Environmental factors affect acidobacterial communities below the subgroup level in grassland and forest soils: Applied and Environmental Microbiology, v. 78, p. 7398–7406. https://doi.org/10.1128/AEM.01325-12.

Osborne, R., 1993, The history of karstification at Wombeyan Caves, New South Wales, Australia, as revealed by palaeokarst deposits: Cave Science, v. 20, p. 1–8.

Pointing, S.B., Chan, Y., Lacap, D.C., Lau, M.C.Y., Jurgens, J.A., and Farrell, R.L., 2009, Highly specialized microbial diversity in hyper-arid polar desert: Proceedings of the National Academy of Sciences, v. 106, p. 19964–19969. https://doi.org/10.1073/pnas.0908274106.

Popović, S., Subakov Simić, G., Stupar, M., Unković, N., Predojević, D., Jovanović, J., and Ljaljević Grbić, M., 2015, Cyanobacteria, algae and microfungi present in biofilm from Božana Cave (Serbia): International Journal of Speleology, v. 44, p. 141–149. https://doi.org/10.5038/1827-806X.44.2.4.

Potts, M., 1999, Mechanisms of desiccation tolerance in cyanobacteria: European Journal of Phycology, v. 34, p. 319–328. https://doi.org/10.1080/09670269910001736382.

Rasche, F., Knapp, D., Kaiser, C., Koranda, M., Kitzler, B., Zechmeister-Boltenstern, S., Richter, A., and Sessitsch, A., 2011, Seasonality and resource availability control bacterial and archaeal communities in soils of a temperate beech forest: The ISME Journal, v. 5, p. 389–402. https://doi.org/10.1038/ismej.2010.138.

Reichert, K., Lipski, A., Pradella, S., Stackebrandt, E., and Altendorf, K., 1998, *Pseudonocardia asaccharolytica* sp. nov. and *Pseudonocardia sulfidoxydans* sp. nov., two new dimethyl disulfide-degrading actinomycetes and emended description of the genus Pseudonocardia: International Journal of Systematic Bacteriology, v. 48, p. 441–449. https://doi.org/10.1099/00207713-48-2-441.

Rindi, F., McIvor, L., Sherwood, A.R., Friedl, T., Guiry, M.D., and Sheath, R.G., 2007, Molecular phylogeny of the green algal order Prasiolales (Trebouxiophyceae, Chlorophyta): Journal of Phycology, v. 43, p. 811–822. https://doi.org/10.1111/j.1529-8817.2007.00372.x.

Saarela, M., Alakomi, H.-L., Suihko, M.-L., Maunuksela, L., Raaska, L., and Mattila-Sandholm, T., 2004, Heterotrophic microorganisms in air and biofilm samples from Roman catacombs, with special emphasis on actinobacteria and fungi: International Biodeterioration and Biodegradation, v. 54, p. 27–37. https://doi.org/10.1016/j.ibiod.2003.12.003.

Saghaï, A., Zivanovic, Y., Zeyen, N., Moreira, D., Benzerara, K., Deschamps, P., Bertolino, P., Ragon, M., Tavera, R., and López-Archilla, A.I., 2015, Metagenome-based diversity analyses suggest a significant contribution of non-cyanobacterial lineages to carbonate precipitation in modern microbialites: Frontiers in Microbiology, v. 6, p. Article 797. https://doi.org/10.3389/fmicb.2015.00797.

Schabereiter-Gurtner, C., Saiz-Jimenez, C., Piñar, G., Lubitz, W., and Rölleke, S., 2004, Phylogenetic diversity of bacteria associated with Paleolithic paintings and surrounding rock walls in two Spanish caves (Llonín and La Garma): FEMS Microbiology Ecology, v. 47, p. 235–247. https://doi.org/10.1016/S0168-6496(03)00280-0.

Scheerer, S., Ortega-Morales, O., and Gaylarde, C., 2009, Microbial deterioration of stone monuments—an updated overview: Advances in Applied Microbiology, v. 66, p. 97–139. https://doi.org/10.1016/S0065-2164(08)00805-8.

Schloss, P.D., Westcott, S.L., Ryabin, T., Hall, J.R., Hartmann, M., Hollister, E.B., Lesniewski, R.A., Oakley, B.B., Parks, D.H., and Robinson, C.J., 2009, Introducing mothur: Open-source, platform-independent, community-supported software for describing and comparing microbial communities: Applied and Environmental Microbiology, v. 75, p. 7537–7541. https://doi.org/10.1128/AEM.01541-09.

Smith, H.D., Baqué, M., Duncan, A.G., Lloyd, C.R., McKay, C.P., and Billi, D., 2014, Comparative analysis of cyanobacteria inhabiting rocks with different light transmittance in the Mojave Desert: A Mars terrestrial analogue: International Journal of Astrobiology, v. 13, p. 271–277. https://doi.org/10.1017/S1473550414000056.

Thompson, J.D., Higgins, D.G., and Gibson, T.J., 1994, CLUSTAL W: Improving the sensitivity of progressive multiple sequence alignment through sequence weighting, position-specific gap penalties and weight matrix choice: Nucleic Acids Research, v. 22, p. 4673–4680. https://doi.org/10.1093/nar/22.22.4673.

Tourney, J., and Ngwenya, B.T., 2009, Bacterial extracellular polymeric substances (EPS) mediate CaCO3 morphology and polymorphism: Chemical Geology, v. 262, p. 138–146. https://doi.org/10.1016/j.chemgeo.2009.01.006.

Urzì, C., 2004, Microbial deterioration of rocks and marble monuments of the Mediterranean basin: A review: Corrosion Reviews, v. 22, p. 441–458. https://doi.org/10.1515/CORRREV.2004.22.5-6.441.

Urzì, C., Brusetti, L., Salamone, P., Sorlini, C., Stackebrandt, E., and Daffonchio, D., 2001, Biodiversity of Geodermatophilaceae isolated from altered stones and monuments in the Mediterranean basin: Environmental Microbiology, v. 3, p. 471–479. https://doi.org/10.1046/j.1462-2920.2001.00217.x.

Ward, N.L., Challacombe, J.F., Janssen, P.H., Henrissat, B., Coutinho, P.M., Wu, M., Xie, G., Haft, D.H., Sait, M., and Badger, J., 2009, Three genomes from the phylum Acidobacteria provide insight into the lifestyles of these microorganisms in soils: Applied and Environmental Microbiology, v. 75, p. 2046–2056. https://doi.org/10.1128/AEM.02294-08.

Warscheid, T., and Braams, J., 2000, Biodeterioration of stone: A review: International Biodeterioration and Biodegradation, v. 46, p. 343–368. https://doi.org/10.1016/S0964-8305(00)00109-8.

de Wever, A., Leliaert, F., Verleyen, E., Vanormelingen, P., Van der Gucht, K., Hodgson, D. a, Sabbe, K., and Vyverman, W., 2009, Hidden levels of phylodiversity in Antarctic green algae: Further evidence for the existence of glacial refugia: Proceedings of the Royal Society B: Biological Sciences, v. 276, p. 3591–3599. https://doi.org/10.1098/rspb.2009.0994.

Wong, F.K.Y., Lacap, D.C., Lau, M.C.Y., Aitchison, J.C., Cowan, D.A., and Pointing, S.B., 2010, Hypolithic microbial community of quartz pavement in the high-altitude tundra of central Tibet: Microbial Ecology, v. 60, p. 730–739. https://doi.org/10.1007/s00248-010-9653-2.

Yergeau, E., Bokhorst, S., Kang, S., Zhou, J., Greer, C.W., Aerts, R., and Kowalchuk, G.A., 2012, Shifts in soil microorganisms in response to warming are consistent across a range of Antarctic environments: The ISME Journal, v. 6, p. 692–702. https://doi.org/10.1038/ismej.2011.124.

Yin, B., Crowley, D., Sparovek, G., De Melo, W.J., and Borneman, J., 2000, Bacterial functional redundancy along a soil reclamation gradient: Applied and Environmental Microbiology, v. 66, p. 4361–4365. https://doi.org/10.1128/AEM.66.10.4361-4365.2000.

Yoshinaka, T., Yano, K., and Yamaguchi, H., 1973, Isolation of highly radioresistant bacterium, *Arthrobacter radiotolerans* nov. sp: Agricultural and Biological Chemistry, v. 37, p. 2269–2275. https://doi.org/10.1080/00021369.1973.10861003.

J. Czerwik-Marcinkowska, W. Wróblewski, M. Gradziński, and B. Uher. Diatom species diversity and their ecological patterns on different substrates in two karstic streams in the Slovak karst. *Journal of Cave and Karst Studies*, v. 80, no. 3, p. 133-144. DOI:10.4311/2017MB0124

DIATOM SPECIES DIVERSITY AND THEIR ECOLOGICAL PATTERNS ON DIFFERENT SUBSTRATES IN TWO KARSTIC STREAMS IN THE SLOVAK KARST

Joanna Czerwik-Marcinkowska[1, C], Wojciech Wróblewski[2], Michal Gradziński[2], Bohuslav Uher[3]

Abstract

Many karstic streams are threatened both by anthropogenic and climate changes, but little is known about their algal biodiversity and conservation value, especially in the Slovak Karst. Diatom assemblages occurring on seven substrates, including stones, mud, submerged mosses and filamentous algae: *Cladophora glomerata, Vaucheria* sp., *Ulothrix zonata*, *Spirogyra* sp. in two nameless karstic streams in the Krásnohorská Dlhá Lúka Village and the Gombasek Cottage Settlement (the Slavec Village) in the Košice Region of central-eastern Slovakia (the Silická Plateau) were studied. A total of 124 diatom taxa were found at four sites, where epilithic and epiphytic diatom assemblages dominated. Both species' richness and Shannon-Wiener indices showed congruent biotic integrity. The dominant taxa were alkaliphilous, halophobous-oligohalobous, requiring xeno-oligosaprobic and oligotrophic waters. Diatoms include: *Diploneis krammeri, Encyonema ventricosum, Gomphonema acuminatum, Gyrosigma attenuatum, Navicula tripunctata*, and *Paraplaconeis cracoviensis*. The latter species is a new report for Slovakia, reflecting the calcareous, geological nature of the Silická Plateau (the Slovak Karst). Diatom assemblages in two karstic streams consisted mainly of small-celled species of *Achnanthidium, Amphora, Caloneis, Planothidium*, and *Stauroneis.* Our results showed that the diatom assemblages were mostly structured by environmental factors of calcium and pH gradients, confirmed by canonical **variates** analysis (CVA) and Monte Carlo permutation tests. However, unique spatial and biological gradients, specific to different guilds related to each other, were also evident. The Slovak karstic streams should be especially protected and regularly monitored.

Introduction

Karstic formations are extremely complex, and, due to a number of geological and hydrological characteristics, can be included among the most fragile and vulnerable environments in the world (Brinkmann and Parise, 2012). Complexity of karst is expressed by the enormous variations existing in different karst regions (White, 1988). Karstic areas cover 10 to 20% of the earth's surface and provide 40 to 50% of the world's drinking water (Ford and Williams, 2007), and it requires a specific approach to mitigate negative human impacts and allow sustainable development. Karstic streams are considered among the most sensitive, water-dependent ecosystems, and their ecological value is important as strategic water sources. Karst is a landscape that results from the chemical weathering and collapse of carbonate rocks (limestone, dolomite, and gypsum), which creates such features as sinkholes, caves, and underground drainage. The Slovak Karst area located in eastern Slovakia is a typical upland karst, consisting of several karst plateaus (Gradziński et al., 2013). These plateau tops and some slopes are partly covered by deciduous forests, and south-facing, steep, partly rocky slopes are occupied by xerothermic grasslands and bushes. The karstic waters from the Slovak Karst are drained by the autochthonous and allochthonous rivers, streams, and springs located in the non-karstic region of the adjacent mountains. Karstic streams are widespread in European regions, where Paleozoic, Mesozoic and Cenozoic limestone formations are subject to present-day karstification (Arp et al., 2010).

The Slovak Karst is a hotspot area for biodiversity, representing specific environments; it is included in the URL UNESCO World Heritage List. Karst regions interact with the environment to produce complex ecosystems supporting specialist plants, animals, and microorganisms. In karstic streams, CO_2 degassing drives the increase of calcite saturation to maximum values of approximately 10-fold, independent from the initial Ca^{2+}-alkalinity ratio. Diatoms are potentially involved in $CaCO_3$ mineral nucleation via exopolymers and/or alternating $CaCO_3$ mineral saturation within microenvironments. Diatoms, by far, are the most dominant eukaryotic microalgal group in karst water streams (Arp et al., 2010). According to Smol and Stoermer (2015), these microhabitats are the most interesting aquatic environments for the study of algae, especially diatoms. They are considered as useful indicators of environmental quality and reflect the ecological integrity of stream habitats. Diatoms are pioneering, autotrophic colonizers in river and stream ecosystems, and they are the main element used for monitoring studies due to their rapid assemblages' response to stress (Potapova et al., 2004; Bellinger et al., 2006). Diatom assemblages are adapted to the local environmental conditions

[1]Department of Botany, Institute of Biology, Jan Kochanowski University, Świętokrzyska 15, 25-420 Kielce, Poland
[2]Institute of Geological Sciences, Jagiellonian University, Oleandry 2a, 30-063 Kraków, Poland
[3]Department of Microbiology, Immunobiology and Genetics, Max F. Perutz Laboratories, University of Vienne, Dr. Bohr Gasse 9, A-1030 Vienna, Austria
[C]Corresponding author: marcinko@kielce.com.pl

in relation to changes in water residence time and to the variations in the ionic content in water, due to flow volume variations (Aboal et al., 1996).

Streams may flow all year round or only intermittently due to desiccation, freezing, or karst phenomena, and they present unique, but understudied, habitats. The karst water streams often sink, particularly on substrates of loose moraine deposits, and reappear again after a certain distance (Kawecka, 2012). Thus, the study of diatoms, both in typical and karstic streams, are an important element of monitoring and assessment programs in countries around Europe. Diatom assemblages are not only useful for an assessment of the relative role of environmental and spatial factors (Heino et al., 2010), but also for assessing the relevance of biological species sorting (Arp et al., 2010).

Consequently, the aim of the present study was to evaluate changes in the structure and species richness of diatoms occurring in karst water streams in middle-eastern Slovakia (the Silická Plateau), and their relationship with environmental variables that influence the diatom assemblages. This study describes the biodiversity of epilithic and epiphytic diatom assemblages, with particular interest in the significance of such habitats for conservation. However, there is the likelihood of underestimating local control and overestimating regional control of karstic stream assemblages. More specifically, we predicted that different diatoms indicate a similar, strong response to the environmental gradient, and a similar, weak response to the spatial gradient, due to the small study area, and different responses to the biotic gradient, due to differences in ecologically-sensitive species.

Materials and Methods

Sampling Sites and Procedures – Four water sites were sampled for physical, chemical, and biological variables in September 2014: three (GP 4.4, GP 4.7, and GP 4.8) from a nameless stream in the Gombasek Cottage Settlement (the Slavec Village) and one (KP 3.5) in the Krásnohorská Dlhá Lúka Village. The two nameless streams belong to the Čremošná tributary (Krásnohorská Dlhá Lúka; N 48º37´02.29" E 20º35'14.97") and to the Slaná tributary (Gombasek; N 48º33'46.21" E 20º27'57.57"). They are situated in headwater streams draining the Silická Plateau (in Slovak; Silická Planina), which is an extensive karst massif, built predominantly of carbonate rocks (Fig. 1). Presently, tufa precipitations are situated at both studied sites (Kilík, 2008; Gradziński et al., 2013), forming barrages and intervening pools (Figs 2-3), colonized by cyanobacteria, coccoid and filamentous algae, and mosses.

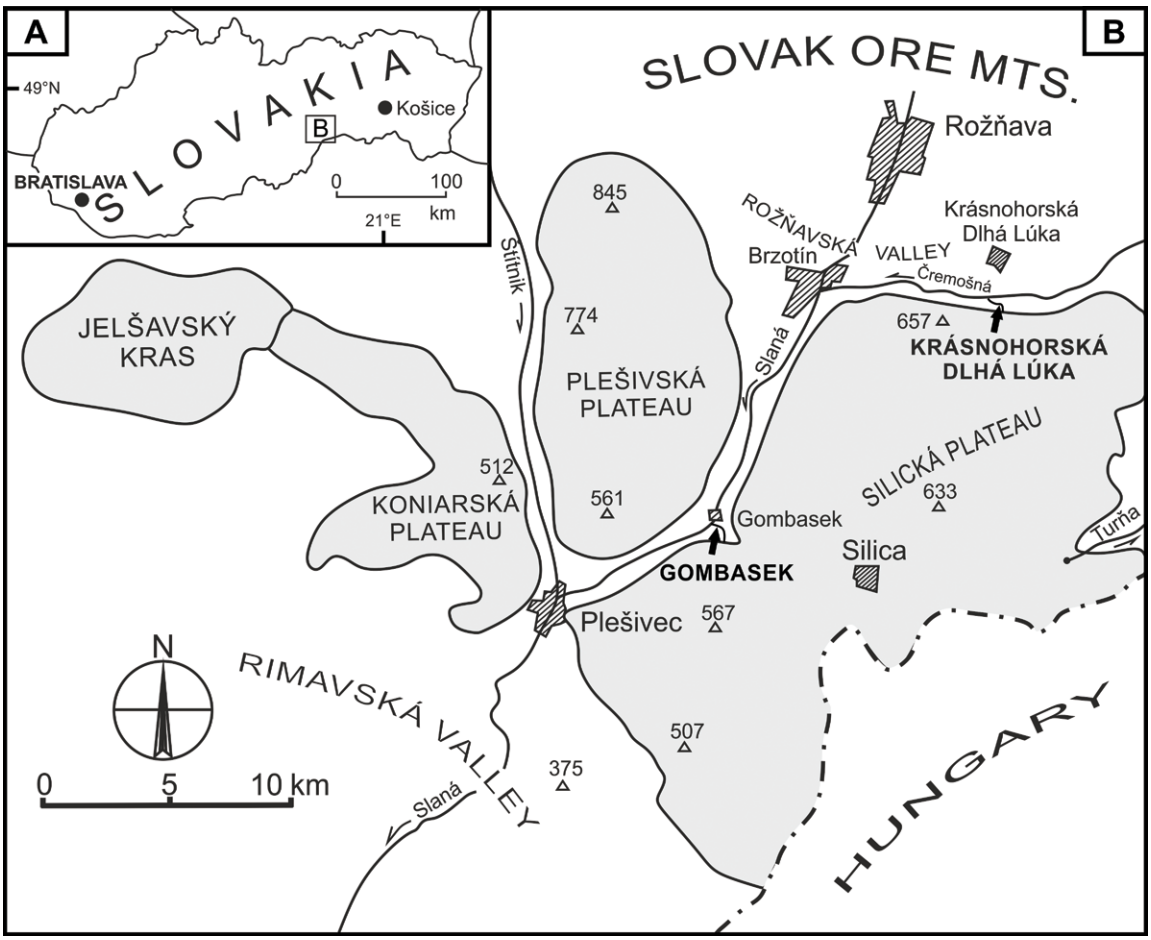

Figure 1. Sampling sites located in the Slovak Karst. A – The map of Slovakia with reference points, B – The collection sites (two streams) are indicated by black arrows.

Figure 2. Barrages and pools in Krásnohorská Dlhá Lúka Village, arrow indicates sampling site.

Figure 3. Barrage colonized by cyanobacteria, algae, and mosses, Gombasek Cottage Settlement site.

Water samples for all analyses were collected from running water. Temperature, pH, dissolved oxygen and conductivity were measured *in situ* with the Barnant 30 pH meter,and DO with the YSI 51B DO meter. The water parameters are listed in Table 1. In the karst water streams, calcium concentrations were high: 125.34 mg/L, the pH was alkaline, from 7.82 to 8.10 (Table 1). The water of Gombasek site (GP) showed high values of SiO_2, whereas the Krásnohorská Dlhá Lúka (KP) site revealed low values. The KP site had high values of conductivity and Mg^{2+} and SO_4^{2-} ions. The physical and chemical conditions in the karstic streams from Slovak Karst, such as: pH, EC, Ca, HCO_3, and TDS, were relatively constant over the sampling period 2011−2013.

Diatom assemblages from different substrates, such as stones, mud, submerged mosses and filamentous algae (*Cladophora glomerata, Vaucheria* sp., *Ulothrix zonata*, *Spirogyra* sp.) were collected from the open water (0.5 × 0.5 m). From the stones (epiphytic), material was scraped using a scalpel; the mud (epipelon) was sampled with a pipette; from submerged mosses, entire portions were cut; and filamentous algae was transferred by hand and placed directly into the same plastic container (with a capacity of 100 mL) as the scraped materials. The collected samples were preserved by adding commercially available, neutralized formalin to the water sample at a rate of about 4%. Light microscope (LM) observation used a Carl Zeiss microscope, Jenamed 2, whereas micrographs were made using a Nikon E 600 Eclipse microscope. The relative abundance of particular taxa and the richness of the species assemblages were estimated on the basis of at least 200 diatoms per sample. For SEM, 10−20 mL aliquots of sample were digested with concentrated H_2O_2 and heated for 24 hours in a sand bath. The sample was allowed to cool and settle and 80−90% of the supernatant was removed by vacuum aspiration. Coating with platinum was accomplished using the BAL-TECMED 020 Modular High Vacuum System for 30 s at 100 mA. Micrographs were digitally processed and plates containing LM and SEM images were prepared using Photoshop CS3 and CorelDRAW X5. Diatoms were identified according to Krammer and Lange-Bertalot (1986, 1991, 2004), Krammer (2002), Lange-Bertalot (2001) and Lange-Bertalot and Wojtal (2014). The diatom ecology, preferences of the species with respect to pH, moisture, and trophy were determined by Van Dam et al. (1994), and the diversity of assemblages was quantified using the H^7 (Shannon-Wiener diversity index).

Statistical Analysis

Data are presented in a three-step scale, where one means species encountered sporadically, two means frequently, and three is a dominant species, and the data were used to calculate H^7 (Shannon-Wiener diversity index). The diversity t test of difference significance between the diversity indexes of studied habitats was performed. Diatom

Table 1. Average of physico-chemical waters parameters in study sites KP and GP during observation period 2011–2013.

Site	pH	EC*	tH_2O	Q**	Ca	Mg	Na	K	HCO_3	SO_4	Cl	SiO_2	TDS†
		[µS/cm]	[ºC]	[L/s]	[mg/L]	[mg/L]	[mg/L]	[mg/L]	[mg/L]	[mg/L]	[mg/L]	[mg/L]	[mg/L]
KP	7.82	617	9.4	179	125.14	10.37	1.19	0.65	368.35	51.77	3.59	4.90	559
GP	8.10	608	8.4	25	125.34	8.50	3.93	4.91	374.86	30.85	10.38	30.99	567

* EC – electric conductivity
** Q – discharge
† TDS – total dissolved solids

assemblages and their relation to environmental variables were examined using principal component analysis (PCA) in PAST, ver. 3.0 (Hammer et al., 2001). Data were analyzed and the factors differentiating studied habitats were determined. Diatoms were subjected to the correspondence variate analysis (CVA), and this analysis was repeated. The CVA analysis was used to determine if there was a difference between the sites in terms of diatom species composition, whereas the second analysis determined whether the correlation between the diatoms occurrence and the kind of substrate is significant. In the first, CVA analysis with environmental data represent a properly constructed file in which information about studied positions was coded. In the second analysis, the substrates of four studied sites was encoded. The file of the species in both cases was the same with the diatom data in a three-point scale. Monte Carlo permutation tests were used to select a set of environmental variables that relate best with species assemblages. The diagram ordination was illustrated by principal component analysis (PCA), where the diatoms' species composition is related to the sites; if the site point is closer to the species point, then there is greater participation of the species in the sample. In the diagrams of the PCA analysis, the environmental variables were presented as the vectors, the sites or substrates as the points, and the species as the triangles. A location of the point near the vector of a given variable indicates that this species prefers the conditions set precisely by this variable. Both of the above, multivariate analysis ordinations (PCA, CVA) were performed using the Canoco 4.5 software (ter Braak & Šmilauer, 2002). The PCA indirect ordination was presented as the diagram of diatom species and their appropriate genera.

Results

A total of 124 diatom species belonging to 39 genera were found in two nameless karst water streams in the Krásnohorská Dlhá Lúka Village and in the Gombasek Cottage Settlement in central-eastern Slovakia (the Silická Plateau). The vast majority of the diatoms were typically epilithic or epiphytic forms, which developed on the stone surfaces, mud, filamentous algae (*Cladophora glomerata, Vaucheria* sp., *Ulothrix zonata, Spirogyra* sp.), and submerged mosses (*Brachythecium rivulare, Polytrichum strictum*, and *Scapania undulata*). Diatom assemblages were dominated by *Gomphonema acuminatum* (25%), *Cocconeis placentula* (12%), and *Frustulia vulgaris* (10%) and are illustrated by LM micrographs. The most frequently encountered diatoms were members of the genera *Pinnularia* (10 species), followed by *Gomphonema* (8), *Eunotia* (7), *Neidium* (7), *Nitzschia* (6), and *Staurosirella* (5). Only five species appeared in four sampling sites: *Paraplaconeis cracoviensis*, *Navicula tripunctata*, *Gomphonema acuminatum*, *Gyrosigma attenuatum* and *Amphora ovalis*.

The rare species *Paraplaconeis cracoviensis* (Fig. 4), which, until now, was only identified in the Kobylanka stream ca. 30 km northwest of Kraków in Poland (sample 6 found by Lange-Bertalot and Wojtal, 2014) as a new species for science was described. This species is characteristic for alkaline springs and streams, mesotrophic, oligo- β-mesosaprobic, calcium-rich waters with moderate-high conductivity. It is also a species occurring in two studied, nameless karst water streams in the Silická Plateau (Slovak Karst).

The most interesting taxa from the ecological point of view were: *Luticola nivalis* from waters with the highest values of calcium (125.34 mg/L) and SiO_2 (30.99 mg/L), *Encyonema ventricosum* and *Gomphonema truncatum* from streams with water of high conductivity.

The frequency occurrence of every recorded taxa was based on the observation of four samples from each site (Table 2). The number of diatom species varied depending on the type of microhabitat substrate specificity; on stones there were 62 species, whereas nearly twice more were on mosses (119). The Shannon-diversity index was 3.0 for stones and 4.6 for mosses. Both microhabitats contained abundant populations of *Cyclotella distinguenda*, *Cymatopleura elliptica*, and *Gomphonema truncatum,* occurring on stones and accompanied by *Cocconeis pediculus* Ehr. Whereas on mosses, there were large populations of *Diploneis krammeri*, *Gyrosigma attenuatum* and *Amphora ovalis*.

The highest species diversity was in the sampling sites GP4.8 and GP4.4, and the lowest on KP3.5 and GP4.7. Site GP4.4 was the most atypical, and characterized by the absence of small species and the presence of many large-size diatoms: *Hantzschia calcifuga*, *Gyrosigma attenuatum, Stauroneis phoenicenteron* and *Frustulia vulgaris*. Green alga *Cladophora glomerata* provides a suitable substrate for colonization by following diatoms: *Cymatopleura distinguenda*,

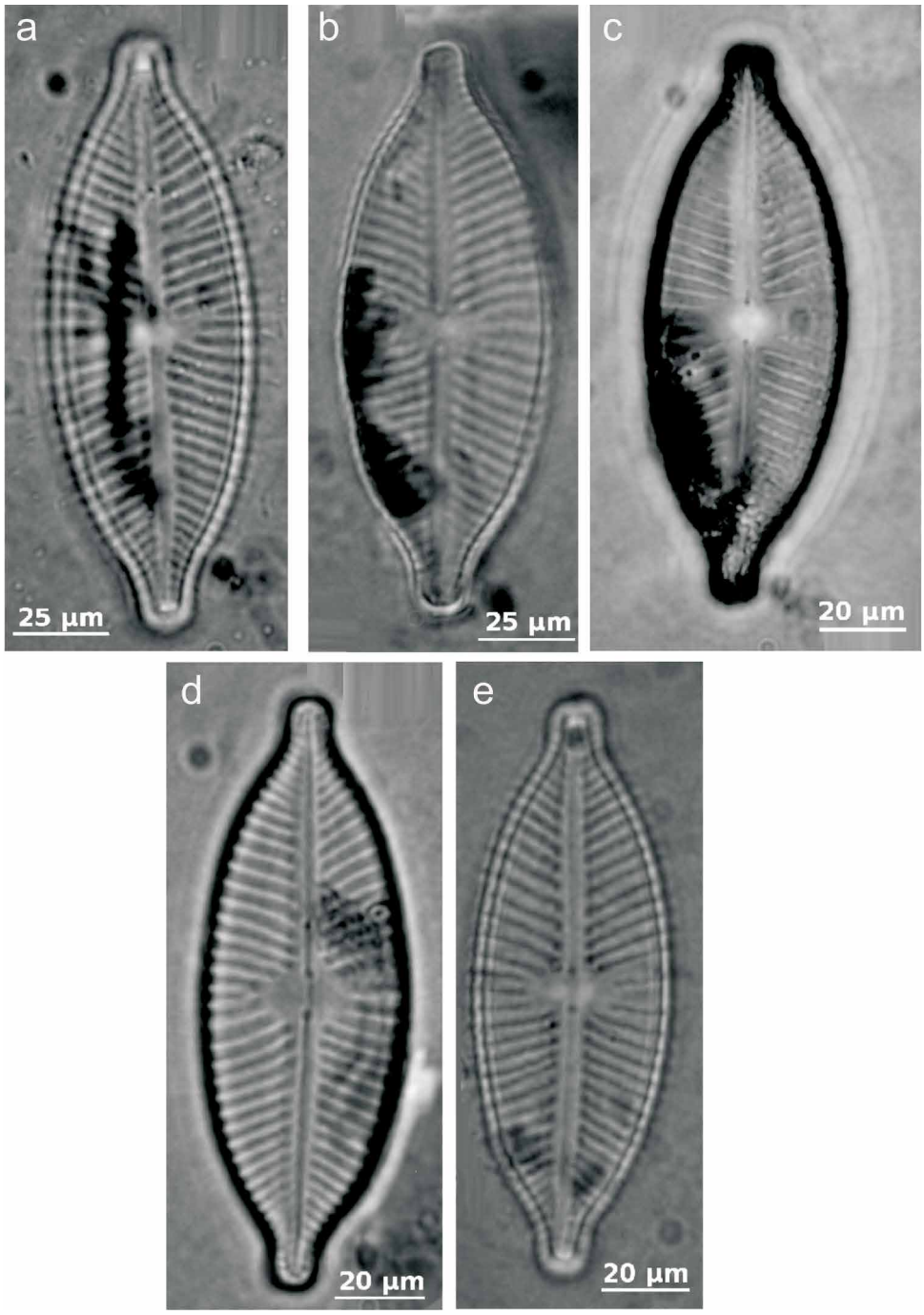

Figure 4, a,b,c,d,e *Paraplaconeis cracoviensis* Lange-Bertalot and Wojtal***, sp. nov. LM***. Light micrographs (LM) of valves from two nameless streams (the Krásnohorská Dlhá Lúka Village and the Gombasek Cottage Settlement). LM views of several specimens showing variation in valve size and shape.

C. elliptica, *C. solea* and *Frustulia vulgaris*. While xanthophyte *Vaucheria* sp. was substrate for species: *Achnanthidium minutissimum, Nitzschia commutata* and *Denticula tenuis*. Other common taxa included: *Navicula tripunctata* (on mud)*, Hantzschia calcifuge* (on filamentous algae) and *Ulnaria biceps* (both on stones and mosses), observed in karst water streams, characteristic for waters neutral to alkaline pH. Among dominating species from the genus *Achnantidium,* e.g. *Achnanthidium minutissimum* prefers waters with circumneutral pH, whereas *A. pyrenaicum* indicated the alkaline waters. *Gomphonema pumilum*, recorded in the material collected from thalli of *Vaucheria sp.,* showed high vitality in environments ranging from mesotrophy to eutrophy.

The Shannon-Wiener diversity index (Fig. 5) was calculated for diatoms, and its highest value *H´* was recorded for site GP 4.8 (*H´* = 4.25), and the lowest for KP 3.5 (*H´* = 4.06). This analysis showed that the significance of the correlation data depends on the substrate type, e.g. *Vaucheria* sp. thalli. The intermediary ordination analysis for the complete data from the four sampling sites was performed. It was concluded that the gradient along first ordination axis is connected with *Eunotia implicata, E. intermedia, E. minor*. On the other side of the axis were the species preferring a different type of substrate. PCA analysis showed a relation between diatom assemblages at each site and selected environmental variables. The first ordination axis accounted for 37.7% of the variation in diatom species composition among sites, and the second ordination axis accounted for 23.5% (Fig. 6). Discrimination analysis was done to determine the species differences between four sampling sites. The results analysis showed that these sites do not differ in terms of diatom species composition. None of the canonical axes were significant in the presented model. Therefore, the analogical CVA analysis was done for the same diatom data, but the substrate was taken into account (Fig. 7). The analysis showed that the significance of the correlation data depends on the substrate type, e.g. *Vaucheria sp.* thalli. The species that preferred this type of substrate were: *Neidium affine*, *Gomphonema acuminatum, G. brebissonii* and *G. truncatum*. This dependent variable was explained by 4.8%, the total data of the variance (Fig. 8). Correlations of remaining substrata with species turned out to be insignificant.

Table 2. Selected diatom species with highest occurrence in seven substrates, such as stone surfaces, mud, submerged mosses and filamentous algae: *Cladophora glomerata, Vaucheria* sp., *Ulothrix* sp., *Spirogyra* sp.

Species	Study Sites																											
	GP 4.7							GP 4.4							KP 35							GP 4.8						
	stone	mud	*Cl.gl*	*V.*	*U.*	*S.*	mosses	stone	mud	*Cl.gl*	*V.*	*U.*	*S.*	mosses	stone	mud	*Cl.gl*	*V.*	*U.*	*S.*	mosses	stone	mud	*Cl.gl*	*V.*	*U.*	*S.*	mosses
Achnanthes sp.	1		1			2		1		2	3				3	1	2				2		3		2	1		3
Achnanthidium affine	2	2	1	1	1	2		2	2	3		1	2	1	1	3			2	2		2		3			3	
Achnantidium minutissimum	2	1		1	1		2	2	1		3				2		3			3		2	1		1			1
Achnantidium minutissima var. *cryptocephala*	2	1	3		2	1	1	1	3	1					2	1	1	2		1	1		1			2	3	3
Achnantidium pyrenaicum		1						1	2	1	1	1							2					2				3
Amphora copulata			1		3		1								2			1				3			3			2
Anomoeoneis sphaerophora	1						2	2		2	2			2			2				2					2		
Aulacoseira ambigua			1			1		1			2				1						1	2						
Brachysira neoexilis				3				1		1			3		3	2			1			2		1		2		
Brachysira vitrea	1		2		2				2	1				3				2		2			2		1			
Caloneis alpestris	2	1									2				2							1						1
Caloneis amphisbaena	1							2				3	2								1					2		
Caloneis silicula	2							2	2					1	2	2	3			2		2		1				3
Caloneis sp.			2			1	2	1			2		2					2					3					
Campylodiscus hibernicus		1			2				2							1						1		2		1		1
Cocconeis pediculus	1			3							1				2				1	2		1						
Co. placentula var. *euglypta*								1		1			1					1			2		2			1		
Craticula cuspidata			2		2				2		2	2		2		2						1		1				
Cyclotella distinguenda	3						3																					
Cyclotella meneghiniana		1				1	2		1								3		1			1				1	2	
Cymatopleura elliptica			3					2							2			2		1	1	2	1			1		3
Cymatopleura solea	2							2			1			1			1					1		1			1	
Cymbella affinis			*2*	*3*	*2*	*1*			*1*							*2*		*2*	*1*			*1*			*1*			*1*
Cymbella aspera	*2*	*1*							*1*	*1*		*2*	*1*				*1*		*1*				*1*			*2*		
Cymbella sp.	1	1					1				1			3	2		1		1		1		1			1		
Denticula tenuis	2		2			1			1	1							1											
Diatoma mesodon	1			2	1		2		1						2							2				1	1	
Diatoma tenuis	2		2					2					1		2					1	1		1			1		1
Diatoma vulgaris	1	1						1				1						2									1	
Diploneis krammeri	2						1	1	1	1	1			2	2						1	3		2				2
Encyonema minutum	1			1		2		2	1								1		1			2				1	1	
Encyonema prostratum					1						2			1		2				1		1		1				1
Encyonema ventricosum	1	1	2					2									1				1		1		2		2	
Epithemia turgida	1						1					2	2			2										1		
Eunotia arcus	3							2	1	1	2				2					3		2	1					

Table 2. (*Continued*).

Species	Study Sites																											
	GP 4.7							GP 4.4							KP 35							GP 4.8						
	stone	mud	*Cl.gl*	*V.*	*U.*	*S.*	mosses	stone	mud	*Cl.gl*	*V.*	*U.*	*S.*	mosses	stone	mud	*Cl.gl*	*V.*	*U.*	*S.*	mosses	stone	mud	*Cl.gl*	*V.*	*U.*	*S.*	mosses
Eunotia exigua				1					2					1			1				1	1			2			
Eunotia implicata	2	1	1							1				2			2			1			2			3		
Eunotia intermedia	1	2	2	2				1			2		2		2			1	1					2			2	
Eunotia maior		2	2		2		1			1			1		2	2	3				2	1			1	1		2
Eunotia paludosa		1		1		3	1	1			2					2					2		1					1
Eunotia praerupta			2					3		1		3			3			1	1					1			1	
Eunotia sp.	3	1		1	1				3								1			3	1				2			
Fragilaria capucina	2				1		1	2			3							2				1			3	1		
Fragilaria crotonensis		1	2	2	2			1					2									2	2			1		2
Fragilaria sp.									3	1				1	1			1		3						2		
Fragilariforma virescens	2		2				3				3	3				1									3			
Frustulia rhomboides	2			1	1			2	3									1						2				
Frustulia vulgaris		1	2			3			3	1							2		1			1				2		3
Gomphonema acuminatum		2		2					2	3	3		2	2		1				3		1	1				1	
Gomphonema angustum			1	2		3		2			1	1		1	1			1		2		1			3			
Gomphonema brebissonii		3			3		3	3		3		3		2		2		2										
Gomphonema clavatum	1	3			1	2	3		2		2							2				2				2		
Gomphonema gracile			2	1				1				3				2							2					1
Gomphonema parvulum		1	1	1	3		3	2		3		3		3	2				1					1				
Gomphonema pumilum			1	1		1		1	2		2	2	2										1	2		2	1	
Gomphonema truncatum	2				1			2	1	3	2				2		3			2		1			3	2		
Gomphonema sp.	1				1							3	2				2				1			1				2
Gyrosigma acuminatum	1	1		2			3			1	1				1		1					2	1			1	1	
Gyrosigma attenuatum	2					2				2	1							2	1				1	2	3			
Gyrosigma obtusatum			2		2			1	1	3	1	2		3		2		2	2	1			1		3	2		
Hantzschia amphioxys				1							2			1	1	2						3					1	
Hantzschia calcifuga			1		2			2		2	1					1			1		2		3		1	1		
Luticola nivalis		1				2		3		3		2					2					2				1		1
Melosira varians	1		1					1	1		1		3		1					1		1						
Meridion circulare var. *constrictum*	2			1	2			1	2		3			1	2				2			2			3			
Navicula angusta	1						3	1		3		2		1		2							1	1				
Navicula tripunctata		1				1			1					1				1				1			2	2		1
Navicula sp.			1		2				1						1				1									
Neidium affine				2				3	1		1	1					1				2				3			
Neidium alpinum			1			1			1						2			2					2					1

Table 2. (*Continued*).

Species	Study Sites																							
	GP 4.7							GP 4.4							KP 35							GP 4.8						
	stone	mud	*Cl.gl*	*V.*	*U.*	*S.*	mosses	stone	mud	*Cl.gl*	*V.*	*U.*	*S.*	mosses	stone	mud	*Cl.gl*	*V.*	*U.*	*S.*	mosses	stone	mud	*Cl.gl*	*V.*	*U.*	*S.*	mosses
Neidium ampliatum		1			2					1	2					3			1			1		2		1		
Neidium dubium			1		3			1						2	1		2					1	1					
Neidium productum		2				1	3		3			2			1				2	2		1				3		2
Nitzschia commutata	2		2		2			1	2		1	1					2				2							
Nitzschia dubia	2	1		3						1	2				2			1			1	1						
Nitzschia gracilis	1				3			1				1	2			2				1	1			1	2			
Nitzschia linearis			1						1					3		1			2		2	1	1					2
Nitzschia sp.	3	1		3		1	1		1		1			2		1					1				3			
Paraplaconeis cracoviense	3	3	2	2			2	3			3	1			3			1	3	2			2	3				2
Pinnularia borealis	1	1	2					2	3	1	3			2	1				1	1				1		1		
Pinnularia gibba	2	2	2		3	1	3	1						1	2			2		2		1		2	2			
Pinnularia interrupta		1		1				1				1				1				1			1					2
Pinnularia macilenta	3		1					1			3				2				1			2			3			
Pinnularia neomaior	2	1	1			1		1		1			3		1		2					2			1			
Pinnularia mesolepta		2							3	1				2		2		1				2						2
Pinnularia microstauron	2	1		1	3					2					3				1	2		2	1			2	3	
Pinnularia viridis	2		1				3				2			1	1					1								
Pinnularia sp.		2		1		1		1		3					3			1	1				1		3			
Placoneis anglica		1		2			2		3								3			1		1		2	1			1
Planothidium lanceolatum	2	1		2				1		2		1	3		1							2						
Rhoicosphaenia abbreviata	1		1			1					1			1						1		1		2		2		
Sellaphora pupula	2		3	1				2								2			1			2			3			1
Stauroneis agrestis		1		2		1		1		2		2			1			1					1			1		
Stauroneis anceps		1	1	1					3						1					1							1	
Stauroneis construens	2		1		3	2			2		1			2		2		1	1			2	1			1		
Stauroneis phoenicenteron		1		1						1																		
Staurosirella leptostauron var. *leptostauron*		1		2				2		2			2		2							2	11		2			1
Surirella angusta							3	1				2				2		1	2			1			1	2		
Surirella brebissonii				2						2	2			3			1					1						
Surirella sp.		1	1			2		1	1		2					2				1				2	1	1	1	1
Tabellaria fenestrata	2				3			2		2					2			2	2			2						
Tabelaria flocculosa	2			2				2					3		2		1					2	3		3	3		
Tabelaria ventricosa		1		1				2				2				1							1		2		2	
Ulnaria biceps			1					1		1					1					1				1				
Ulnaria ulna	2		1		3	2	1	1	1	2	1			3			1	2	2	1		2		1		1		1

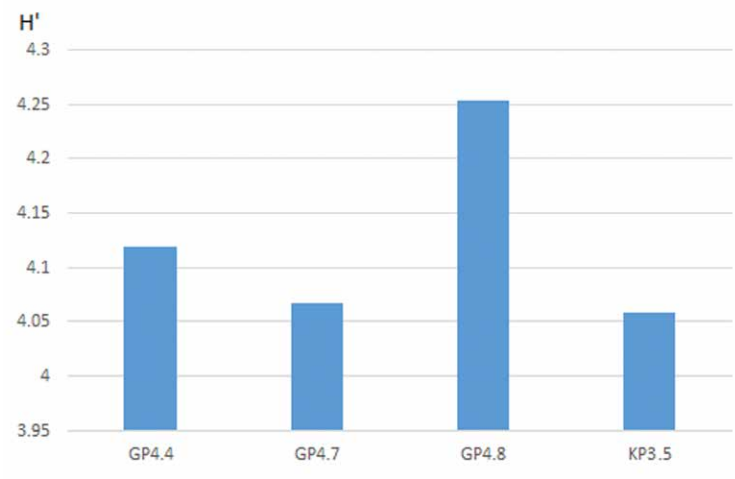

Figure 5. The Shannon diversity index for diatoms from four sites (GP4.4, GP4.7, GP4.8, KP3.5). The only statistically significant difference was between sites KP3.5 and GP4.8 ($p < 0.005$, Kruskal-Wallis test).

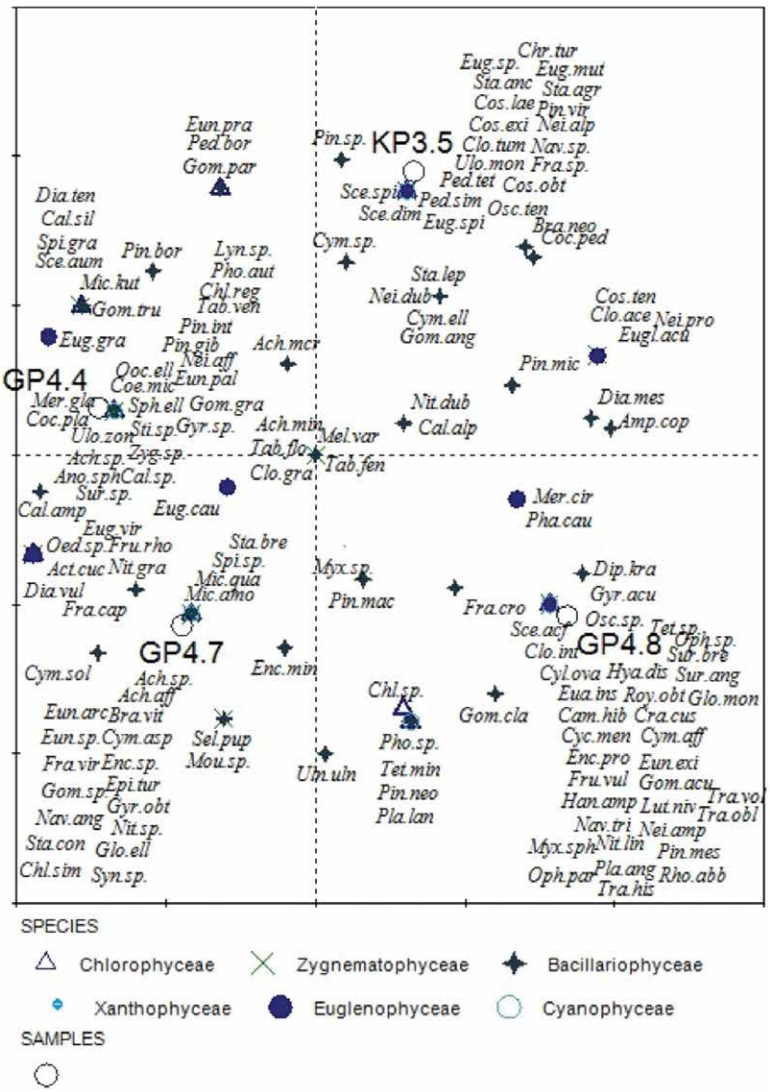

Figure 6. Principal component analysis (PCA) for the diatom assemblages in four sites (GP4.4, GP4.7, GP4.8, KP3.5). The first ordination axis accounted for 37.7% of the variation in diatom species composition among sites. Abbreviations of species names in Fig. 6 consist of three letters of a generic name and three letters of a species name.
Abbreviations of species names: *Achnanthes* sp. (Ach. sp.); *Achnanthidium affine* (Ach. aff.); *Achn.`minutissimum* (Ach. min.); *Achn. minutissima* var. *cryptocephala* (Ach. cry.); *Achn. pyrenaicum* (Ach. pyr.); *Amphora copulata* (Amp. cop.); *Anomoeoneis sphaerophora* (Ano. sph.); *Aulacoseira ambigua* (Aul. amb.); *Brachysira neoexilis* (Bra. neo.); *Brachysira vitrea* (Bra. vit.); *Caloneis alpestris* (Cal. alp.); *Caloneis amphisbaena* (Cal. amp.); *Caloneis silicula* (Cal. sil.); *Caloneis* sp. (Cal. sp.); *Campylodiscus hibernicus* (Cam. hib.); *Cocconeis pediculus* (Coc. ped.); *Cocconeis placentula* var. *euglypta* (Coc. eug.); *Craticula cuspidata* (Cra. cus.); *Cyclotella distinguenda* (Cyc. dis.); *Cyclotella meneghiniana* (Cyc. men.); *Cymatopleura elliptica* (Cyc. ell.); *Cyclotella solea* (Cyc. sol.); *Cymbella affinis* (Cym. aff.); *Cymbella aspera* (Cym. asp.); *Cymbella* sp. (Cym. sp.); *Denticula tenuis* (Den. ten.); *Diatoma mesodon* (Dia. mes.); *Diatoma tenuis* (Dia. ten.); *Diatoma vulgaris* (Dia. vul.); *Diploneis krammeri* (Dip. kra.); *Encyonema minutum* (Enc. min.); *Encyonema prostratum* (Enc. pro.); *Encyonema ventricosum* (Enc. ven.); *Epithemia turgida* (Epi. tur.); *Eunotia arcus* (Eun. arc.); Eunotia *exigua* (Eun. exi.); *Eunotia implicata* (Eun. imp.); *Eunotia intermedia* (Eun. int.); *Eunotia maior* (Eun. mai.); *Eunotia paludosa* (Eun. pal.); *Eunotia praerupta* (Eun. pre.); *Eunoti* sp. (*Eun.* sp.); *Fragilaria capucina* (Fra. cap.); *Fragilaria crotonensis* (Fra. cro.); *Fragilaria* sp. (Fra. sp.); *Fragilariformis virescens* (Fra. vir.); *Frustulia rhomboides* (Fru. rho.); *Frustulia vulgaris* (Fru. vul.); *Gomphonema acuminatum* (Gom. acu.); *Gomphonema angustum* (Gom. ang.); *Gomphonema brebissonii* (Gom. bre.); *Gomphonema clavatum* (Gom. cla.); *Gomphonema gracile* (Gom. gra.); *Gomphonema parvulum* (Gom. par.); *Gomphonema pumilum* (Gom. pum.); *Gomphonema truncatum* (Gom. tru.); *Gomphonema* sp. (Gom. sp.); *Gyrosigma acuminatum* (Gyr. acu.); *Gyrosigma attenuatum* (Gyr. att.); *Gyrosigma obtusatum* (Gyr. obt.); *Hantzschia amphioxys* (Han. amp.); *Hantzschia calcifuga* (Han. cal.); *Luticola nivalis* (Lut. niv.); *Melosira varians* (Mel. var.); *Meridion circulare* var. *constrictum* (Mer. cir.); *Navicula angusta* (Nav. ang.); *Navicula tripunctata* (Nav. tri.); *Navicula* sp. (Nav. sp.); *Neidium affine* (Nei. aff.); *Neidium alpinum* (Nei. alp.); *Neidium ampliatum* (Nei. aml.); *Neidium dubium* (Nei. dub.); *Neidium productum* (Nei. prod.); *Nitzschia commutata* (Nit. *com.*); *Nitzschia dubia* (Nit. dub.); *Nitzschia gracilis* (Nit. grac.); *Nitzschia linearis* (Nit. lin.); *Nitzschia* sp. (Nit. sp.); *Paraplaconeis cracoviense* (Par. cra.); *Pinnularia borealis* (Pin. bor.); *Pinnularia gibba* (Pin. gib.); *Pinnularia interrupta* (Pin. int.); *Pinnularia macilenta* (Pin. mac.); *Pinnularia neomajor* (Pin. neo.); *Pinnularia mesolepta* (Pin. mes.); *Pinnularia microstauron* (Pin. mic.); *Pinnularia viridis* (Pin. vir.); *Pinnularia* sp. (Pin. sp.); *Placoneis anglica* (Pla. ang.); *Planothidium lanceolatum* (Pla. lan.); *Rhoicosphaenia abbreviata* (Rho. abb.); *Selaphora pupula* (Sel. pup.); *Stauroneis agrestis* (Sta. agr.); *Stauroneis anceps* (Sta. anc.); *Stauroneis construens* (Sta. con.); *Stauroneis phoenicenteron* (Sta. pho.); *Staurosirella leptostauron* var. *leptostauron* (Sta. lep.); *Surirella angusta* (Sur. ang.); *Surirella brebissonii* (Sur. bre.); *Surirella* sp. (Sur. sp.); *Tabellaria fenestrata* (Tab. fen.); *Tabellaria flocculosa* (Tab. flo.); *Tabelaria ventricosa* (Tab. ven.); *Ulnaria biceps* (Uln. bic.); *Ulnaria ulna* (Uln. uln.).

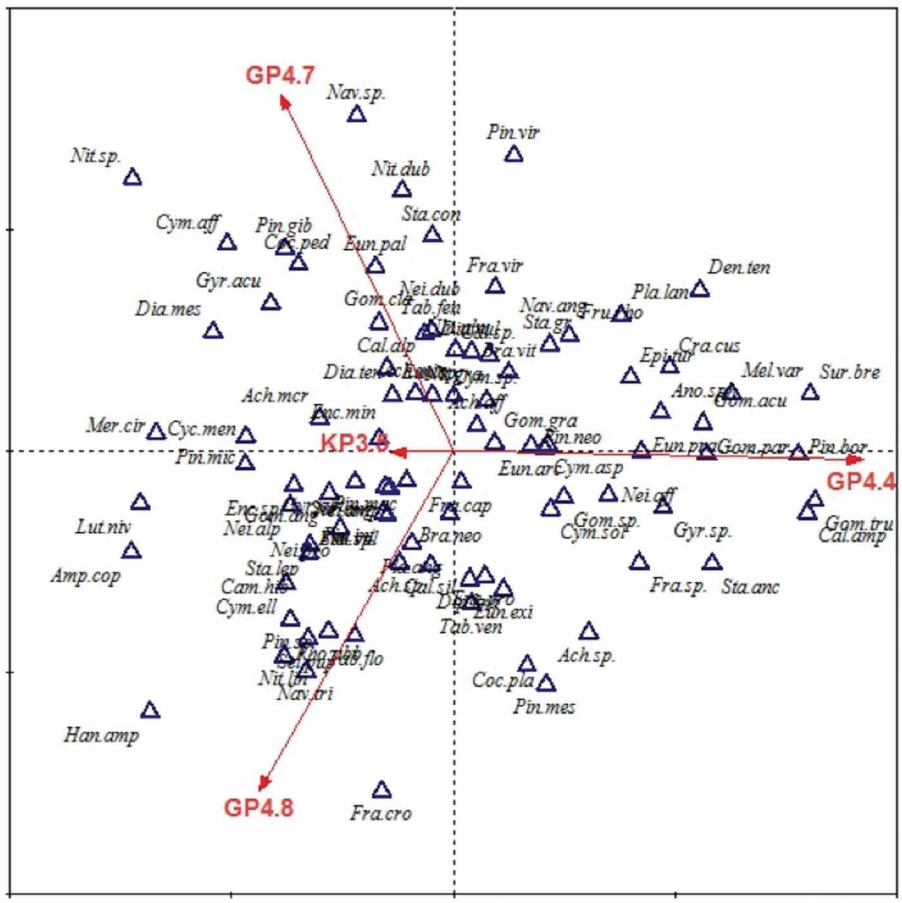

Figure 7. Canonical variates analysis (CVA) of diatoms species composition was done on four sites (GP4.4, GP4.7, GP4.8, KP3.5). The differentiation along the 1st axis was not statistically significant (F = 1.08, p = 0.7). Names of species - see abbreviations Fig. 6.

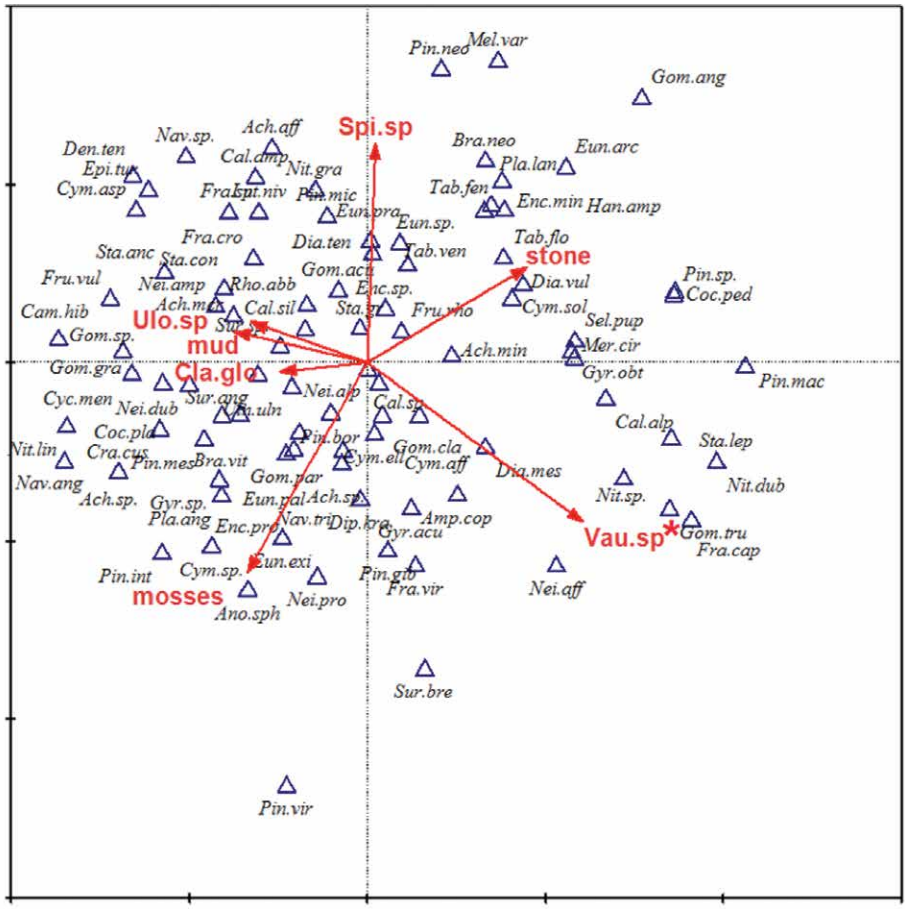

Figure 8. Canonical variates analysis (CVA) of diatoms on diversified substratum: stone, mud, mosses and filamentous algae (*Cladophora glomerata* – Cla. glo.; *Vaucheria* sp. – Vau. sp.; *Ulothrix* sp. – Ulo. sp.; *Spirogyra* sp. – Spi. sp.). Diversification along first canonical axis was statistically significant (F = 1.4, p = 0.02). The only variable differentiating data was *Vaucheria sp.* thalli (Monte Carlo test, p = 0.03). The variable marked with an asterisk explains 4.8% of the total variability. Names of species - see abbreviations, Fig. 6.

Discussion

Although observational studies like ours limit the assessment of mechanisms, the individual and collective patterns emerging from environmental, biological and spatial factors, and their shared variance, provided us with further detailed insight into what factors determine the structure of diatom assemblages in the karst water streams of the Slovak Karst. The inclusion of the biological component was particularly relevant. It helped to increase our understanding of the potential role of biological interactions at the microhabitats scale in karstic streams, for which our current knowledge is still limited. Studies on diatom biodiversity in the karst water streams of Slovak Karst are important because these microhabitats are considered to be more sensitive toward the structure of the substrate than the typical streams (Cantonati, 1998; Poulíčková et al., 2004; Buczkó, 2006). According to our knowledge, there are not many studies about karst phenomena and photosynthetic organisms. The indices of biotic integrity in this study revealed high species richness, diversity, and balanced distribution of the diatom species assemblages. The composition of natural karst water streams is related to factors such as the weathering resistance of carbonate rocks, reflected mainly in total mineral content (Wojtal and Sobczyk, 2012).

Generally, it is important to recognize the substrate and to understand mechanisms of tufa calcification in karst waters. Stones and filamentous algae are two of the most common substrates in fast-running waters, which are rare in the karstic areas. In our two karst streams in central-eastern Slovakia, macroalgae, such as *Cladophora, Vaucheria*, *Ulothrix* and *Spirogyra,* were relevant substrates for development of diatom assemblages, compared to the results of Wojtal and Sobczyk (2012), suggesting that two kinds of strata, epilithic and bryophytic, influenced the diatom assemblages and could provide data useful for water-quality monitoring. Barbiero (2000) observed epilithic diatoms on natural and artificial substrates and determined that the differences between the substrates were insignificant.

Diatom assemblages in karst water streams were dominated by *Pinnularia, Gomphonema* and *Achnanthidium* species. The widespread distribution of adnate species *Achnanthidium minutissimum* and *A. pyrenaicum* may indicate the importance of the physical environment in controlling biotic assemblages (Weilhoefer and Pan, 2006). *Achnanthidium minutissimum,* found in two karst water streams, is considered to represent a benthic periphytic habitat, however it has also been reported as tychoplanktonic or planktonic (Ehrlich, 1995). Krammer and Lange-Bertalot (1991) and Poulíčková et al. (2017) noted that *A. minutissimum* is one of the most frequently occurring diatoms in freshwater benthic samples. This species was reported from alkaline and acidic, oligotrophic and hypertrophic waters, and its apparent ubiquity is puzzling; and therefore, sometimes questioned (Round et al., 1990). Potapova and Hamilton (2007) concluded from SEM observations that ultrastructural characters do not discriminate among taxa within the *Achnanthidium minutissimum* complex.

The relatively large species richness generally confirms the findings of other studies carried out in the Wyżyna Krakowsko-Częstochowska Upland (Poland). This karst is formed in Upper Jurassic calcareous rock, where Wojtal (2009) described 307 taxa from Kobylanka stream, while Kawecka (2012) found 414 species in 27 karst streams in the Tatra National Park. The karst springs diatom epilithic assemblages in Bosnia and Herzegovina were studied by Dedić et al. (2015). Lai et al. (2016) also noted epilithic diatom assemblages in a karst spring of Sardinia (Italy) and confirmed ecological potential of the karst features. In relation to trophy, diatoms of a wide ecological spectrum, from oligo- to eutrophic, were most frequent in the typical streams but rare in the karst streams. Diatoms are a significant constituent of epilithic assemblages in karst water streams of central-eastern Slovakia.

Our studies contribute to improving the knowledge of the diatoms in the Slovak Karst and suggested that all kinds of substrates can be successfully inhabited by diatoms. Hall and Smol (1999) mentioned that the diatom assemblages on various substrates become uniform in meso- and eutrophic waters, where there is nutrient limitation. The general variability of the karstic streams environment in central-eastern Slovakia play a very important role in determining the distribution of diatoms. In all cases, our study showed that diatom assemblages in karst water streams of the Slovak Karst required ecological monitoring. However, spatial gradients were also evident over these relatively small microhabitats, which may reflect high dispersal effects, although biotic factors have largely been overlooked in karst water stream studies at similar or larger spatial scales. Our data offered that it seems to be crucial to assess an effect of biotic factors on diatom assemblage structure in addition to environmental and spatial indicators. On the other hand, we could risk underestimating the total conservation of these diatom assemblages.

Conclusions

In two nameless karstic streams of the Slovak Karst (Krásnohorská Dlhá Lúka Village and Gombasek Cottage Settlement), 124 species on seven substrates, such as stones, mud, submerged mosses and filamentous algae, i.e., *Cladophora glomerata, Vaucheria* sp., *Ulothrix* zonata, and *Spirogyra* sp., were observed. Both species richness and Shannon-Wiener indices showed congruent biotic integrity. The diatom assemblages were mostly structured by environmental factors, calcium and pH gradients, confirmed by canonical variates analysis (CVA) and Monte Carlo permutation tests. The unique spatial and biological gradients, specific to different guilds related to each other, were also evident. The Slovak karstic streams should be especially protected and regularly monitored.

Acknowledgments

The authors wish to express their gratitude to Anna Wojciechowska for statistical comments. We also thank two reviewers for valuable comments on the manuscript. This research was supported by the National Science Centre under Grant N N307 600640.

References

Aboal, M., Prefasi, M. and Asencio, M.D., 1996, The aquatic microphytes and macrophytes of the Transvase Tajo-Segura irrigation system, southeastern Spain: Hydrobiology, v. 340, no. 1−3, p. 101−107.

Arp, G., Bissett, A., Brinkmann, N., Cousin, S., de Beer, D., Friedl, T., Mohr, K., Neu, T.R., Reimer, A., Shiraishi, F., Stackebrandt, E. and Zippel, B., 2010, Tufa-forming biofilms of German karstwater streams: microorganisms, exopolymers, hydrochemistry and calcification, *in* Rogerson, M. and Pedly, M.M., eds., Tufas and Speleotherms: Unravelling the Microbial and Physical Controls: Geological Society, London, Special Publication, v. 336, p. 83−118. https://doi.org/10.1144/SP336.6.

Barbiero, R.P., 2000, A multi-lake comparison of epilithic diatom communities on natural and artificial substrates: Hydrobiology, v. 438, p. 157−170.

Bellinger, B.J., Cocquyt, Ch. and O'Reilly, Ch.M., 2006, Benthic diatoms as indicators of eutrophication in tropical streams: Hydrobiology, v. 573, p. 75−87. https://doi.org/10.1007/s10750-006-0262-5.

Brinkmann, R. and Parise, M., 2012, Karst environments: problems, management, human impacts, and sustainability an introduction to the special issue: Journal of Cave and Karst Studies, v. 7, p. 135−136. https://doi.org/10.4311/2011JCKS0253.

Buczkó, K., 2007, The occurrence of the epiphytic diatom *Lemnicola hungarica* on different European Lemnaceae species: Fottea, v. 7, p. 77−84. https://doi.org/10.5507/fot.2007.007

Cantonati, M., 1998, Diatom communities of springs in the southern Alps: Diatom Research, v. 13, p. 210-220.

Dedić, A., Plenković-Moraj, A., Borojević, K.K. and Hafner, D., 2015, The first report on periphytic diatoms on artificial and natural substrate in the karstic spring Bunica, Bosnia and Herzegovina: Acta Botanica Croatia, v. 74, no. 2, p. 393−406.

Ehrlich, A., 1995, Atlas of the Inland-Water Diatom Flora of Israel: Israel Academy of Sciences and Humanities, Jerusalem.

Ford, D.C. and Williams, P., 2007, Karst Hydrology and Geomorphology: John Wiley and Sons, Chichester, UK.

Gradziński, M., Hercman, H., Jaśkiewicz, M. and Szczurek, S., 2013, Holocene tufa in the Slovak Karst: facies, sedimentary environments and depositional history: Geological Quarterly, v. 57, p. 769−788.

Hall, R.I. and Smol, J.P., 1999, Diatoms as indicators of lake eutrophication, *in*: Stoermer, E.F. and Smol, J.P., eds., The Diatoms: Applications for the Environmental and Earth Sciences: Cambridge University Press, Cambridge, p. 128−168.

Hammer, Ø., Harper, D.A.T. and Ryan, P.D., 2001, Past: paleontological statistics software package for education and data analysis: Palaeontologia Electronica, v. 4 no. 1, p. 1−9.

Heino, J., Bini, L.M., Karjalainen, S.M., Mykrä, H., Soininen, J., Vieira, L.C.G. and Diniz-Filho, J.A.F., 2010, Geographical patterns of micro-organismal community structure: are diatoms ubiquitously distributed across boreal streams? Oikos, v. 119, p. 129−137. https://doi/10.1111/j.1600-0706.2009.17778.

Kawecka, B., 2012, Diatom diversity in streams of the Tatra National Park (Poland) as indicator of environmental conditions: W. Szafer Institute of Botany, Polish Academy of Sciences, Kraków.

Kilík, J., 2008, Calcareous tufa in Slovak Karst: Naturae Tutela, v. 12, p. 177−184.

Krammer, K., 2002, Cymbella, *in* Lange-Bertalot, H., ed., Diatoms of Europe 3, A.R.G. Gantner Verlag K.G. Ruggell, p. 31−89.

Krammer, K. and Lange-Bertalot, H., 1986, Bacillariophceae. 1. Naviculaveae, *in* Ettl, H., Gerloff, J., Heyning, H. and Mollenhauer, D., eds., Süßwasserflora von Mitteleuropa, 2/1: Gustav Fischer Verlag, Stuttgart, p. 759.

Krammer, K. and Lange-Bertalot, H., 1991, Bacillariophceae. 4. Achnanthaceae, Kritische Ergänzungen zu *Navicula* (Lineolatae) und *Gomphonema,* Gesamtliteraturverzeichnis Teil 1-4, *in*: Ettl, H., Gerloff, J., Heyning, H. and Mollenhauer, D., eds., Süßwasserflora von Mitteleuropa 2/4: Gustav Fischer Verlag, Stuttgart., p. 554.

Krammer, K. and Lange-Bertalot, H., 2004, Bacillariophceae. 3. Centrales, Fragilariaceae, Eunotiaceae, *in*: Ettl, H., Gerloff, J., Heyning, H. and Mollenhauer, D., eds., Süßwasserflora von Mitteleuropa 2/3, Spektrum Akademischer Verlag Heidelberg, Berlin, p. 345.

Lai, G., Padedda, B.M., Wetzel, C.E., Luglié, A., Sechi, N. and Ector, L., 2016, Epilithic diatom assemblages and environmental quality of the Su Gologone karst spring (central-eastern Sardinia, Italy): Acta Botanica Croatica, v. 75, no. 1, p. 129−143. https://doi/10.1515/botcro-2016-0008.

Lange-Bertalot, H., 2001, Navicula sensu stricto. 10 genera separated from Navicula sensu lato. Frustulia, *in*: Lange-Bertalot, H., ed., Diatoms of Europe 2, A.R.G. Gantner Verlag K.G. Ruggell.

Lange-Bertalot, H. and Wojtal, A.Z., 2014, Diversity in species complexes of *Placoneis clementis* (Grunow) Cox and *Paraplaconeis placentula* (Ehrenberg) Kulikovskiy, Lange-Bertalot and Metzeltin: Nova Hedwigia, v. 143, p. 403−420.

Potapova, M., Charles, D.F., Ponander, K.C. and Winter, D.M., 2004, Quantifying species indicator values for trophic diatom indices: A comparison of approaches: Hydrobiology, v. 517, p. 25−41.

Potapova, M. and Hamilton, P.B., 2007, Morphological and ecological variation within the *Achnanthidium minutissimum* (Bacillariophyceae) species complex: Journal of Phycology, v. 43, p. 561−575. https://doi/10.1111/j.1529-8817.2007.00332.

Poulíčková, A., Hájková, P., Krenková, P. and Hájek, M., 2004, Distribution of diatoms and bryophytes on linear transect through spring fens: Nova Hedwigia, v. 78, p. 411−424.

Pouličková, A., Letáková, M., Hašler, P., Cox, E. and Duchoslav M., 2017, Species complexes within epiphytic diatoms and their relevance for the bioindication of trophic status: Science of The Total Environment, v. 599−600, p. 820−833. https://doi.org/10.1016/j.scitotenv.2017.05.034.

Round, F.E., Crawford, R.M. and Mann, D.G., 1990, The diatoms. Biology and morphology of the genera: Cambridge University Press, Cambridge.

Smol, J.P. and Stoermer, E.F., 2015, The Diatoms: Applications for the Environmental and Earth Sciences: 2nd Ed, Cambridge University Press, Cambridge.

ter Braak, C.J.F. and Šmilauer, P., 2002, CANOCO reference manual and CanoDraw for Windows user's guide: software for canonical community ordination (version 4.5): Biometrics, Wageningen and Česke Budéjovice.

Van Dam, H., Mertens, A. and Sinkeldam, J., 1994, A coded checklist and ecological indicator values of freshwater diatoms from the Netherlands: Netherlands Journal of Aquatic Ecology, v. 28, no. 1, p. 117−133.

Weilhoefer, Ch.L. and Pan, Y., 2006, Diatom assemblages and their associations with environmental variables in Oregon Coast Range streams, USA: Hydrobiology, v. 561, p. 207−219. https://doi.org/10.1007/1-4020-5070-4_15.

White, W.B., 1988, Geomorphology and Hydrology of Karst Terrains: University Press, New York, Oxford.

Wojtal, A.Z., 2009, The diatoms of Kobylanka stream near Kraków (Wyżyna Krakowsko-Częstochowska Upland, S Poland): Polish Botanical Journal, v. 54, no. 2, p. 129−330.

Wojtal, A.Z. and Sobczyk, Ł., 2012, The influence of substrates and physicochemical factors on the composition of diatom assemblages in karst springs and their applicability in water-quality assessment: Hydrobiology, v. 695, p. 97−108.

M. Rossi, G. Santi, R. Zorzin, D. Döppes, R. Friedrich, S. Lindauer, and W. Rosendahl. The first directly dated cave bear from the Covoli di Velo Cave (Verona Province, Veneto, northern Italy) with some discussion of Italian Alps cave bears. *Journal of Cave and Karst Studies*, v. 80, no. 3, p. 145-152. DOI:10.4311/2017PA0111

THE FIRST DIRECTLY DATED CAVE BEAR FROM THE COVOLI DI VELO CAVE (VERONA PROVINCE, VENETO, NORTHERN ITALY) WITH SOME DISCUSSION OF ITALIAN ALPS CAVE BEARS

Mario Rossi[1], Giuseppe Santi[2, C], Roberto Zorzin[5], Doris Döppes[3], Ronny Friedrich[4], Susanne Lindauer[4], and Wilfried Rosendahl[3]

Abstract

Absolute dates of cave bears from Northern Italy are rare. The first radiocarbon date from Covoli di Velo Cave (Verona Province, Veneto, N. Italy) from a cave bear first phalanx is reported; its value is 29,130 ± 0.90 ^{14}C yr BP. The date, combined with morphological features of dentition suggest that cave bear populations that lived in Northern Italy were relatively underived compared to other European populations, hinting at patters of migration. Comparison of dental morphology suggest that the Covoli di Velo bear is *Ursus spelaeus*.

Introduction

In recent years, knowledge of the paleobiology of the cave bear (*Ursus spelae*us Rosenmüller, 1794) has greatly expanded. This is a consequence of numerous studies on the morphometry (historically the most common study) on the morphodynamics of the dentition (i.e. Torres, 1988 a-f; Withalm, 2001; Rabeder, 1999, 2014; Grandal d'Anglade and López-González, 2004; Sabol, 2005; Tsoukala et al., 2006; Baryshnikov and Puzachenko, 2011; 2017; Cvetković and Dimitrijević, 2014; Frischauf, 2014; Robu, 2016; Plichta et al., 2017), absolute dating, as well as genetics (Hofreiter et al., 2002; Orlando et al., 2002; Rabeder et al., 2004; Pacher and Stuart, 2008; Spötl et al., 2014, 2017; Martini et al., 2014; Döppes et al., 2016, 2018; Baca et al., 2016, 2017; Fortes et al., 2017; Gretzinger et al., 2017; Terlato et al., 2018 and so on). The most important results of this knowledge have been to modify the phylogenetic tree of the cave bear. In fact, when considering overall the genetic data, different species of cave bears have been identified (*Ursus ingressus*, *U. spelaeus eremus* and *U. spelaeus ladinicus*) (Rabeder et al., 2004) with their distribution throughout Europe (Doppes et al, 2018). In Italy, morphometric and morphodynamic studies are numerous (i.e. Santi and Rossi, 2001, 2014; Santi et al., 2003, 2011; De Carlis et al., 2005; Rabeder et al., 2004), but genetic studies and reports on absolute dating are very rare. With this in mind, the present study presents the results of the first absolute dating with ^{14}C (authorization MBAC-SBA-VEN 05 0015108 19/11/2014), performed on the first phalanx of *U. spelaeus* found in recent surveys coordinated by one of the Authors (R.Z.), in sector B L1/Z2 sup. 1 of the excavation in the Covoli di Velo Cave (Grotta inferiore) (Verona, Veneto) (cadastral number 44 V VR) (Fig. 1 A). The specimen (I.G.VR 63925) is stored in the Department of Geology and Paleontology, Civic Museum of Natural History of Verona (Veneto region, Northern Italy). This new information greatly improves the state of knowledge gathered in prior excavations (Bona et al., 2006).

Covoli di Velo Cave: Research History

Since the 18th Century, Covoli di Velo Cave has been the object of study by the most important noted naturalists of the Verona area. The first definite report of this site goes back to the late 1700's, when the Abbot Fortis, in a letter (24 September 1785) sent to the Count de Cassini, (Fortis, 1786) described and identified the bones from the cave as "amfibj" (amphibians). A few years later, Serafino Volta (1796) corrected Fortis, proposing that the bones belonged to continental animals. Later, Catullo (1844) visited the cave confirming the presence of a lot of bones, and Massalongo (1851) accurately described both the Covoli di Velo Cave geology and added to the collection of fossils from the site. With his precisely detailed description of the Covoli di Velo Cave, Massalongo proposed some hypotheses supported by tables and by beautiful illustrations, on the origin of both the cave and bones. Although some of the hypotheses were not accurate, the study by Massalongo is considered the first scientific study on the Covoli di Velo Cave.

Omboni (1875) published an important memoir about this cave in which he described and illustrated various paleontological remains. He pointed out the problem of the lack of research and of excavations using scientific methods, and that this created a risk of lost scientific knowledge about the history and taphonomy of the accumulated fossils. Omboni also mentioned the problem of illegal excavations, which went on for decades and ruined a significant amount of paleontological data. In fact, while some scientists gathered a paltry number of fossils, the locals (Benetti and Cristoferi, 1968; Benetti and Sauro, 1999) made profits by selling cave sediments as topsoil, and sold the bones, whole or

[1]Department of Geology and Paleontology, Civic Museum of Natural History, Lungadige Porta Vittoria 9, I-37129 Verona, Italy
[2]Department of Earth and Environmental Science, University of Pavia, Via Ferrata 1, I-27100 Pavia, Italy
[3]Reiss-Engelhorn-Museen, Zeughaus C5, 68159 Mannheim, Germany
[4]Curt-Engelhorn-Zentrum Archäometrie gGmbH, D6, 3, D-68159 Mannheim, Germany
[5] Geologist freelance, Verona, Italy
[C] Corresponding Author: gsanti@unipv.it

crushed, as good fertilizer. For these reasons, the collection of bones was eventually prohibited. However, the illegal excavations by collectors and dealers, continued for many decades. In the first half of 20th Century, a few authors studied the Covoli di Velo Cave, but did not add scientific data (Fabiani, 1919).

In 1970, speleologists from the Centro Ricerche Idrologiche e Speleologiche Veronese (C.R.I.S.V.) discovered a new room (Benetti, 1973); that discovery confirmed that the explorations of the galleries with fossils was far from completed. Only in 2001 did the Ente Parco Naturale Regionale della Lessinia close the Grotta Inferiore, and the Museo Civico di Storia Naturale di Verona begin a series of paleontological excavations with the authorization of the Ministero dei Beni e delle Attività Culturali that continued until 2008.

Stratigraphy of the Grotta Inferiore of Covoli di Velo Cave

The karst system of Covoli di Velo Cave is located in one of the most interesting areas of the central-eastern part of the Lessini Mountains (Verona province-Veneto) because of its geology and paleontological content (Bon et al., 1991). The cave opens into the Valley of Covolo, a tributary of the deep Valley Illasi (Fig. 1A).

The karst system of the Covoli di Velo Cave is composed of three main chambers: Grotta superiore and Grotta inferiore or Grotta dell´orso (totalling 364 m long), the Covolo dell´Acqua (65 m long), and some minor tunnels. The cave principally has a sub-horizontal direction, with the mouth of the cave opening at about 870 m above sea level. The cave is formed in oolitic calcarenites, a local dolomitization of the Calcari Grigi di Noriglio Formation (Lower Jurassic).

In the cave, the connections between the passageways, are often limited and may be blocked by large alluvial and collapse deposits, that in various ways close the chambers (Zorzin and Rossi, 1999). The Grotta inferiore of the Covoli di Velo (cadastral number 44 V VR), preserves a great quantity of *Ursus* gr. *spelaeus* fossils. For this reason in October 2001, the Geology and Paleontology Section of the Civic Museum of Natural History of Verona (Zorzin and Bona, 2002) began a long series of excavations performed with scientific methods; about 3,000 specimens (most belonging to *Ursus spelaeus*) were gathered.

Besides the *Ursus* fossils, the macrofauna association is composed of: *Crocuta spelaea*, *Canis lupus* and *Capra ibex*. The microfauna assemblage is composed of: *Glis glis*, *Microtus arvalis*, *Microtus agrestis*, *Microtus oeconomus*, *Chionomys nivalis*, *Dinaromys bogdanovi*, *Terricola* sp., *Sorex minutus*, *Myotis blythi*, *Myotis* sp., *Miniopterus schreibersi*, and *Rhinolophus* sp.

Paleontological excavations have been performed in the small areas inside the “sala terminale,” located about 150 m from the entrance, along the western wall, called sector A and another, called sector B on the eastern side (Fig. 1B).

Stratigraphy of Sector A

Sector A is an area of about 12 m^2, divided in squares, where the team started working in 2001 and continues until now. Each 1-meter-grid square, is designated by at least one letter followed by a number (AA1, AA2, AA3, A1, A2, A3, B1, B2, B3, C1, C2, C3). At the conclusion of the last excavation, a depth of 2.8 m had been reached, using the cave floor as the datum mark on the wall of the cave as zero level (Fig. 1C).

From trampling surface these levels have been identified as:

Level 0: It is the uppermost level, principally composed of landslide material coming from the collapse of the above wall, with calcareous blocks of variable dimensions, up to 1 m^2. Among the clasts the matrix is composed of dark clay. This level reaches a maximum depth of 90 cm; a few bones, including ibex, a very important vertebrate for paleoenvironmental interpretations, were found.

Level 1: This level is composed of slightly laminated, clayey silt. The layers alternate between yellow, silty sheets with a maximum thickness of 1 mm, probably formed during periods of slightly fast-moving water through the cave system, and other sheets, black in colour. The dark layers probably are an accumulation of organic material, that perhaps settled out of especially calm waters. Sand lenses, with clasts of 2-3 mm in size, have also been observed. The thickness of level 1 reaches 40 cm and is paleontologically barren.

Level 1B is characterized by layers of laminated, clayey silt among numerous, large rock blocks, some with a volume of up to 250 dm^3, and other smaller clasts. This level can be interpreted like level 1, but the sheets of clayey silt have been deformed by the rock blocks. The thickness of this level is about 40 cm, and this level is very poor in fossils.

Level 2 is composed of especially angular clasts of various sizes. The matrix is of dark clay. Clasts are placed in a sub-horizontal disposition, forming the evident surfaces. At present, three, main paleosurfaces are identified; the surfaces are characterized by clasts and bones, also placed in a sub-horizontal position, and by an increased presence of sandy and clayey components. The matrix shows a blackish coloration from the accumulation of organic material, which is the consequence of animal decomposition. In alternation to these surfaces, there are lenses of laminated, clayey silt with maximum bed thickness of 1 mm. This level is the richest in fossils. On the three paleosurfaces abundant limb bones, a large fragment of a skull belonging to *U. spelaeus*, and one metatarsal of a wolf, were found (Zorzin and Bona, 2002).

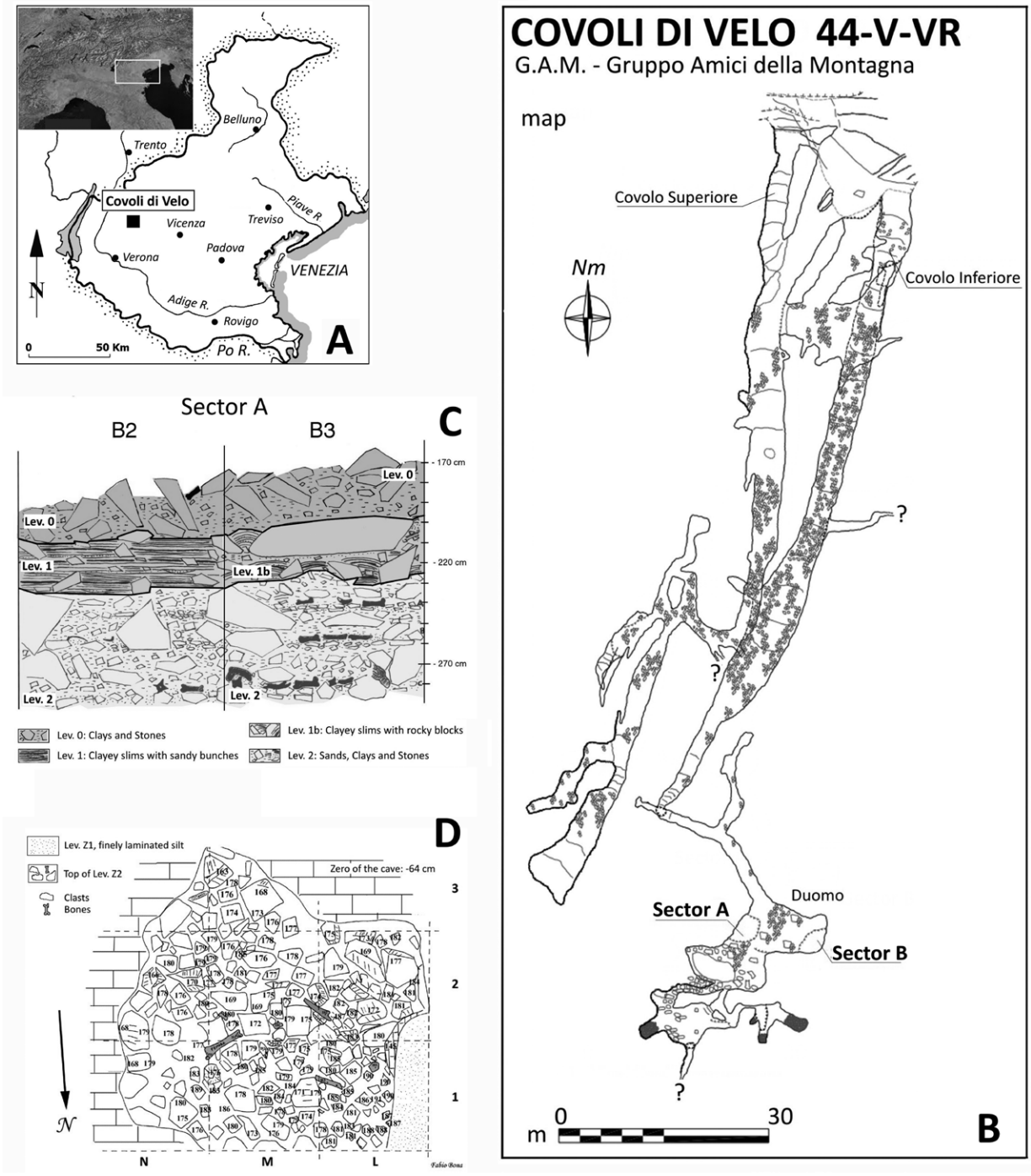

Figure 1. A - Geographical location of the Covoli di Velo Cave (Verona, Veneto region). B - Map view of the Covoli di Velo Cave showing the location of sectors A and B. C - Vertical section of portion of B2 and B3 grids in sector A (drawing F. Bona). D - Map view of the sector B showing some level Z1 sediment, and the distribution of bones and clasts in the Z2 (drawing F. Bona).

Stratigraphy of Sector B

Beginning in 2002, excavations concentrated in sector B on a surface of about 9 m^2. Each 1 m^2 grid is designated by letters and numbers (L1, L2, L3, M1, M2, M3, N1, N2, N3). The depth of the excavation has been 1.8 m (October 2008) from the cave floor, located 1 m below the datum mark (Fig. 1D).

At present there are two stratigraphic levels:

Level Z1: This level is composed of a finely laminated, clayey silt with 1 mm thick beds, alternating with black beds. The yellow layers are mainly composed of silt and probably formed by the accumulation of fine material, carried by water and deposited in relatively calm waters. Alternating with those beds are black layers, formed by the deposition of

organic material, perhaps deposited from remarkably calm waters. Some gravel and sand lenses are also found. The level Z1 is 90 cm thick. Bone fossils are absent.

Level Z2: Five distinct layers (paleosurfaces), formed by poorly sorted and angular clasts and bones, sub-horizontally deposited, have been identified (Fig. 2). The matrix is clayey in composition and brown in color due to accumulation of organic substances. Included within the paleosurfaces are some lenses of clayey silt with laminae of 1 mm maximum thickness. All paleosurfaces of level Z2 are rich in *U. spelaeus* bones, some of which are large in size; among them, some almost complete skulls have been found. Furthermore, some bones of ibex and a femur of a wolf have also been collected (Zorzin et al., 2005).

The clear, stratigraphic similarity between the levels 1 and 2 of sector A and levels Z1 and Z2 of sector B, allows us to hypothesize a depositional uniformity in the levels of two excavation areas. It is still not clear if the paleosurfaces of levels 2 and Z2 can be considered as distinct, separate levels, or if they are different areas of a single level. This question can be solved only by future excavations.

In December 2004, sediment samples from different levels of sector B were collected to search for micromammals (Bona et al., 2006) and three cores were collected to extract pollen. From these studies Bona et al. (2006) preliminarily concluded that at least two analysed pollen samples (lev. Z2 sup. 3 and lev. Z2 sup. 5) indicated an age attributable to about 18,000 years ^{14}C.

Material and Methods

The Curt Engelhorn-Centre for Archaeometry (CEZA) received a bone sample (cave bear, first phalanx from L1/Z2 sup.) to determine the age by ^{14}C with the MICADAS Accelerator at their subsidiary institute, Klaus-Tschira-Archaeometry Center. Collagen was extracted from the bone and the fraction > 30kD separated by ultrafiltration. This fraction was freeze-dried and combusted. The CO_2 was catalytically reduced to graphite.

The radiocarbon data is shown in Table 1. The ^{14}C age is normalized to $\delta^{13}C = -25$ ‰ (Stuiver and Pollach, 1977). The $\delta^{13}C$ value comes from the measurement of the isotope ratios in the accelerator; its error is approximately 2-3 ‰. The value can be different than the true value of the sample material because of isotope separation during sample preparation, and in the ion source of the accelerator. So, the value is only used to correct the fractionation effects. The value is, therefore, not comparable with the measurement in a mass spectrometer for stable isotopes (IRMS) and is not used for further data interpretation.

The C:N ratio and carbon content of the collagen extracted are comparable to modern bones, and the collagen preservation of the sample is good.

Radiocarbon data is, by default, reported as conventional ^{14}C age yr BP. This should not be taken as a calendar age. The origin of this convention lies in the fact that, originally, the ^{14}C data was converted to an age by using the radioactive decay equation, the radiocarbon half-life and the assumption that the atmospheric ^{14}C content is constant over time. Unfortunately, it turned out that the atmospheric content is not constant. Radiocarbon is produced in the atmosphere by interaction of neutrons with nitrogen, while neutrons are produced by galactic, cosmic rays entering the atmosphere. ^{14}C production rates vary due to changes of cosmic ray influx, which is driven by solar and terrestrial magnetic varia-

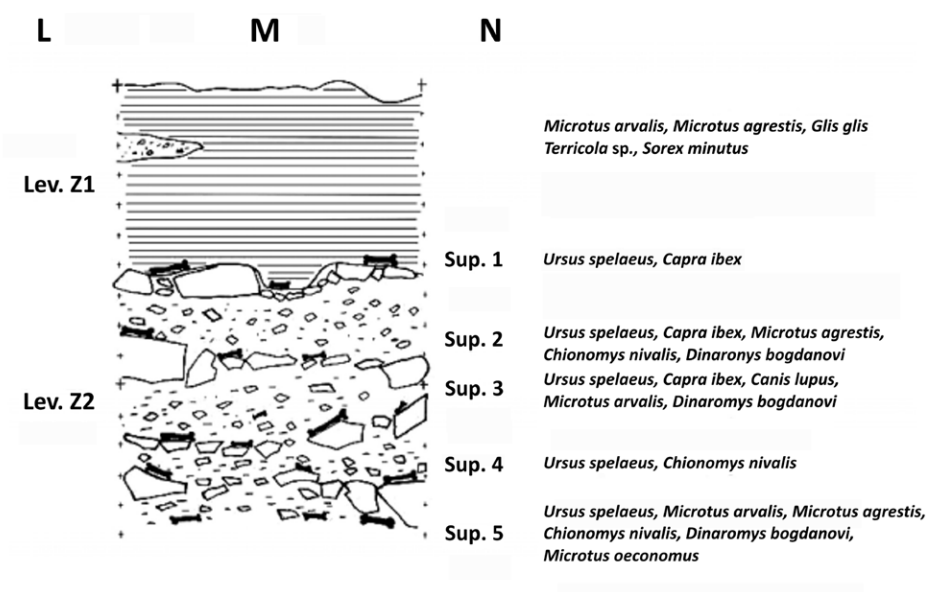

Figure 2. Vertical section of sector B with the list of the species found in stratigraphic sequence (drawing M. Accordini and F. Bona).

Table 1. Dating of the phalanx Iº from Covoli di Velo Cave (Verona, Veneto, North Italy).

Labor No. MAMS	Site	C^{14} (yr BP)	13C (‰)	Cal 1 sigma	Cal 2 sigma	C:N	C (%)	Collagen (%)
24061	Covoli di Velo	29,130 ± 90	−15.6	cal BC 32,110 − 31,461	cal BC 32,518 − 31,382	3.3	37.4	10.7

tions and other sources (Damon et al., 1978). To cope with this, a calibration curve was established using several other methods, such as dendrochronology (until approximately 10,000 BC), Uranium-Thorium dating of speleothems and corals, and varve counting, to name a few. The chronologic limitations of radiocarbon dating are due to the half-life of ^{14}C, which is 5,730 ± 0.40 years. After 10 half-lives, usually, most of the isotopes are decayed, therefore no material older than 50,000 years can be dated reliably with this method (Reimer et al., 2013; Olsson, 2009).

Calibrated ages are usually quoted with a 1-sigma error range, corresponding to a confidence probability of 68.3%. It rises to 95.5% for 2-sigma. The calibration here was performed using the program SWISSCAL 1.0 (L. Wacker, ETH Zurich) with the INTCAL13 dataset.

Discussion and Conclusion

The results of the ^{14}C dating performed on the first phalanx of the *Ursus spelaeus* (I.G.VR 63925) (29,130 ± 0.90 yr BP), combined with pollen and faunal content preserved in the sector B of the cave (Figs. 1C-2), indicates an age of about 10,000 years older than initial estimates (Bona et al., 2006, Table 2). Using pollen data from levels Z2 surfaces 3-5, an indirect date of 18,000 yr BP had been proposed (Bona et al., 2006). These associations suggest the presence of two geological intervals (level Z2 and Z1), corresponding to two different climatic phases. In particular, inside level Z2 (the lower one), the presence of *Capra ibex*, *Chyonomis nivalis*, *Dynaromis bogdanovi*, *Microtus eoconomus*, *Microtus arvalis* and *Microtus agrestis* suggests a cool climate and a landscape characterized by poor forest cover with open spaces. The pollen data from the surfaces 3 and 5 of this level (Bona et al., 2006, Table. 2) confirms this reconstruction. In the level Z1, the disappearance of the *Capra ibex*, *Chionomys nivalis*, *Dinaromys bogdanovi* and *Microtus oeconomus,* and the appearance of the *Glis glis* confirms an increase in forest cover, even if it is characterized by the presence, on its margins or inside it, of open space as indicated by the presence of *Microtus arvalis* and *Microtus agrestis* and the appearance of *Terricola* sp. and *Sorex minutus*. During this phase the climate was more humid and warm, as the pollen data also indicates (Bona et al., 2006).

The new date derived from the phalanx of *U. spelaeus* of the level Z2 surface 1 pushes back earlier age estimates by about 10,000 yr. This new date coincides perfectly with the climatic conditions during the advance of the ALGM (Al-

Table 2. Several radiometric datings of Italian cave bears.

#	SITE	Region	Radiometric dating k yr BP	Source
1	Conturines	Trentino Alto-Adige	87±0.5 to 108+8/-7 (230Th/U)	Withalm (1995)
2	Conturines	Trentino Alto-Adige	107.2-115.8 to 41.9-47.5 (Uran series)	Rabeder et al. (1994)
3	Conturines	Trentino Alto-Adige	40.19±0,9	Döppes et al. (2018)
4	Conturines	Trentino Alto-Adige	>49	Döppes et al. (2018)
5	Conturines	Trentino Alto Adige	>50.579 to >46.435	Spöttl et al. (2018)
6	Grotta Generosa	Lombardy	38.2±1.4	Bianchi-Demicheli and Oppizzi (2001)
7	Grotta Generosa (Level 2)	Lombardy	39.2±1 to 51.2±4	Bona (2004)
8	Grotta Generosa (Level 4)	Lombardy	46.7±2.4	Bona (2004)
9	Grotta Generosa (Level 6)	Lombardy	47.8±2.6 to 50.8±5	Bona (2004)
10	Fontana Marella (FM1)	Lombardy	21.81±0.2	Perego et al. (2001)
11	Fontana Marella (FM2)	Lombardy	22.31±0.2	Perego et al. (2001)
12	Buse di Bernardo	Trentino Alto-Adige	25.78±0.2 to 25.1±0.2	Avanzini et al. (2000)
13	Paina	Veneto	19.686±54	Terlato et al. (2018)
14	Trene	Veneto	19.948±55	Terlato et al. (2018)
15	Chiostraccio Cave	Tuscany	24.030±0.1	Martini et al. (2014)

pine Last Glacial Maximum) before a temperate-humid phase, indicated by the travertine deposits of the Sarca Valley, dated between 28,600 ± 0.300 yr BP and 33,200 ± 0.550 yr BP with AMS ^{14}C dating (R.J. Van de Graaf Laboratorium of Utrecht University) (Avanzini et al., 2000). The date of 29,130 ± 0.90 yr BP for the *U. spelaeus* population of the Covoli di Velo Cave is especially interesting, being close to the estimated time of extinction for cave bears about 24,000 ^{14}C yr ago (Pacher and Stuart, 2008), although a more recent paper has estimated a slightly younger period (20,930 ± 0.140 ^{14}C yr ago) (Baca et al., 2016). Given dates on bears from other caves in Italy (Table 2), the Covoli di Velo cave bear is probably from one of the last populations living in Italy (a specimen found in the Chiostraccio cave, Siena, Tuscany, dated at 24,030 ± 0.100 ^{14}C yr BP (29,200 – 28,550 cal yr BP) is the youngest cave bear in Italy (Martini et al., 2014). It is coeval with the Gamssulzen population (*U. ingressus*) (Austria) (38,000 – 25,400 yr BP) (Rabeder, 1999), a population often utilized for comparison in evolutionary studies. Recently Terlato et al. (2018) produced two new chronological data for Paina and Trene localities (Berici Hills, Veneto region) of 19,686 ± 54 and 19,948 ± 55 respectively and actually considered the youngest cave bear in Italy.

Recently Rabeder (pers. com.) suggested that the Covoli di Velo population belongs to the *U. ingressus* species which inhabited mostly Eastern Europe, having been found in Romania, Slovenia, Ukraine, Czech Republic, Slovakia and Greece, but also found in Switzerland, Austria and Germany.

However, although several morphometric studies (i.e. Stoppini et al., 2007; Santi and Rossi, 2008; Rossi and Santi, 2013) indicated a very similar size range in both populations (the Covoli and Gamssulzen), the Covoli di Velo bears have very simple features in the dentition. The Gamssulzen population and other of *U. ingressus* have derived upper fourth premolars compared to other cave bears (Rabeder et al., 2004). The Covoli di Velo population retains simple premolars, and is, consequently, particularly different from *U. ingressus*. The Covoli di Velo population shows strong similarity to *U. spelaeus*, which is more widely distributed in the western-central Europe regions (Rabeder et al., 2009), unlike *U. ingressus* (Rabeder et al., 2004).

The conclusion is that cave bears in the Italian Alps were evolutionarily conservative with large size and retention of simple dental morphologies. It is possible that a small number of bear populations with more-derived denture, for example the Basura cave population (Liguria region) (Quiles, 2004), migrated from the western Alps region, and/or members of a population from the eastern regions of the Europe, could have migrated into Italy. Rabeder (1995) and Withalm (2014) have hypothesized that the more-derived populations appeared in the eastern regions of Europe and later moved to the west through alpine areas, creating the mix of archaic and modern features that characterized cave bear populations at the end of the Pleistocene. However, the lack of more-derived populations in the eastern Alps might be because the more-derived cave bears migrated to the south toward Greece, as indicated by the presence of *U. ingressus* in the Loutrá Aridéa (Macedonia) (Tsoukala et al., 2006). To test all the hypotheses of evolution and migration, more morphological and genetic data from confidently-dated cave bear populations are necessary.

Acknowledgements

The authors thank the Soprintendenza Archeologia del Veneto, Nucleo Operativo di Verona that has granted permission for the removal of a sample of bone to the dating ^{14}C, and, in particular, to Dr. Gianni De Zuccato, official archaeologist, who attended the sampling operations. We thank Dr. Greg McDonald, associate Editor of the Journal of Cave and Karst Studies and three anonymous reviewers for their useful comments. Dr. Nicoletta Benedetta Carlo-Stella (Cleveland) and Dr. Greg Mc Donald are also thanked for help with the English.

References

Avanzini, M., Bertolini, M., Betti, G., Borsato, A., Calmieri, G., Dellantonio, E., Lazinger, M., and Zambotto, P., 2000, Resti di *Ursus spelaeus* dalle "Buse di Bernardo" e dal "Covelo di Rio Malo" (Trentino-Italia): alcune implicazioni paleoambientali: Studi Trentini di Scienze Naturali - Acta Geologica-, v. 75(1998), p. 155–160.

Baca, M., Popović, D., Stefaniak, K., Marciszak, A., Urbanowski, M., Nadachowski, A., and Mackiewicz, P., 2016, Retreat and extinction of the Late Pleistocene cave bear (*Ursus spelaeus* sensu lato):. The Science of Nature, v. 103, no. 92, p. 1–17. https://doi.org/10.1007/s00114-016-1414-8.

Baca, M., Nadachowski, A., Lipecki, G., Mackiewicz, P., Marciszak, A., Popovic, D., Socha, P., Stefaniak, K., and Wojtal, P., 2017, Impact of climatic changes in the late Pleistocene on migrations and extinctions of mammals in Europe: four case studies: Geological Quarterly, v. 61, no 2, p. 291–304. http://dx.doi.org/10.7306/gq.1319.

Baryshnikov, G.F., and Puzachenko, A.Yu., 2011, Craniometrical variability in the cave bears (Carnivora, Ursidae): multivariate analysis: Quaternary International, v. 245, no 2, p. 350–368. https://doi.org/10.1016/j.quaint.2011.02.035.

Baryshnikov, G.F., and Puzachenko, A.Yu., 2017, Morphometric analysis of metacarpal and metatarsal bones of cave bears (Carnivora, Ursidae): Fossil Imprint, v. 73, no 1-2, p. 7–47, https://doi.org/10.1515/if-2017-0001.

Benetti, A., 1973, La distruzione dei depositi quaternari dei "Covoli di Velo" nei Monti Lessini Veronesi: Natura Alpina, v. 24, no. 1, p. 27–37.

Benetti, A., and Cristoferi, W., 1968, La grotta del "Monte Gaole" e i " Covoli di Velo" nei Lessini Veronesi: Studi Trentini di Scienze Naturali, B, v. 45, p. 270–283.

Benetti, A., and Sauro, F., 1999, Storia delle ricerche sul complesso carsico dei Covoli di Velo. Atti della Tavola Rotonda: "Un importante sistema carsico dei Monti Lessini: i Covoli di Velo": Verona-Camposilvano, 16-17 aprile 1999, Tipolitografia "La Grafica" Vago di Lavagno (VR), p. 5–12.

Bianchi-Demicheli, F., and Oppizzi, N., 2001, Ricerche speleologiche e paleontologiche nella regione del Monte Generoso: la Caverna Generosa: Bolletino della Società Ticinese di Scienze Naturali, v. 89, p. 61–66.

Bon, M., Piccoli, G., and Sala, B., 1991, I giacimenti quaternari di vertebrati fossili nell'Italia nord-orientale: Memorie Scienze Geologiche Padova, v. 43, p. 185–231.

Bona, F., Zorzin, R., Accordini, M., Mazzi, R., Gatto, R., Accorsi, C.A., Bandini Mazzanti, M., Bosi, G., Trevisan, G., and Torri, P., 2006, First paleo-environmental considerations on the Pleistocene deposits of the lower cave of Covoli di Velo (VR-Italy): Scientific Annals. School of Geology Aristotle University of Thessaloniki (AUTH), Spec. Vol. 98, p. 229–239.

Catullo, T.A., 1844, Su le caverne delle Province venete: Atti dell'I. R. Veneto Istituto, Venezia.

Cvetković, N.J., and Dimitrijević, V.M., 2014, Cave bears (Carnivora, Ursidae) from the Middle and Late Pleistocene of Serbia: A revision: Quaternary International, v. 339-340, p. 197–208. https://doi.org/10.1016/j.quaint.2013.10.045.

Damon, P.E, Lerman, J.C. and Long, A., 1978, Temporal fluctuations of atmospheric ^{14}C: casual factors and implications: Annual Review of Earth and Planetary Sciences, v. 6, p. 457–494. https://doi.org/10.1146/annurev.ea.06.050178.002325.

De Carlis, A., Alluvione, E., Fonte, A., Rossi, M., & Santi, G., 2005, Morphometry of the *Ursus spelaeus* remains from Valstrona (Northern Italy): GeoAlp, v. 2, p. 115–126.

Döppes, D., Pacher, M., Rabeder, G., Lindauer, S., Friedrich, R., Kromer, B., and Rosendahl, W., 2016, Unexpected! New AMS dating from Austrian cave bear sites: Cranium, v. 33, no 1, p. 26–30.

Döppes, D., Rabeder, G., Frischauf, C., Kavcik-Graumann, N., Kromer, B., Lindauer, S., Friedrich, R., and Rosendahl, W., 2018, Extinction pattern of Alpine cave bears-new data and climatological interpretation. Historical Biology, https://doi.org/10.1080/08912963.2018.1487422.

Fabiani, R., 1919, I Mammiferi quaternari della regione veneta: Memorie Istituto di Geologia dell'Università di Padova, v. 5, p. 1–174.

Fortes, G.G., Grandal-d'Anglade, A., Kolbe, B., Fernandes, D., Meleg, I.N., Vázquez, A.G., Pinto-Llona, A.C., Constantin, S., de Torres, T.R., Ortiz, J.E., Frischauf, C., Rabeder, G., Hofreiter, M., and Barlow, A., 2017, Insights into bear behaviour from aDNA data: Aragonit, v. 22, no 1, p. 11.

Fortis, A., 1786, Extrait d'une lettre de M. l'abbé Fortis datée de Vérone le 24 Septembre 1785 à M. le Comte de Cassini de l'Académie des Sciences sur différentes pétrifications: Journal Physique, v. 28, no 1, p. 161–168.

Frischauf, C., 2014, The Cave Bear Incisors from Križna jama (Slovenia): Mitteilungen der Kommission für Quartärforschung der Österreichischen Akademie der Wissenschaften, v. 21, p. 75–83.

Grandal d'Anglade, A., and López-González, F., 2004, A study of the evolution of the Pleistocene cave bear by a morphometric analysis of the lower carnassial: Oryctos, v. 5, p. 83–94.

Gretzinger, J., Reiter, E., Urban, C., Bocherens, H., Sabol, M., Schuenemann, V., and Krause, J., 2017, Genetic analysis of a cave bear-morphothype specimen from Prepoštská cave, Slovakia featuring carnivorous-like isotopic signature: Aragonit, v. 22, no 1, p. 11–12.

Hofreiter, M., Capelli, C., Krings, M., Waits, L., Conard, N., Münzel, S., Rabeder, G. Nagel, D., Paunovic, M., Jambrēsić, G., Meyer, S., Weiss, G., and Pääbo, S., 2002, Molecular Biology and Evolution, v. 19, no 8, p. 1244–1250. https://doi.org/10.1093/oxfordjournals.molbev.a004185.

Martini, I., Coltorti, M., Mazza, P.P.A., Rustioni, M., and Sandrelli, F., 2014, The latest *Ursus spelaeus* in Italy, a new contribution to the extinction chronology of the cave bear: Quaternary Research, v. 81, p. 117–124. http://doi.org/10.1016/j.yqres.2013.10.003.

Massalongo, O., 1851, Osteologia degli Orsi fossili nel Veronese, con un saggio sopra le principali caverne del Distretto di Tregnago: Naturwissenschaftliche Abhandlungen, v. 4, p. 1–110.

Olsson, I.U., 2009, Radiocarbon dating history: early days, questions, and problems met. Radiocarbon, v. 51, p. 1–43. https://doi.org/10.1017/S0033822200033695.

Omboni, G., 1875, Di alcuni oggetti preistorici delle caverne di Velo Veronese: Atti della Società Italiana di Scienze Naturali e del Museo Civico di Storia Naturale di Milano, v. 18, p. 69–82.

Orlando, L., Bonjean, D., Bocherens, H., Thenot, A., Argant, A., Otte, M., and Hänni, C., 2002, Ancient DNA and the population genetics of cave bears (*Ursus spelaeus*) through space and time: Molecular Biology and Evolution, v. 19, no 11, p. 1920–1933. https://doi.org/10.1093/oxfordjournals.molbev.a004016.

Pacher, M., and Stuart, A.J., 2008, Extinction chronology and paleobiology of the cave bears (*Ursus spelaeus*): Boreas, v. 38, p. 189–206. https://doi.org/10.1111/j.1502-3885.2008.00071.x.

Perego, R., Zanalda, C., and Tintori, A., 2001, *Ursus spelaeus* from Grotta Sopra Fontana Marella, Campo dei Fiori Massif (Varese, Italy) : morphometry and paleoecology : Rivista Italiana di Paleontologia e Stratigrafia, v. 197, no 3, p. 451–462.

Plichta, A., Rablíčkova, M., and Káňa, V., 2017, Morphometrical analyses of cave bear populations from Barová cave in moravian karst (Czech Republic): Aragonit, v. 22, no 1, p. 20–21.

Quiles, J., 2004, Analyse morphodynamique de l'ours des caverne (Carnivora, Ursidae) de cinq sites du pourtour Méditerranéen : Cahiers scientifique du Muséum d'Histoire naturelle de Lyon Hors Série, v. 2, p. 149–161.

Rabeder, G., 1995, Evolutionsniveau und Chronologie der Höhlenbären aus der Gamssulzen-Höhle im Toten Gebirge (Oberösterreich). Mitteilungen der Kommission für Quartärforschung der Österreichischen Akademie der Wissenschaften, Band 9, p. 69–81.

Rabeder, G., 1999, Die Evolution des Höhlenbärengebisses. Mitteilungen der Kommission für Quartärforschung der Österreichischen Akademie der Wissenschaften, Band 11, p. 1–102.

Rabeder, G., 2014, Metrics and Evolutionary Level of Teeth of the Bears from Križna jama (Slovenia): Mitteilungen der Kommission für Quartärforschung der Österreichischen Akademie der Wissenschaften, v. 21, p. 57–63.

Rabeder, G., Steffan, I., and Wild, E., 1994, The chronological position of the cave bears from Conturines cave: Abstract, 2nd International Cave Bears Symposium Alta Badia.

Rabeder, G., Frischauf, C., and Nielsen, E., 2017, Steigelfadbalm, eine fossilführende Bärenhöhle in der Nagelfluh der Rigibei Luzern (Zentralschweiz): Die Höhle, v. 68, no 1–4, p. 124–133.

Rabeder, G., Hofreiter, M., Nagel, D., and Withalm, G., 2004, New taxa of alpine cave bears (Ursidae, Carnivora): Cahiers scientifique du Muséum d'Histoire naturelle de Lyon Hors Série, v. 2, p. 49–68.

Reimer, P.J., Baillie, M.G.L., Bard. E., et al., 2013, IntCal09 and Marine09 radiocarbon age calibration curves, 0–50,000 years cal BP: Radiocarbon, v. 51, p. 1111–1150. https://doi.org/10.1017/S0033822200034202.

Robu, M., 2016, Age re-assessment of the cave bear assemblage from Urşilor Cave, north-western Romania: International Journal of Speleology, v. 45, no. 2, p. 123–133. http://doi.org/10.5038/1827-806X.45.2.1947.

Rosenmüller, J.CH., 1794, Quaedam de ossibus fossilibus animalis cujusdam, historiam ejus et cognitionem accuratiorem illustrantia, dissertatio, quam d. 22.October 1794. ad disputandum proposuit Ioannes Christ : Rosenmüller Heßberga-Francus, LL. AA. M. in Theatro anatomico

Lipsiensi Prosector assumto socio Io. Chr. Aug. Heinroth Lips. Med. Stud. Cum tabula aenea.- Leipzig.

Rossi, M., and Santi, G., 2013, Studio morfometrico e morfodinamico di resti craniali, dentali e mandibolari di *Ursus spelaeus* dalla Grotta del Buco del Frate e dall'Altopiano di Cariadeghe (Brescia) nel quadro evolutivo degli orsi delle caverne: Natura Bresciana, Annali del Museo Civico di Storia Naturale Brescia, v. 38, p. 33–43.

Sabol, M., 2005, Cave Bears (Ursidae, Mammalia) from the Trojuholník Cave (Slovakia): Mitteilungen der Kommission für Quartärforschung der Österreichischen Akademie der Wissenschaften, v. 14, p. 161–175.

Santi, G., and Rossi, M., 2001, Bears from the Buco dell'Orso Cave (Laglio-Como, Lombardy-Northern Italy). I : Morphometric study of the cranial and mandibular fossil remains: Atti Ticinensi di Scienze della Terra, Pavia, v. 42, p. 75–100.

Santi, G., and Rossi, M., 2008, Fossili craniali e mandibolari di *Ursus* da grotte del Veneto (Italia Settentrionale) nuove osservazioni sul quadro evolutivo degli orsi italiani: Atti del Museo Civico di Storia Naturale di Trieste, suppl. al v. 53, p. 3–12.

Santi, G., and Rossi, M., 2014, Metapodial bones of *Ursus* gr. *spelaeus* from selected caves of the North Italy. A biometrical study and evolutionary trend. Annales de Paléontologie, v. 100, p. 237–256. https://doi.org/10.1016/j.annpal.2014.01.003.

Santi, G., Rossi, M., and Pomodoro, S., 2003, *Ursus spelaeus* Rosenmüller-Heinroth, 1974 remains from Buco dell'Orso Cave (Laglio, Como, Lombardy-Northern Italy-). III – Metapodial bones: morphometric analysis: Bulletin de l'Institut Royal des Sciences Naturelles de Belgique, v. 73, p. 195–219.

Santi, G., Rossi, M., and Dellantonio, E., 2011, *Ursus spelaeus* Rosenmüller, 1794 from the "Buse di Bernardo" (Tesero, Trento Province, Northern Italy): morphometric, morphodynamic and evolutionary frame. Revue de Paléobiologie Genève, v. 30, no. 1, p. 223–249.

Spötl, C., Reimer, P.J., Rabeder, G., and Scholz, D., 2014, Presence of cave bears in western Austria before the onset of the Last Glacial Maximum: new radiocarbon dates and palaeoclimatic considerations: Journal of Quaternary Science, v. 29, no 8, p. 760–766. https://doi.org/10.1002/jqs.2747.

Spötl, C., Reimer, P.J., Rabeder, G., and Bronk-Ramsey, C., 2018, Radiocarbon constraints on the age of the world's highest-elevation cave-bear population, Conturines cave (Dolomites, Northern Italy): Radiocarbon, v. 60, no 1, p. 299-307. https://doi.org/10.1017/RDC.2017.60.

Stoppini, M., Bonin, M., Gironi, B., Rossi, M., and Santi, G., 2007, Morphodynamic analysis of *Ursus spelaeus* dentition from caves of the Lombardia and Veneto Regions caves (North Italy): preliminary data on $P^4/_4$ and lower carnassials (M_1): Grzybowski Foundation Special Publication, v. 12, p. 93–103.

Stuiver, M., and Polach, H.A., 1977, Discussion: reporting of ^{14}C data: Radiocarbon, v. 19, p. 355–363. https://doi.org/10.1017/S0033822200003672.

Terlato, G., Bocherens, H., Romandini, M., Nannini, N., Hobson, K.A. and Peresani, M., 2018, Chronological and isotopic data support a revision for the timing of cave bear extinction in the Mediterranean Europe: Historical Biology, https://doi.org/10.1080/08912963.2018.1448395.

Torres Pérez Hidalgo, T., 1988a, Osos (Mammalia, Carnivora, Ursidae) del Pleistocene Ibérico (*U. deningeri* Von Reichenau, *U. spelaeus* Rosemüller-Heinroth, *U. arctos* Linneo). I. Filogenia, distribution stratigrafca y geografca. Estudio anatomico y metrico del craneo. Boletín Geológico y Minero, v. 99, no 1, p. 3–46.

Torres Pérez Hidalgo, T., T. (1988b): Osos (Mammalia, Carnivora, Ursidae) del Pleistocene Ibérico (*U. deningeri* Von Reichenau, *U. spelaeus* Rosemüller-Heinroth, *U. arctos* Linneo). II. Estudio anatomico y metrico de la mandibula, hioides, atlas y axis: Boletín Geológico y Minero, v. 99, no 2, p. 220–249.

Torres Pérez Hidalgo, T., 1988c, Osos (Mammalia, Carnivora, Ursidae) del Pleistocene Ibérico (*U. deningeri* Von Reichenau, *U. spelaeus* Rosemüller-Heinroth, *U. arctos* Linneo). III. Estudio anatomico y metrico del miembro toracico, carpo y metacarpo: Boletín Geológico y Minero, v. 99, no 3, p. 356–412.

Torres Pérez Hidalgo, T., 1988d, Osos (Mammalia, Carnivora, Ursidae) del Pleistocene Ibérico (*U. deningeri* Von Reichenau, *U. spelaeus* Rosemüller-Heinroth, *U. arctos* Linneo). IV. Estudio anatomico y metrico del miembro pelviano, tarso, metatarso y dedos: Boletín Geológico y Minero, v. 99, no 4, p. 516–577.

Torres Pérez Hidalgo, T., 1988e, Osos (Mammalia, Carnivora, Ursidae) del Pleistocene Ibérico (*U. deningeri* Von Reichenau, *U. spelaeus* Rosemüller-Heinroth, *U. arctos* Linneo).V. Denticion decidual, formula dentaria y denticion superior: Boletín Geológico y Minero, v. 99, no 5, p. 660–714.

Torres Pérez Hidalgo, T., 1988f, Osos (Mammalia, Carnivora, Ursidae) del Pleistocene Ibérico (*U. deningeri* Von Reichenau, *U. spelaeus* Rosemüller-Heinroth, *U. arctos* Linneo).VI. Denticion inferior: Boletín Geológico y Minero, v. 99, no 6, p. 886–940.

Tsoukala, E., Chatzopoulou, K., Rabeder, G., Pappa, S., Nagel, D., and Withalm, G., 2006, Paleontological and stratigraphical research in Loutrá Aridéas bear cave (Almopia Speleopark, Pella, Macedonia, Greece): Scientific Annals, School of Geology Aristotle University of Thessaloniki (AUTH), Special Vol. 98, p. 41–67.

Volta, S., 1796, Ittiolitologia Veronese, Giuliari, Verona, p. 46–48.

Withalm, G., 2011, Analysis of cave bear metapodial bones from Ajdovska jama near Krško (Slovenia): Mitteilungen der Kommission für Quartärforschung der Österreichischen Akademie der Wissenschaften, v. 20, p. 65–71.

Withalm, G., 2014, Analysis of the Cave Bear metapodial bones from Križna jama (Slovenia): Mitteilungen der Kommission für Quartäforschung der Österreichischen Akademie der Wissenschaften, Band 21, p. 117–122.

Zorzin, R., and Bona, F., 2002, Covoli di Velo (VR), Prima campagna paleontologica: risultati preliminari: Bollettino del Museo Civico di Storia Naturale di Verona, Geologia Paleontologia Preistoria, v. 26, p. 43–46.

Zorzin, R., and Rossi, G., 1999, Il sistema carsico dei Covoli di Velo. Atti Tavola Rotonda: "Un importante sistema carsico dei Monti Lessini (VR): i Covoli di Velo": Verona-Camposilvano, 16-17 aprile 1999, Tipolitografia "La Grafica" Vago di Lavagno (VR), p. 13–22.

Zorzin, R., Bona, F., and Accordini, M., 2005, From 2001 to 2004: paleontological excavations in the Grotta inferiore dei Covoli di Velo (Veneto - Italy): 4th International Congress of Speleology, 21-28 August 2005, Kalamos, Hellas, Hellenic Speleological Society, O-23, p.1–8.

R. Ogórek. Speleomycology of air in Demänovská Cave of Liberty (Slovakia) and new airborne species for fungal sites. *Journal of Cave and Karst Studies*, v. 80, no. 3, p. 153-160. DOI:10.4311/2018MB0104

SPELEOMYCOLOGY OF AIR IN DEMÄNOVSKÁ CAVE OF LIBERTY (SLOVAKIA) AND NEW AIRBORNE SPECIES FOR FUNGAL SITES

Rafał Ogórek

Abstract

The study is the first report of the fungal air quality in the Demänovská Cave of Liberty, Slovakia, which is one of the most visited caves in Slovakia (Low Tatras). A total of 108 air samples were collected in June 2014 using the microbiological air sampler "Air Ideal 3P" and Potato Dextrose Agar medium. Fungi were identified based on phenotypic tests and ITS regions analysis. Air samples collected from underground sites contained fewer propagules of fungi (from 86.7 to 126.7 colony-forming units per m^3 of air) than outdoor air samples (391.7). Altogether, the incidence of 18 different fungal species were found in the air of the cave, and most of them were isolated from the indoor samples. *Cladosporium macrocarpum* spores dominated in this study. The fungal species such as *Bjerkandera adusta*, *Exophiala xenobiotica*, *Fusarium lateritium*, *Penicillium aurantiacobrunneum,* and *Trichoderma citrinoviride* were detected for the first time in the internal air of underground sites. Overall, fungal air quality of the Demänovská Cave does not pose a biological threat to people and animals with undamaged immune systems according to most standards of fungal sir contamination. However, some of the airborne fungi detected in the cave can pose a risk to persons and animals with weakened immune systems or people who have fungal allergies.

Introduction

The earth's atmosphere has a great impact on the quality of life, especially in these times when the air quality has dropped significantly (Bruce et al., 2000; Darçın, 2014). However, Hippocrates mentioned in the *Corpus Hippocraticum* manuscript that some of the air components can be the cause of human illness (Mammas and Spandidos, 2016). Assessment of outdoor and indoor air pollution of buildings and public places is more frequent than underground sites. Poor indoor air quality of buildings can affect the deterioration of the health of residents such as skin and respiratory problems, poisoning, malaise and general weakness (Stolwijk, 1991; Romagnoli et al., 2016). The problem of poor indoor air quality is very serious and it can affect up to 3 billion people worldwide. The term "sick building syndrome" (SBS) was introduced in 1983 to describe the situation where a building affects human health (WHO, 1983). Moreover, it should be emphasized that microscopic fungi and their secondary metabolites (i.e. mycotoxins) play a major role in SBS. The fungal spores can constitute up to 70% of all bioaerosol pollution of indoor air (Brickus et al., 1998; Reynolds et al., 2001).

Atmospheric air and subterranean ecosystems are among the most inhospitable habitats for mycobiota, mainly due to lack of nutrients, and in the case of underground sites, also due to low temperatures (Poulson and White, 1969). Consequently, fungi usually occur as spores suspended in the air in these environments, which are also reproductive dispersal structures (Barton and Northup, 2007; Kokurewicz et al., 2016). On the other hand, environmental stress is one of the main factors determining evolution; and therefore, fungi that can tolerate or adapt to unfavorable living conditions in the underground are usually extremophile species (Rampelotto, 2013). These species most often have a high potential to secrete various biologically active compounds that, among others, may pose a risk to human and animal health, e.g. mycotoxins (Barton and Northup, 2007; Zain, 2011).

Natural and artificial underground ecosystems are mainly the place of occurrence of fungi belonging to the phylum *Ascomycota* (Vanderwolf, et al., 2013). In the summer, fungi of the genera *Cladosporium* usually dominate underground sites, and *Penicillium* species in the winter (Pusz et al., 2015; Ogórek et al., 2017). Currently, 44 genera of airborne fungi have been detected in Slovakian caves, and most species belong to the *Penicillium* (Nováková, 2009; Ogórek et al., 2016 a, b, c, d; 2018). Moreover, *Penicillium* species are significantly related to increased incidence of SBS, allergic respiratory diseases, and they can also cause opportunistic mycosis in humans and animals (Eschete et al., 1981; Hoffman et al., 1992; Pekkanen et al., 2007). Thus, it is important to do mycological monitoring of air in underground habitats, especially in the case of tourist facilities and/or those used by hibernating bats.

The main goal of this research was to assess the fungal air quality during summer in Demänovská Cave of Liberty, which is open to tourists, by determining the number and species composition of cultivable, microscopic fungi in the air of this cave. Additionally, we wanted to check: (1) whether the mycological quality of air within the investigated underground sites poses a risk to the health of workers and tourists, and (2) influence of air temperature and humidity on the concentration of fungal spores in the air.

University of Wroclaw, Institute of Genetics and Microbiology, Department of Genetics, Przybyszewskiego Street 63/77, 51-148 Wroclaw, Poland, E-mail: rafal-ogorek@wp.pl,

Material and Methods

Description of the study area

The study was carried out in the Demänovská Cave of Liberty, "Demänovská jaskyňa slobody" (48°99′8″ N, 19°58′5″ E), which is part of the biggest cave system in Slovakia – the Demänová Caves system (Fig. 1). The cave passages are 8126 m long, and its entrance lies at an elevation of 870 m a.s.l. It is formed in the Middle Triassic, dark-gray Gutenstein limestones of the Krížna Nappe, along the tectonic faults. These faults are shaped by corrosive and erosive activity of ponor allochthonous water flows of the Demänovká River and its tributaries (Marušin, 2003). Currently, the cave is inhabited by four species of bats, with the most frequent being the greater mouse-eared bat (*Myotis* Borkhausen) and the whiskered bat (*Myotis mystacinus* Kuhl) (Slovak Caves Administration, 2018). According to Nudziková (2014), this cave is the most visited underground facility in Slovakia, e.g. it is estimated that 111,261 tourists visited the caves in 2014. However, there are no reports about mycological air quality in this cave.

Air sampling

The air samples were collected on June 5, 2014 from indoor and outdoor air of the cave (Fig. 1), using the microbiological air sampler "Air Ideal 3P" (bioMérieux), and Potato Dextrose Agar (PDA, Biocorp) (Ogórek et al., 2013). It was programmed for air sample volumes of 50 L, 100 L, and 150 L, and the measurement in particular sampling sites was performed in six-plicate for each volume. Additionally, the air temperature and relative humidity were measured nine times at each sampling site, using a LB-522 thermohygrometer (Label, accuracy: ±1%). The air samples in Petri dishes with PDA were incubated from 4 to 21 days at 25±1 °C. After incubation, the colonies that appeared on the medium

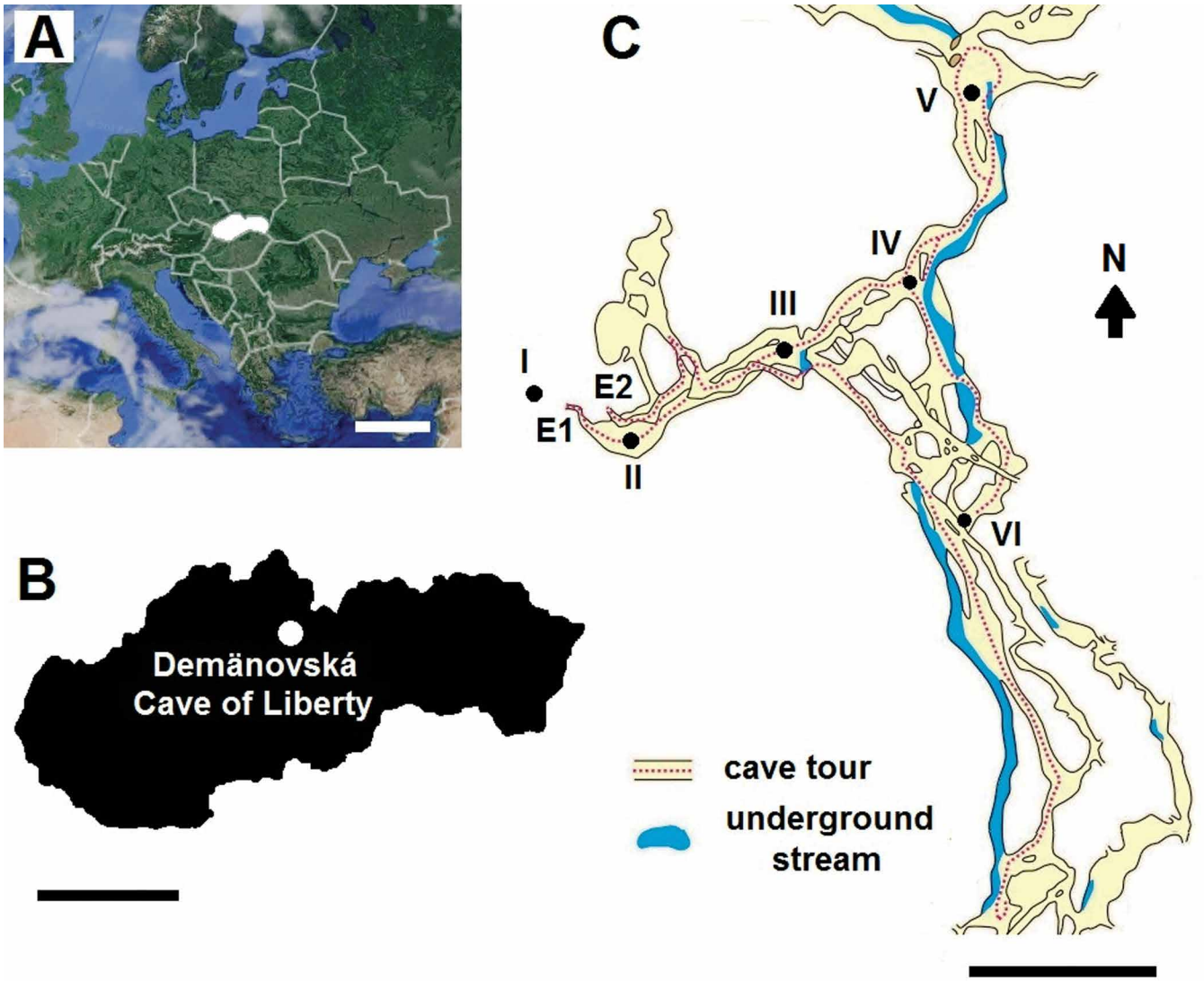

Figure 1. Geographic location of Slovakia (A) and Demänovská Cave of Liberty (B). Sampling location (C) on the tourist route: E1 – entrance to the cave, E2 – exit from the cave, I – sampling location outside the cave, from II to VI – sampling locations inside the cave. Scale bars: A = 500 km, B = 100 km, C = 100 m.

were counted. The colony-forming unit concentrations were expressed as CFU per cubic meter of air using the formula $X = (a \times 1000) / V$, where a is the number of colonies obtained on a Petri dish, and V is the air volume sampled (m^3). Then, fungal colonies were subcultured on PDA medium for phenotypic and molecular identification.

Morphological and molecular identification

Overall, fungal structures were observed on PDA, and additionally on Malt Extract Agar (MEA, Biocorp), Czapek-Dox Agar (1.2% agar, Biocorp), and Czapek Yeast Autolysate Agar (CYA) for *Penicillium* and *Aspergillus*. Then, fungi were identified using the taxonomic literature (Jülich, 1979; Golubev, 1981; Tanaka et al., 2001; Frisvad and Samson, 2004; Keirle et al., 2004; Chilvers and du Toit, 2006; de Hoog et al. 2006; Houbraken et al., 2011; Vitale et al., 2011; Bensch et al., 2012; Jung et al., 2014; Visagie et al., 2014; Hernández-Restrepo et al., 2016; Kim et al., 2016). DNA was isolated from fungal colonies cultured on PDA according to the original, hexadecyltrimethylammonium bromide- (CTAB) based method (Doyle and Doyle, 1987), modified as described by Ogórek et al. (2012). The internal, transcribed spacer region of fungal rDNA was amplified using the primer ITS1 (5′-TCCGTAGGTGAACCTGCGG-3′) and ITS4 (5′-TCCTCCGCTTATTGATATGC-3′) (White et al., 1990). Polymerase chain reactions were performed in a T100 Thermal Cycler (Bio-Rad), according to Ogórek et al. (2016a). The PCR products were verified by electrophoretic separation on the gel of 1.2% agarose. Then, they were purified by using Clean-UP (A&A Biotechnology) and sequenced by Macrogen Europe (Netherlands).

Data analyses

BioEdit Sequence Alignment Editor was used for the analysis of the obtained fungal ITS sequences (http://www.mbio.ncsu.edu/bioedit/bioedit.html). Next, fungi were identified to species by using the BLAST algorithm (http://www.ncbi.nlm.nih.gov/), that compared the obtained sequences with those deposited in the GenBank database. The sequences were placed in GenBank databases (Table 1). The data from the number of airborne fungal colonies were subjected to statistical analysis by using a Statistica 12.0 package. For this purpose, one-way analysis of variance

Table 1. Airborne fungi detected in the Demänovská Cave of Liberty and results of BLAST (all E values were zero). A + indicates that the fungus was cultured from the air samples.

		Air		Identity with Sequence from GenBank			
	Fungi	Outside	Inside	Accession	Query Cover, %	Identity, %	GenBank Accession No.
1	*Aspergillus elegans* Gasperini		+	FM201287.1	97	99	KX426973.1
2	*A. flavus* Link		+	LN482443.1	99	99	KX426971.1
3	*A. niger* Tiegh.		+	KP940595.1	100	99	KX426976.1
4	*Bjerkandera adusta* (Willd.) P. Karst.	+	+	FJ228211.1	98	99	KX426963.1
5	*Botrytis cinerea* Pers.	+		KP151610.1	98	99	KX426964.1
6	*Cladosporium cladosporioides* (Fresen.) G.A. de Vries		+	KJ589547.1	98	88	KX426970.1
7	*C. macrocarpum* Preuss 1848	+	+	KM977762.1	98	99	KX426960.1
8	*Coprinellus disseminatus* (Pers.) J.E. Lange 1938	+		JN159561.1	97	100	KX247294.1
9	*Cutaneotrichosporon curvatus* (Diddens & Lodder) A.M. Yurkov, X.Z. Liu, F.Y. Bai, M. Groenew. & Boekhout		+	NR_130657.1	99	99	KX426975.1
10	*Discosia* sp.	+	+	KU325138.1	90	96	KX426977.1
11	*Exophiala xenobiotica* de Hoog, J.S. Zeng, Harrak & Deanna A. Sutton		+	KJ522804.1	96	99	KX426972.1
12	*Fusarium lateritium* Nees	+	+	JN391185.1	99	99	KX426966.1
13	*Microdochium seminicola* M. Hern.-Restr., Seifert, Clear & B. Dorn	+	+	KP859023.1	98	99	KX426969.1
14	*Penicillium aurantiacobrunneum* Houbraken, Frisvad & Samson	+	+	NR_121509.1	97	99	KX426962.1
15	*P. brevicompactum* Dierckx	+	+	KT876695.1	100	99	KX426968.1
16	*P. crustosum* Thom		+	HQ850913.1	97	82	KX426967.1
17	*Phlebiopsis gigantea* (Fr.) Jülich	+		KP676120.1	97	99	KX426965.1
18	*Trichoderma citrinoviride* Bissett		+	JX125617.1	97	99	KX426974.1
	∑ species	10	15		...		

(ANOVA) and the Tukey HSD (honest significant differences) test at α ≤ 0.05 were used. The Pearson correlation coefficient r was used to determine the relation between the temperature and humidity of the air and the concentrations of airborne fungal propagules.

Results and Discussion

The results of this study show that the indoor air temperature (6.8–8.5 °C) of the examined cave in the summer was lower than the outdoor air (16.9 °C) and correlated positively with the concentration of airborne fungal propagules ($p < 0.05$, $r = 0.98$). A similar situation was not reported for relative humidity of the air, which was lower outside the cave (61.1%) than inside (81.7–98%) (Table 2, Fig. 2). According to Tang (2009), these factors most affect the survival of fungi in the environment. However, the survival of mycobiota in the air also depends on other factors that were not measured in these studies, such as ultraviolet radiation, pres-

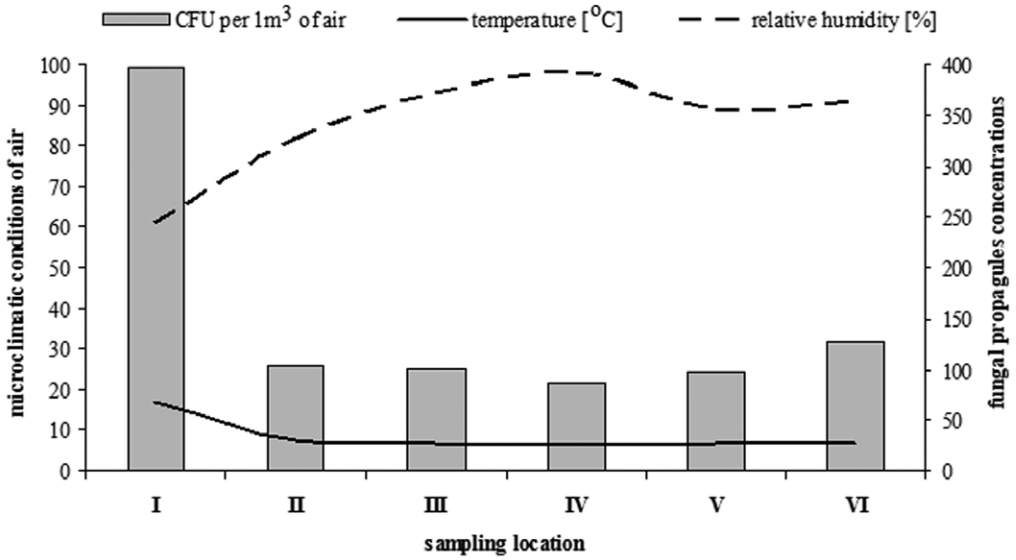

Figure 2. The climate parameters and measured concentrations of airborne fungal propagules at the sampled locations in the Demänovská Cave of Liberty: location I – outside the cave, locations from II to VI – inside the cave.

Table 2. Average number of airborne fungal propagules (CFU m^{-3}) detected in the Demänovská Cave of Liberty (ND = not detected).

	Sampling Location					
Fungi	**Ia**	**II**	**III**	**IV**	**V**	**VI**
Aspergillus elegans	N D	ND	10.1 a	ND	ND	ND
A. flavus	ND	16.7 abc	15.0 a	11.7 ab	15.0 abc	8.3 a
A. niger	ND	ND	23.4 a	20.0 ab	25.0 ab	28.3 a
Bjerkandera adusta	63.0 b**	26.7 ab	18.3 a	11.7 ab	13.3 ab	ND
Botrytis cinerea	51.6 bc	ND	ND	ND	ND	ND
Cladosporium cladosporioides	ND	ND	ND	ND	ND	15.0 a
C. macrocarpum	146.8 a	31.7 a	26.7 a	28.3 a	30.0 a	46.7 a
Coprinellus disseminatus	4.5 d	ND	ND	ND	ND	ND
Cutaneotrichosporon curvatus	ND	ND	ND	ND	3.3 c	ND
Discosia sp.	6.2 d	3.3 c	ND	ND	ND	ND
Exophiala xenobiotica	ND	1.7 c	ND	1.7 b	ND	ND
Fusarium lateritium	5.0 d	ND	ND	ND	5.0 bc	11.7 a
Microdochium seminicola	13.3 cd	5.0 c	ND	ND	ND	ND
Penicillium aurantiacobrunneum	48.0 bc	6.7 c	ND	ND	ND	ND
P. brevicompactum	33.3 bcd	ND	6.7 a	ND	ND	ND
P. crustosum	ND	11.7 bc	ND	13.3 ab	ND	ND
Phlebiopsis gigantea	20.0 cd	ND	ND	ND	ND	ND
Trichoderma citrinoviride	ND	ND	ND	ND	6.7 bc	ND
Total	391.7 A**	103.3 C	100.2 CD	86.7 D	98.6 CD	126.7D

[a] I – the outdoor air samples, II-VII – the indoor air samples;
[b] For each location, the number of fungal spores followed by the same letter are not statistically different, and others are (Tukey HSD test, α ≤ 0.05). Small letters indicate the differences between fungal species in a given location; they refer to means in columns. Capital letters indicate the effect of a particular location on the total concentration of fungal spores; they refer to means in rows.

sure, and atmospheric pollution, mainly by chemical particles (Niazi et al., 2015). Additionally, the presence of aeromycota in underground niches is closely related to the season of the year, the external environment, air currents, anthropogenic factors, and the presence of bats (Pusz et al., 2014, 2015 Kokurewicz et al., 2016; Ogórek et al., 2017; 2018).

This study is the first report of mycological air quality in the Demänovská Cave of Liberty. The external air of the cave was more contaminated by fungal propagules than the indoor air ($p_{I, VI} < 0.001$), but aeromycota occurring in the underground sites is richer in species. Overall, we detected from 86.7 to 126.7 fungal spores per m^3 of indoor air of the cave, and these values of fungal spore contaminations were similar to those in other Slovakian caves (Ogórek et al., 2016b, c, d). The highest number of airborne spores was discovered in Location VI, and the smallest number of spores was recorded in Locations IV ($p_{IV, VI} < 0.001$) (Tables. 1, 2). The concentration of fungal spores in the air is an important factor of biosafety, because elevated levels can have a negative effect on the health of people and animals (WHO, 1990; Choi et al., 1999).

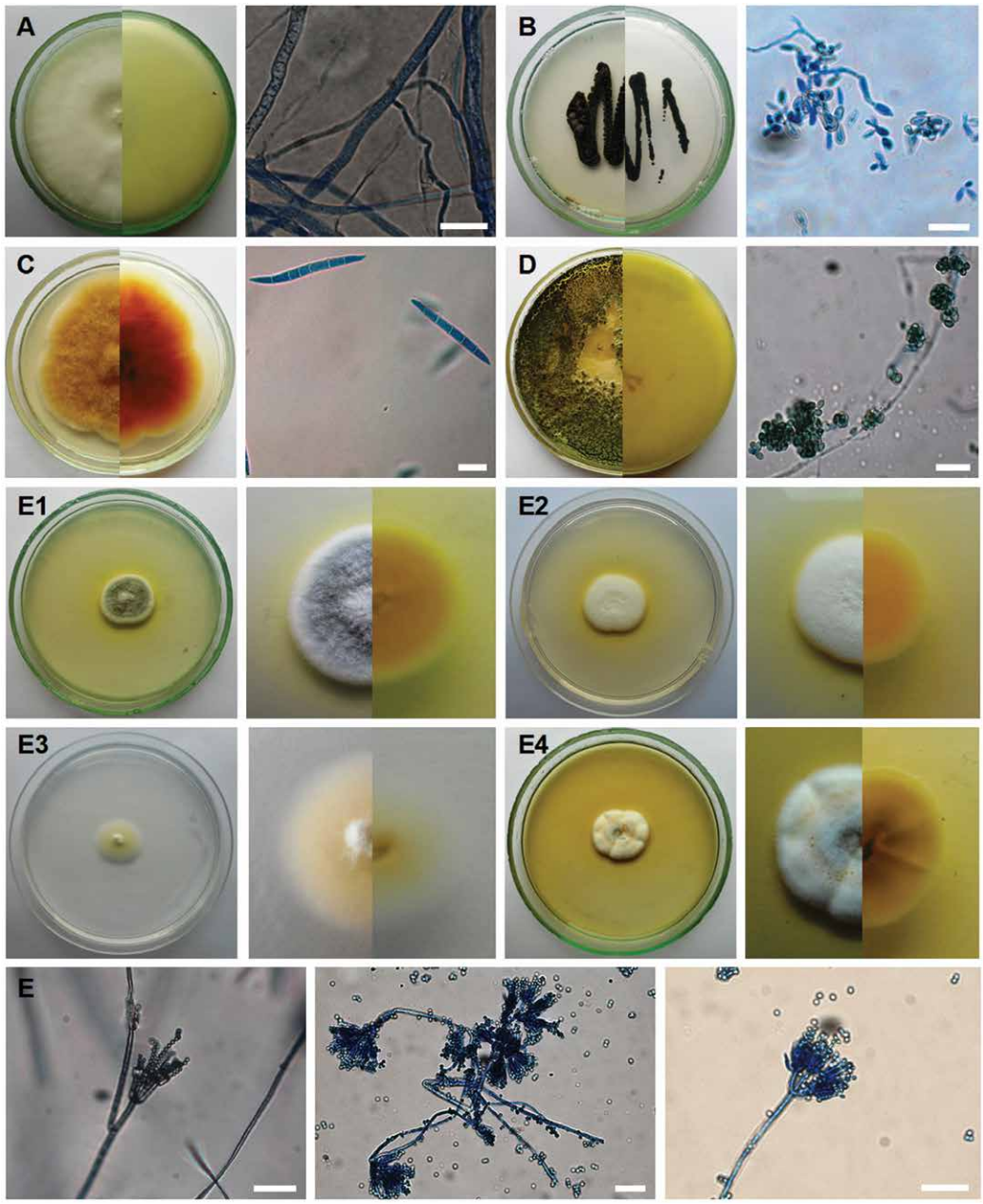

Figure 3. New airborne fungal species for underground sites discovered in Demänovská Cave of Liberty, 7-day-old (A, B, C, E) or 21-day-old culture (D) at 25±1 °C, top and bottom view of a colony on media PDA (A, B, C, D, E1), MEA (E2), Czapek-Dox Agar (E3), and CYA (E4), and the characteristic structure of fungi under the optical microscope on PDA: A – *Bjerkandera adusta* B – *Exophiala xenobiotica*, C – *Fusarium lateritium*, D – *Trichoderma citrinoviride*, E – *P. aurantiacobrunneum*. Scale bars: A – D = 10 µm, E = 20 µm.

Currently, there are no official mycological air quality standards relating specifically to underground sites, but there are such requirements with respect to indoor air of buildings. Therefore, we could conclude that the mycological quality of air in the investigated sites does not pose a risk to human health with an unimpaired immune system, according to most standards of fungal air contamination, i.e. the American Industrial Hygiene Association, the World Health Organization, or the European Confederation Commission. For example, the most stringent standard among them states that the concentration of airborne fungi should not be higher than 500 spores per m^3 (WHO, 1990; Choi et al., 1999). Thus, in this study, the numbers of airborne fungal spores were at much lower levels.

The species diversity of airborne fungi was higher in the air inside Demänovská Cave of Liberty than outside it (Tables. 1, 2). This trend is consistent with other reports on aeromycological research of underground sites during the summer (Pusz et al., 2014, 2015). Altogether, 18 different fungal spores were detected in the air samples of the cave. Fungal spores

belonging to *Bjerkandera adusta*, *Exophiala xenobiotica*, *Fusarium lateritium*, *Penicillium aurantiacobrunneum*, and *Trichoderma citrinoviride* were discovered for the first time in underground sites (Tables. 1, 2; Fig. 3). The presence of these new species can be associated with anthropogenic factors, and the presence of bats in the Demänovská Cave of Liberty, because those factors can contribute to the qualitative and quantitative changes of fungal communities inhabiting underground areas (Griffin et al., 2014; Kokurewicz et al., 2016; Ogórek et al., 2016b).

Aerobiological investigations of mycobiota show that the fungal propagules of *Cladosporium* are most commonly detected in the atmosphere, as well as in the indoor air of underground sites (Larsen and Gravesen, 1991; Stępalska et al., 1999; Pusz et al., 2014). These spores also dominated in the air of Demänovská Cave of Liberty, especially *C. macrocarpum* spores ($p < 0.001$), which constituted for over 32% of all detected spores (Table 2). *Cladosporium* spores are one of the most allergenic biological particles in the air, which can cause allergic rhinitis, asthma or allergic alveolitis. However, almost 3,000 spores of this fungi in one cubic meter of air are required for the emergence of respiratory allergies in humans (Rapiejko et al., 2004). Therefore, the level of *Cladosporium* spores detected in the air samples of the Demänovská Cave of Liberty does not constitute a significant allergic risk to visitors, because we detected a maximum of 61.7 spores of *Cladosporium* in 1 m^3 in the air of this cave.

An important group of the fungal community in the internal air of Demänovská Cave of Liberty constituted species belonging to *Aspergillus* and *Penicillium* (Tables. 1, 2), which are also commonly found in the bioaerosols of underground sites (Nováková, 2009; Vanderwolf et al., 2013). Their spores, as with the above-mentioned *Cladosporium*, are also strongly associated with allergic respiratory diseases, especially asthma (Pekkanen et al., 2007). Additionally, they can also cause opportunistic mycosis in mammals, including humans (Eschete et al., 1981; Hoffman et al., 1992). Overall, it should be noted that many of these fungal spores obtained from the Demänovská Cave of Liberty are not pathogenic. Still, some of them can pose a risk to persons with weakened immune systems (Nowicka, 2003).

Conclusions

Mycological monitoring carried out in underground ecosystems, with particular emphasis on sites open to tourists, or important from the point of view of wintering bats, is a relatively new venture. Regular monitoring will allow observation of qualitative and quantitative changes taking place in fungal communities inside underground ecosystems, and it will be possible to maintain biological safety for people and animals in such sites. The species diversity of airborne fungi was higher in the air inside the Demänovská Cave of Liberty than outside it, and *Cladosporium macrocarpum* spores dominated in this study. Moreover, research of this type has allowed the detection of new airborne species for underground ecosystems (*Bjerkandera adusta*, *Exophiala xenobiotica*, *Fusarium lateritium*, *Penicillium aurantiacobrunneum,* and *Trichoderma citrinoviride*).

Nevertheless, it is difficult to explain the occurrence of these new species. One of the reasons may be the accuracy of research methods, but it can also be associated with anthropogenic factors, as well as the presence of bats in this cave. Pearson correlation analysis showed that the levels of airborne fungal spores were correlated positively with air temperature. The concentration of fungi in the air of the investigated sites does not pose a health risk for people with an unimpaired immune system. However, some of the airborne fungi detected in the Demänovská Cave of Liberty can pose a risk to persons and animals with weakened immune systems or people who have fungal allergies. Moreover, it is likely that the mycological quality of air in these sites may deteriorate, which is why their further monitoring is important, and should be regularly performed.

Acknowledgements

This work was co-financed by the Ministry of Science and Higher Education, carried out by the University of Wroclaw ‘‘Grant to Young Researchers,” Grant number: 0420/2299/17.

References

Barton, H.A., and Northup, D.E., 2007, Geomicrobiology in cave environments: past, current, and future perspectives: Journal of Cave and Karst Studies, v. 69, p. 163–178.

Bensch, K., Braun, U., Groenewald, J.Z., and Crous, P.W., 2012, The genus *Cladosporium*: Studies in Mycology, v. 72, p. 1–401. https://doi.org/10.3114/sim0003.

Brickus, L.S.R., Siqueira, L.F.G., Aquino Neto, F.R., and Cardoso, J.N., 1998, Occurrence of airborne bacteria and fungi in bayside offices in Rio de Janeiro, Brazil: Indoor and Built Environment, v. 7, p. 270–275. https://doi.org/10.1177/1420326X9800700504.

Bruce, N., Perez-Padilla, R., and Albalak, R., 2000, Indoor air pollution in developing countries: a major environmental and public health challenge: Bulletin of the World Health Organization, v. 78, no. 9, p. 1078–1092.

Chilvers, M.I., and du Toit, L.J., 2006, Detection and identification of *Botrytis* species associated with neck rot, scape blight, and umbel blight of onion: Online. Plant Health Progress, htttps://doi.org/10.1094/PHP-2006-1127-01-DG.

Choi, Y.W., Hyde, K.D., and Ho, W.H., 1999, Single spore isolation of fungi: Fungal Diversity, v. 3, p. 29–38.

Darçın, M., 2014, Association between air quality and quality of life: Environmental Science and Pollution Research, v. 21, p. 1954–1959. https://doi.org/10.1007/s11356-013-2101-3.

de Hoog, G.S., Zeng, J.S., Harrak, M.J., and Sutton, D.A., 2006, *Exophiala xenobiotica* sp. nov., an opportunistic, black, yeast- inhabiting environment, rich in hydrocarbons: Antonie van Leeuwenhoek, v. 90, no. 3, p. 257–68. https://doi.org/10.1007/s10482-006-9080-z.

Doyle, J.J., and Doyle, J.L., 1987, A rapid DNA isolation procedure for small quantities of fresh leaf tissue: Phytochemical Bulletin, v. 19, p. 11–15.

Eschete, M.L., King, J.W., West, B.C., and Oberle, A., 1981, *Penicillium chrysogenum* endophthalmitis: first reported case: Mycopathology, v. 74, p. 125–127. https://doi.org/10.1007/BF01259468.

Frisvad, J.C., and Samson, R.A., 2004, Polyphasic taxonomy of *Penicillium* subgenus Penicillium A guide to identification of food and air-borne terverticillate *Penicillia* and their mycotoxins: Studies in Mycology, v. 49, p. 1–173.

Golubev, V.I., 1981, New combinations in the yeast genus *Cryptococcus*: Mikologiya i Fitopatologiya, v. 15, no. 6, p. 467–468.

Griffin, D.W., Gray, M.A., Lyles, M.B., and Northup, D.E., 2014, The transport of nonindigenous microorganisms into caves by human visitation: A case study at Carlsbad Caverns National Park: Geomicrobiology Journal, v. 31, no. 3, p. 175–185. https://doi.org/10.1080/01490451.2013.815294.

Hernández-Restrepo, M., Groenewald, J.Z., and Crous, P.W., 2016. Taxonomic and phylogenetic re-evaluation of *Microdochium*, *Monographella* and *Idriella*: Persoonia, v. 36, p. 57– 82. https://doi.org/10.3767/003158516X688676.

Hoffman, M., Bash, E., Berger, S.A., Burke, M., and Yust, I., 1992, Fatal necrotizing esophagitis due to *Penicillium chrysogenum* in a patient with acquired immunodeficiency syndrome: European Journal of Clinical Microbiology & Infectious Diseases, v. 11, p. 1158–1160. https://doi.org/10.1007/BF01961135.

Houbraken, J., Frisvad, J.C., and Samson, R.A., 2011, Taxonomy of *Penicillium* section Citrina: Studies in Mycology, v. 70, p. 53–138. https://doi.org/10.3114/sim.2011.70.02

Jülich, W., 1979, Studies in resupinate Basidiomycetes - V. Some new genera and species: Persoonia, v. 10, no. 1, p. 137–140.

Jung, P.E., Fong, J.J., Park, M.S., Oh, S.-Y., Kim, C., and Lim, Y.W., 2014, Sequence validation for the identification of the White-Rot fungi *Bjerkandera* in public sequence databases: Journal of Microbiology and Biotechnology, v. 24, no. 10, p. 1313–1319. https://doi.org/10.4014/jmb.1404.04021

Keirle, M.R., Hemmes, D.E., and Desjardin, D.E., 2004, Agaricales of the Hawaiian Islands. 8. Agaricaceae: *Coprinus* and *Podaxis*; Psathyrellaceae: Coprinopsis, Coprinellus and Parasola: Fungal Diversity, v. 15, p. 33–124.

Kim, J.Y., Kwon, H.W., Yun, Y.H., and Kim, S.H., 2016, Identification and characterization of *Trichoderma* species damaging shiitake mushroom bed-logs infested by *Camptomyia* Pest: Journal of Microbiology and Biotechnology, v. 26, no. 5, p. 909–917. https://doi.org/10.4014/jmb.1602.02012.

Kokurewicz, T., Ogórek, R., Pusz, W., and Matkowski, K., 2016, Bats increase the number of cultivable airborne fungi in the "Nietoperek" bat reserve in Western Poland: Microbial Ecology, v. 72, no. 1, p. 36–48. https://doi.org/10.1007/s00248-016-0763-3.

Larsen, L., and Gravesen, S., 1991, Seasonal variation of outdoor airborne viable microfungi in Copenhagen, Denmark: Grana, v. 30, p. 467–471. https://doi.org/10.1080/00173139109432011

Mammas, I.N., and Spandidos, D.A., 2016, Paediatric virology in the hippocratic corpus: Experimental and Therapeutic Medicine, v. 12, p. 541–549. https://doi.org/10.3892/etm.2016.3420.

Marušin, M., 2003, Geological conditions - factor of origin of two different cave systems in two adjacent valleys (the Demänovská Valley and the Jánska Valley, the Low Tatras, Slovakia): Acta Carsologica, v. 32, no. 1, p. 121–130.

Niazi, S., Hassanvand, M.S., Mahvi, A.H., Nabizadeh, R., Alimohammadi, M., Nabavi, S., Faridi, S., Dehghani, A., Hoseini, M., Moradi-Joo, M., Mokamel, A., Kashani, H., Yarali, N., and Yunesian, M., 2015, Assessment of bioaerosol contamination (bacteria and fungi) in the largest urban wastewater treatment plant in the Middle East: Environmental Science and Pollution Research, v. 22, p. 16014–16021. https://doi.org/10.1007/s11356-015-4793-z.

Nováková, A., 2009, Microscopic fungi isolated from the Domica Cave system (Slovak Karst National Park, Slovakia). A review: International Journal of Speleology, v. 38, no. 1, p. 71–82. https://doi.org/10.5038/1827-806X.38.1.8.

Nowicka, J., 2003, Czynniki ryzyka, epidemiologia i klinika grzybic w ostrych białaczkach (Risk factors, epidemiology and clinics of mycoses in acute leukemia): Mikologia Lekarska, v. 10, p. 135–143 [In Polish].

Nudziková, Ľ., 2014, Vývoj návštevnosti sprístupnených jaskýň na Slovensku od roku 2009 (Course of show caves attendance in Slovakia since 2009): Aragonit, v. 19, no. 1–2, p. 35–38 [in Slovak].

Ogórek, R., 2018, Fungal Communities on Rock Surfaces in Demänovská Ice Cave and Demänovská Cave of Liberty (Slovakia): Geomicrobiology Journal, v. 35, no. 4, p. 266–276. https://doi.org/10.1080/01490451.2017.1348409.

Ogórek, R., Dyląg, M., and Kozak, B., 2016a, Dark stains on rock surfaces in Driny Cave (Little Carpathian Mountains, Slovakia): Extremophiles, v. 20, p. 641–652. https://doi.org/10.1007/s00792-016-0853-7.

Ogórek, R., Dyląg, M., Kozak, B., Višňovská, Z., Tančinová, D., and Lejman, A., 2016b, Fungi isolated and quantified from bat guano and air in Harmanecká and Driny Caves (Slovakia): Journal of Cave and Karst Studies, v. 78, no. 1, p. 41–49. https://doi.org/10.4311/2015MB0108.

Ogórek, R., Dyląg, M., Višňovská, Z., Tančinová, D., and Zalewski, D., 2016c, Speleomycology of air and rock surfaces in Driny Cave (Lesser Carpathians, Slovakia): Journal of Cave and Karst Studies, v. 78, no. 2, p. 119–127. https://doi.org/10.4311/2015MB0128.

Ogórek, R., Kozak, B., Lejman, A., Kalinowska, K., and Dyląg, M., 2012, Analiza genetyczna szczepów *Candida albicans* za pomocą techniki RFLP-PCR (Molecular typing of *Candida albicans* isolates using RFLP-PCR): Mikologi Lekarska, v. 9, no. 3, p. 109–114 [in Polish].

Ogórek, R., Kozak, B., Višňovská, Z., and Tančinová, D., 2018, Phenotypic and genotypic diversity of airborne fungal spores in Demänovská Ice Cave (Low Tatras, Slovakia): Aerobiologia, v. 34, no. 1, p. 13–28. https://doi.org/10.1007/s10453-017-9491-5.

Ogórek, R., Lejman, A., and Matkowski, K., 2013, The fungi isolated from the Niedźwiedzia Cave in Kletno (Lower Silesia, Poland): International Journal of Speleology, v. 42, no. 2, p. 161–166. https:// doi.org/10.5038/1827-806X.42.2.9.

Ogórek, R., Pusz, W., Zagożdżon, P.P., Kozak, B., and Bujak, H., 2017, Abundance and diversity of psychrotolerant cultivable mycobiota in winter of a former aluminous shale mine: Geomicrobiology Journal, v. 34, no. 10, p. 823–833. https://doi.org/10.1080/01490451.2017.1280860.

Ogórek, R., Višňovská, Z., and Tančinová, D., 2016d, Mycobiota of underground habitats: case study of Harmanecká Cave in Slovakia: Microbial Ecology, v. 71, no. 1, p. 87–99. https://doi.org/10.1007/s00248-015-0686-4.

Pekkanen, J., Hyvarinen, A., Haverinen-Shaughnessy, U., Korppi, M., Putus, T., and Nevalainen, A., 2007, Moisture damage and childhood asthma: a population-based incident case-control study: European Respiratory Society, v. 29, no. 3, p. 509–515. https://doi.org/10.1183/09031936.00040806.

Poulson, T.L., and White, W.B., 1969, The cave environment: Science, v. 165, no. 3897, p. 971–981. https://doi.org/10.1126/science.165.3897.971.

Pusz, W., Ogórek, R., Knapik, R., Kozak, B., and Bujak, H., 2015, The occurrence of fungi in the recently discovered Jarkowicka cave in the Karkonosze Mts. (Poland): Geomicrobiology Journal, v. 32, no. 1, p. 59–67. https://doi.org/10.1080/01490451.2014.925010.

Pusz, W., Ogórek, R., Uklańska-Pusz, C., and Zagożdżon, P., 2014, Speleomycological research in underground Osówka complex in Sowie Mountains (Lower Silesia, Poland): International Journal of Speleology, v. 43, no. 1, p. 27–34. https://doi.org/10.5038/1827-806X.43.1.3.

Rampelotto, P.H., 2013, Extremophiles and extreme environments: Life, v. 3, no. 3, p. 482–485. https://doi.org/10.3390/life3030482.

Rapiejko, P., Lipiec, A., Wojdas, A., and Jurkiewicz, D., 2004. Threshold pollen concentration necessary to evoke allergic symptoms: International Review of Allergology and Clinical Immunology in Family Medicine, v. 10, p. 91–94.

Reynolds, S.J., Black, D.W., Borin, S.S., Breuer, G., Burmeister, L.F., Fuortes, L.J, Smith, T.F., Stein, M.A., Subramanian, P., Thorne, P.S., and Whitten, P., 2001, Indoor environmental quality in six commercial office buildings in the Midwest United States: Applied Occupational and Environmental Hygiene, v. 16, p. 1065–1077. https://doi.org/10.1080/104732201753214170.

Romagnoli, P., Balducci, C., Perilli, M., Vichi, F., Imperiali, A., and Cecinato, A., 2016, Indoor air quality at life and work environments in Rome, Italy: Environmental Science and Pollution Research, v. 23, no. 4, p. 3503–3516. https://doi.org/10.1007/s11356-015-5558-4.

Slovak Caves Administration, 2018, Demänovská Ice Cave, http://www.ssj.sk/en/jaskyna/5-demanovska-ice-cave, access: 25.01.2018.

Stępalska, D., Harmata, K., Kasprzyk, I., Myszkowska, D., and Stach, A., 1999, Occurrence of air borne *Cladosporium* and *Alternaria* spores in Southern and Central Poland in 1995–1996: Aerobiologia, v. 15, p. 39–47. https://doi.org/10.1023/A:1007536513836.

Stolwijk, J.A.J., 1991, Sick-Building Syndrome: Environmental Health Perspectives, v. 95, p. 99–10. https://doi.org/10.1289/ehp.919599.

Tanaka, K., Endo, M., Hirayama, K., Okane, I., Hosoya, T., and Sato, T., 2001, Phylogeny of *Discosia* and *Seimatosporium*, and introduction of *Adisciso* and *Immersidiscosia* genera nova: Persoonia, v. 26, p. 85–98. https://doi.org/10.3767/003158511X576666.

Tang, J.W., 2009, The effect of environmental parameters on the survival of airborne infectious agents: Journal of the Royal Society Interface, v. 6, no. 6, p. 737–746. https://doi.org/10.1098/rsif.2009.0227.focus.

Vanderwolf, K.J., Malloch, D., McAlpine, D.F., and Forbes, G.J., 2013, A world review of fungi, yeasts, and slime molds in caves: International Journal of Speleology, v. 42, no. 1, p. 77–96. https:// doi.org/10.5038/1827-806X.42.1.9.

Visagie, C.M., Varga, J., Houbraken, J., Meijer, M., Kocsubè, S., Yilmaz, N., Fotedar, R., Seifert, K.A., Frisvad, J.C., and Samson, R.A., 2014, Ochratoxin production and taxonomy of the yellow aspergilli (*Aspergillus* section Circumdati): Studies in Mycology, v. 78, p. 1–61. https://doi.org/10.1016/j.simyco.2014.07.001.

Vitale, S., Santori, A., Wajnberg, E., Castagnone-Sereno, P., Luongo, L., and Belisario, A., 2011, Morphological and molecular analysis of *Fusarium lateritium*, the cause of gray necrosis of hazelnut fruit in Italy: Phytopathology, v.101, no. 6, p. 679–86. https://doi.org/10.1094/PHYTO-04-10-0120.

White, T.J., Bruns, T., Lee, S., and Taylor, J.W., 1990, Amplification and direct sequencing of fungal ribosomal RNA genes for phylogenetics. *in* Innis, M.A., Gelfand, D.H., Sninsky, J.J., and White, T.J., ed., PCR Protocols: A Guide to Methods and Applications: New York, Academic Press, pp. 315–322. https://doi.org/10.1016/B978-0-12-372180-8.50042-1.

WHO, 1983, Indoor Air Pollutants: exposure and health effects. WHO EURO Reports and studies. Copenhagen: World Health Organization. Report No 1983:78.

WHO, 1990, Indoor Air Quality: Biological contaminants: report on a WHO meeting, Rautavaara, 29 August – 2 September 1988, WHO Regional Publications, European Series no. 31. WHO Regional Office for Europe, Copenhagan.

Zain, M.E., 2011, Impact of mycotoxins on humans and animals: Journal of Saudi Chemical Society, v. 15, no. 2, p. 129–144. https://doi.org/10.1016/j.jscs.2010.06.006.

GUIDE TO AUTHORS

The *Journal of Cave and Karst Studies* is a multidisciplinary journal devoted to cave and karst research. The *Journal* is seeking original, unpublished manuscripts concerning the scientific study of caves or other karst features. Authors do not need to be members of the National Speleological Society, but preference is given to manuscripts of importance to North American speleology.

LANGUAGES: The *Journal of Cave and Karst Studies* uses American-style English as its standard language and spelling style, with the exception of allowing a second abstract in another language when room allows. In the case of proper names, the *Journal* tries to accommodate other spellings and punctuation styles. In cases where the Editor-in-Chief finds it appropriate to use non-English words outside of proper names (generally where no equivalent English word exist), the *Journal* italicizes them. However, the common abbreviations i.e., e.g., et al., and etc. should appear in roman text. Authors are encouraged to write for our combined professional and amateur readerships

CONTENT: Each paper will contain a title with the authors' names and addresses, an abstract, and the text of the paper, including a summary or conclusions section. Acknowledgments and references follow the text. Manuscripts should be limited to 6,000 words and no more than 10 figures and 5 tables. Larger manuscripts may be considered, but the *Journal* reserves the right to charge processing fees for larger submissions.

ABSTRACTS: An abstract stating the essential points and results must accompany all articles. An abstract is a summary, not a promise of what topics are covered in the paper.

STYLE: The *Journal* consults The Chicago Manual of Style on most general style issues.

REFERENCES: In the text, references to previously published work should be followed by the relevant author's name and date (and page number, when appropriate) in brackets. All cited references are alphabetical at the end of the manuscript with senior author's last name first, followed by date of publication, title, publisher, volume, and page numbers. Geological Society of America format should be used (see http://www.geosociety.org/documents/gsa/pubs/GSA_RefGuide_Examples.pdf). Please do not abbreviate periodical titles. Web references are acceptable when deemed appropriate. The references should follow the style of: Author (or publisher), year, Webpage title: Publisher (if a specific author is available), full URL (e.g., http://www.usgs.gov/citguide.html), and the date the website was accessed in brackets. If there are specific authors given, use their name and list the responsible organization as publisher. Because of the ephemeral nature of websites, please provide the specific date. Citations within the text should read: (Author, Year).

SUBMISSION: Manuscripts are to be submitted via the PeerTrack submission system at http://www.edmgr.com/jcks/. Instructions are provided at that address. At your first visit, you will be prompted to establish a login and password, after which you will enter information about your manuscript and upload your manuscript, tables, and figure files. Manuscript files can be uploaded as DOC, WPD, RTF, TXT, or LaTeX. Note: LaTeX files should not use any unusual style files; a LaTeX template and BiBTeX file may be obtained from the Editor-in-Chief. Table files can be uploaded as DOC, WPD, RTF, TXT, or LaTeX files and figure files can be uploaded as TIFF, AI, EPS, or CDR files. Extensive supporting data may be placed on the Journal's website as supplemental material at the discretion of the Editor-in-Chief. The data that are used within a paper must be made available upon request. Authors may be required to provide supporting data in a fundamental format, such as ASCII for text data or comma-delimited ASCII for tabular data.

DISCUSSIONS: Critical discussions of papers previously published in the *Journal* are welcome. Authors will be given an opportunity to reply. Discussions and replies must be limited to a maximum of 1000 words and discussions will be subject to review before publication. Discussions must be within 6 months after the original article appears.

MEASUREMENTS: All measurements will be in Systeme Internationale (metric) except when quoting historical references. Other units will be allowed where necessary if placed in parentheses and following the SI units.

FIGURES: Figures and lettering must be neat and legible. Figure captions should be on a separate sheet of paper and not within the figure. Figures should be numbered in sequence and referred to in the text by inserting (Fig. x). Most figures will be reduced, hence the lettering should be large. Photographs must be sharp and high contrast. Figures must have a minimum resolution of 300 dpi for acceptance. Please do not submit JPEG images.

TABLES: See http://caves.org/pub/journal/PDF/Tables.pdf to get guidelines for table layout.

COPYRIGHT AND AUTHOR'S RESPONSIBILITIES: It is the author's responsibility to clear any copyright or acknowledgement matters concerning text, tables, or figures used. Authors should also ensure adequate attention to sensitive or legal issues such as land owner and land manager concerns or policies and cave location disclosures.

PROCESS: All submitted manuscripts are sent out to at least two experts in the field. Reviewed manuscripts are then returned to the author for consideration of the referees' remarks and revision, where appropriate. Revised manuscripts are returned to the appropriate Associate Editor who then recommends acceptance or rejection. The Editor-in-Chief makes final decisions regarding publication. Upon acceptance, the senior author will be sent one set of PDF proofs for review. Examine the current issue for more information about the format used.

Journal of Cave and Karst Studies

Volume 80 Number 3 September 2018

CONTENTS